

1950

Vapor-Liquid Equilibrium of Non-Ideal Solutions.

Virgil Orr

Louisiana State University and Agricultural & Mechanical College

Follow this and additional works at: https://digitalcommons.lsu.edu/gradschool_disstheses



Part of the [Chemical Engineering Commons](#)

Recommended Citation

Orr, Virgil, "Vapor-Liquid Equilibrium of Non-Ideal Solutions." (1950). *LSU Historical Dissertations and Theses*. 7950.
https://digitalcommons.lsu.edu/gradschool_disstheses/7950

This Dissertation is brought to you for free and open access by the Graduate School at LSU Digital Commons. It has been accepted for inclusion in LSU Historical Dissertations and Theses by an authorized administrator of LSU Digital Commons. For more information, please contact gradetd@lsu.edu.

VAPOR-LIQUID EQUILIBRIUM OF NON-IDEAL SOLUTIONS

A Dissertation

Submitted to the Graduate Faculty of the
Louisiana State University and
Agricultural and Mechanical College
in partial fulfillment of the
requirements for the degree of
Doctor of Philosophy

in

The Department of Chemical Engineering

by

Virgil Orr

B.S., Louisiana Polytechnic Institute, 1944

M.S., Louisiana State University, 1948

June, 1950

UMI Number: DP69328

All rights reserved

INFORMATION TO ALL USERS

The quality of this reproduction is dependent upon the quality of the copy submitted.

In the unlikely event that the author did not send a complete manuscript and there are missing pages, these will be noted. Also, if material had to be removed, a note will indicate the deletion.



UMI DP69328

Published by ProQuest LLC (2015). Copyright in the Dissertation held by the Author.

Microform Edition © ProQuest LLC.

All rights reserved. This work is protected against
unauthorized copying under Title 17, United States Code



ProQuest LLC.
789 East Eisenhower Parkway
P.O. Box 1346
Ann Arbor, MI 48106 - 1346

MANUSCRIPT THESES

Unpublished theses submitted for the master's and doctor's degrees and deposited in the Louisiana State University Library are available for inspection. Use of any thesis is limited by the rights of the author. Bibliographical references may be noted, but passages may not be copied unless the author has given permission. Credit must be given in subsequent written or published work.

A library which borrows this thesis for use by its clientele is expected to make sure that the borrower is aware of the above restrictions.

LOUISIANA STATE UNIVERSITY LIBRARY

1187
Deposit
Gen.

36
S9419

ACKNOWLEDGMENTS

The author is very deeply indebted to Dr. Jesse Coates, director of this project, for his advice and suggestions.

Grateful acknowledgment is also made:

To Dr. P. M. Horton for his many helpful suggestions.

To Mr. E. E. Snyder for fabricating and maintaining the equipment.

To Mrs. Grace Cameron, chemistry librarian, for her invaluable assistance in preparing the literature survey.

To Mr. A. J. Gully for his assistance in performing the statistical analyses on the analytical methods and in preparing the graphs.

To his fellow students for their advice and constructive criticisms.

378.76
L930 d
1950
C.2

TABLE OF CONTENTS

CHAPTER	PAGE
I. INTRODUCTION	1
II. THEORETICAL CONSIDERATIONS	3
A. Derivation of the Thermodynamic Relations	3
B. Development of the Integrated Forms of the Gibbs-Duhem Equation	8
C. Effect of Temperature on Activity Coefficients	22
D. Other Correlations	27
E. Conclusions	28
III. AN EQUILIBRIUM STILL FOR PARTIALLY MISCIBLE LIQUIDS	33
A. Resume' of Previous Designs	33
B. Design of the New Type of Still	39
C. Operating Procedure and Characteristics .	45
D. Proof of the Equilibrium Still	50
E. Reagents	64
F. Conclusions	65
IV. EXPERIMENTAL DATA	66
V. DISCUSSION OF RESULTS	100
A. Development of a More Versatile Equilibrium Still	100

CHAPTER	PAGE
B. Proposed Modifications of the Existing	
Design	103
C. Experimental Results	103
D. Correlation of Data	105
VI. SUMMARY	120
BIBLIOGRAPHY	122
APPENDIX	126
BIOGRAPHY	137

LIST OF TABLES

TABLE		PAGE
I.	Experimental Vapor-Liquid Equilibrium Data for Ethanol-Water at Atmospheric Pressure	52
II.	Experimental Vapor-Liquid Equilibrium Data for n-Butanol-Water at Atmospheric Pressure	55
III.	Vapor-Liquid Equilibrium Data of Stockhardt and Hull on n-Butanol-Water at Atmospheric Pressure	57
IV.	Vapor-Liquid Equilibrium Data on Smith and Bonner on n-Butanol-Water at Atmospheric Pressure	60
V.	Experimental Vapor-Liquid Equilibrium Data on Ethyl Acetate-Water at Atmospheric Pressure	62
VI.	Physical Properties of Reagents	64
VII.	Experimental Data for n-Hexane-Ethanol at 250 mm. Hg.	72
VIII.	Experimental Data for n-Hexane-Ethanol at 393 mm. Hg.	76
IX.	Experimental Data for n-Hexane-Ethanol at 760 mm. Hg.	80
X.	Experimental Data on n-Hexane-Ethanol at 1270 mm. Hg.	84

TABLE	PAGE
XI. Experimental Data on n-Hexane-Ethanol at 1545 mm. Hg.	88
XII. Experimental Data on n-Hexane-Ethanol at 2510 mm. Hg.	92
XIII. Experimental Data on n-Hexane Ethanol at 2830 mm. Hg.	96
XIV. Calibration Data for Copper-Constantan Thermocouples	129
XV. Solubility of n-Butanol in Water	131
XVI. Solubility of Ethyl Acetate in Water	133

LIST OF FIGURES

FIGURE	PAGE
1. Van Laar Constants for Ethanol-Water at 50°C. . . .	13
2. Activity Coefficient Curves for Ethanol-Water at 50°C.	14
3. Van Laar Constants for Ethanol-Water at Atmospheric Pressure	15
4. Van Laar Constants for Ethanol-Water at Atmospheric Pressure	16
5. Activity Coefficient Curves for Ethanol-Water at Atmospheric Pressure	17
6. Activity Coefficient Curves for Ethanol- Chloroform at 45°C.	18
7. Van Laar Constants for Ethanol-Chloroform at 45°C.	19
8. Othmer Still	34
9. Jones, Schoenborn, and Colburn Still	35
10. Detail Drawing of New Type Equilibrium Still . . .	40
11. Oblique View of Original Design	41
12. Front View of Original Design	42
13. Front View of Modified Still	48
14. Oblique View of Modified Still	49
15. x - y Diagram for Ethanol-Water at Atmospheric Pressure	51

FIGURE	PAGE
16. x - y Diagram for n-Butanol-Water at Atmospheric Pressure	53
17. Boiling Point Diagram for n-Butanol-Water at Atmospheric Pressure	54
18. Experimental Activity Coefficient Curves for n-Butanol-Water	56
19. Activity Coefficient Curves for n-Butanol-Water from the Data of Stockhardt and Hull	58
20. Activity Coefficient Curves for n-Butanol-Water from the Data of Smith and Bonner	59
21. x - y Diagram for Ethyl Acetate-Water at Atmospheric Pressure	63
22. Laboratory Distilling Column	67
23. Jones, Schoenborn, and Colburn Still	71
24. x - y Diagram for n-Hexane-Ethanol at 250 mm. Hg.	73
25. Boiling Point Diagram for n-Hexane-Ethanol at 250 mm. Hg.	74
26. Activity Coefficient Curves for n-Hexane-Ethanol at 250 mm. Hg.	75
27. x - y Diagram for n-Hexane-Ethanol at 393 mm. Hg.	77
28. Boiling Point Diagram for n-Hexane-Ethanol at 393 mm. Hg.	78
29. Activity Coefficient Curves for n-Hexane-Ethanol at 393 mm. Hg.	79

FIGURE		PAGE
30.	x - y Diagram for n-Hexane-Ethanol at 760 mm. Hg. .	81
31.	Boiling Point Diagram for n-Hexane-Ethanol at 760 mm. Hg.	82
32.	Activity Coefficient Curves for n-Hexane-Ethanol at 760 mm. Hg.	83
33.	x - y Diagram for n-Hexane-Ethanol at 1270 mm. Hg.	85
34.	Boiling Point Diagram for n-Hexane-Ethanol at 1270 mm. Hg.	86
35.	Activity Coefficient Curves for n-Hexane-Ethanol at 1270 mm. Hg.	87
36.	Boiling Point Diagram for n-Hexane-Ethanol at 1545 mm. Hg.	89
37.	x - y Diagram for n-Hexane-Ethanol at 1545 mm. Hg. .	90
38.	Activity Coefficient Curves for n-Hexane-Ethanol at 1545 mm. Hg.	91
39.	x - y Diagram for n-Hexane-Ethanol at 2310 mm. Hg. .	93
40.	Boiling Point Diagram for n-Hexane-Ethanol at 2310 mm. Hg.	94
41.	Activity Coefficient Curves for n-Hexane-Ethanol at 2310 mm. Hg.	95
42.	x - y Diagram for n-Hexane-Ethanol at 2830 mm. Hg. .	97
43.	Boiling Point Diagram for n-Hexane-Ethanol at 2830 mm. Hg.	98
44.	Activity Coefficient Curves for n-Hexane-Ethanol at 2830 mm. Hg.	99

FIGURE		PAGE
45.	Corrected Activity Coefficient Curves for n-Hexane-Ethanol at 2310 mm. Hg.	106
46.	Corrected x - y Diagram for n-Hexane-Ethanol at 2310 mm. Hg.	107
47.	Correlation of the Data on n-Hexane-Ethanol at 1545 mm. Hg. by Proposed Equation	109
48.	x - y Diagram for n-Hexane-Ethanol at 1545 mm. Hg. with Limiting Slopes	111
49.	White Correlation of Activity Coefficient Data . . .	115
50.	Copper-Constantan Thermocouple Calibration	130
51.	Physical Properties of the n-Butanol-Water System .	132
52.	Physical Properties of the Ethanol-Water System . .	134
53.	Physical Properties of the n-Hexane-Ethanol System .	135
54.	Cox Vapor Pressure Plot	136

ABSTRACT

Previous investigators developed apparatus for obtaining vapor-liquid equilibrium data and derived methods of correlating this data based on thermodynamic considerations. The methods used to obtain vapor-liquid equilibrium data have limitations that are usually imposed by the physical nature of the systems being studied. These limitations have prevented determination of a sufficient amount of reliable data on the various types of systems encountered to permit development of suitable correlations for the extension of limited data or prediction of values from a minimum amount of related data. Some of the relations previously presented have found wide application as approximations and in some cases have been applied under conditions for which they are not valid.

A more versatile recirculation type equilibrium still has been developed for the determination of vapor-liquid equilibrium data on miscible or partially miscible systems at pressures ranging from below atmospheric to considerably above atmospheric. The still is of metal construction utilizing a centrifugal pump with a large by-pass line as a condensed vapor receiver. The pump will agitate the two liquid phases so completely that they behave as a homogeneous, single phase fluid and can be removed from this receiver in the ratio that is present. This still was found to satisfactorily duplicate literature values for the miscible system, Ethanol-Water, and the partially miscible system, n-Butanol-Water, at atmospheric pressure.

Vapor-liquid equilibrium data for Ethanol-Water, n-Butanol-Water, Ethyl Acetate-Water, and n-Hexane-Ethanol at atmospheric pressure and for n-Hexane-Ethanol at 250 mm., 393 mm., 1270 mm., 1545 mm., 2310 mm., and 2830 mm. total pressure are presented.

The following equation is proposed for the correlation of activity coefficients derived from vapor-liquid equilibrium data for binary systems rather than the commonly used empirical power series:

$$\log \frac{r_1}{r_2} = \log \frac{y_1 x_2}{x_1 y_2} + \log \frac{f_{P_2}}{f_{P_1}} + \log \frac{\sqrt{\pi_1}}{\sqrt{\pi_2}} + \frac{V_{M_2}(\pi - P_2)}{2.303RT} - \frac{V_{M_1}(\pi - P_1)}{2.303RT}$$

where

- r_1 -- activity coefficient of component 1
- r_2 -- activity coefficient of component 2
- y_1 -- mole fraction of component 1 in vapor
- x_1 -- mole fraction of component 1 in liquid
- y_2 -- mole fraction of component 2 in vapor
- x_2 -- mole fraction of component 2 in liquid
- f_{P_1} -- fugacity of component 1 when under its own vapor pressure at the temperature of the solution
- f_{P_2} -- fugacity of component 2 when under its own vapor pressure at the temperature of the solution
- $\sqrt{\pi_1}$ -- fugacity coefficient of component 1 evaluated at a reduced temperature corresponding to the critical temperature of component 1 and a reduced pressure corresponding to the total pressure and critical pressure of component 1
- $\sqrt{\pi_2}$ -- fugacity coefficient of component 2 evaluated at a reduced

temperature corresponding to the critical temperature of component 2 and a reduced pressure corresponding to the total pressure and critical pressure of component 2

V_{M_1} -- molal volume of component 1 in the liquid

V_{M_2} -- molal volume of component 2 in the liquid

P_1 -- vapor pressure of component 1

P_2 -- vapor pressure of component 2

R -- Gas Constant

T -- absolute temperature

π -- total pressure

An improved method for prediction of activity coefficients and vapor-liquid equilibrium over moderate pressure ranges from accurate isobaric boiling point measurements over the entire composition range is presented. This method is based on the proposed correlation equation and seems to permit prediction of this data as accurately as it can be determined experimentally. The equipment necessary to obtain the basic data is much less involved than that for determination of the vapor-liquid equilibrium data.

CHAPTER I

INTRODUCTION

The development of azeotropic and extractive distillation as important industrial processes has stimulated many investigations of the vapor-liquid equilibria of non-ideal systems. While a large amount of data have been obtained, correlation of this data in a generalized and conveniently usable form has proved to be an exceedingly difficult problem.

The usual approach to correlation is by evaluation of the deviations from the laws of ideal solutions employing equations based on thermodynamic considerations. Use of thermodynamic analysis has proved to be very valuable in correlation of vapor-liquid equilibrium. For example, the Gibbs-Duhem equation, which in differential form expresses the necessary conditions for any phase equilibrium under conditions of constant temperature and pressure, is commonly employed as a test for thermodynamic consistency of vapor-liquid equilibrium data. While thermodynamic consistency does not in itself constitute a proof of equilibrium, it does give strong evidence of such. Incorrect data may be consistent, but thermodynamically inconsistent data cannot be correct. Thermodynamic consistency should always be used as a guide when drawing a line through experimental vapor-liquid equilibrium data.

Instead of using the differential form of the Gibbs-Duhem equation, certain investigators^{27, 5, 50, 51} have developed integrated forms which

will be discussed more fully in later sections. These equations are commonly applied under conditions of constant pressure and varying temperature for which they are not valid, having been derived at constant temperature. Of these integrated forms the Van Laar^{50, 51} equations are probably the most widely used. They contain two empirical constants which are supposedly independent of composition at constant temperature for any particular substance, but which are known to vary with temperature. The assumption that these constants are independent of temperature has lead to poor results in many cases and points up a very definite need for investigation of the effects of temperature variation on these constants. Since liquid "activity coefficients" are a qualitative measure of the deviations from ideal solution behavior, and since the constants of the various integrated forms of the Gibbs-Duhem equation are easily related to these activity coefficients, there is a need for a study of the variation of these coefficients with temperature.

CHAPTER II

THEORETICAL CONSIDERATIONS

A. DERIVATION OF THE THERMODYNAMIC RELATIONS.

The Gibbs-Duhem equation is a rigorous thermodynamic expression of the necessary conditions for phase equilibrium of a closed system at constant temperature and pressure. It was first deduced by J. Willard Gibbs¹⁰ in 1875 and later, independently by P. Duhem⁹ in 1886. It has been shown that the change in free energy, F , in a homogeneous phase as a function of the temperature, T , the pressure, P , and the number of moles of each component present, n_1, n_2, \dots , is

$$dF = \left(\frac{\partial F}{\partial T} \right)_{P, n_1, n_2, \dots} dT + \left(\frac{\partial F}{\partial P} \right)_{T, n_1, n_2, \dots} dP + \left(\frac{\partial F}{\partial n_1} \right)_{T, P, n_2, \dots} dn_1 + \left(\frac{\partial F}{\partial n_2} \right)_{T, P, n_1, \dots} dn_2 + \dots \quad (1)$$

Since one of the conditions of a closed system in equilibrium at constant temperature and pressure is $(\delta F)_{T, P} = 0$, Equation (1) reduces to

$$\left(\frac{\partial F}{\partial n_1} \right)_{T, P, n_2, \dots} dn_1 + \left(\frac{\partial F}{\partial n_2} \right)_{T, P, n_1, \dots} dn_2 + \dots = 0 \quad (2)$$

where

$$\left(\frac{\partial F}{\partial n_i} \right)_{T, P, n_2, \dots} = \bar{F}_i$$

which is known as the partial molal free energy. Since Equation (2) is a partial molal equation, the independent and dependent variables can be switched yielding the following expression for a binary system:

$$n_1 \left(\frac{\partial \bar{F}_1}{\partial n_1} \right)_{T, P} + n_2 \left(\frac{\partial \bar{F}_2}{\partial n_2} \right)_{T, P} = 0 \quad (3)$$

In order to define some terms, a digression is in order. The partial molal free energy, \bar{F} , is related to the fugacity, f , at constant temperature by the following equation which is a partial definition of fugacity.

$$\left(d\bar{F} = RT d \ln f \right)_T \quad (4)$$

Qualitatively, fugacity is a measure of the escaping tendency of any particular substance in any particular phase and the concept was introduced by G. N. Lewis²⁴ to account for the behavior of real gases as compared to perfect gases. It should be remembered that when two phases are in equilibrium, the fugacity of any particular component is the same in both phases, so if the fugacity of a component in the vapor phase can be calculated, the fugacity in the liquid phase is obtained simultaneously.

Fugacity of pure gases is related to pressure through the basic thermodynamic functions as described by Hougen and Watson¹⁷ with the following results:

$$\ln \left(\frac{f}{P} \right) = \int_0^P (z-1) \frac{dP}{P} \quad (5)$$

where

f = the fugacity of the pure gas at temperature, T .
 P = the pressure.
 z = the compressibility factor, $z = \frac{PV}{RT}$ for one mole.

This equation is easily integrated graphically or analytically if a suitable equation of state is evaluated. This integration has been carried out in conjunction with the theorem of corresponding states and the ratio of fugacity to pressure ($\frac{f}{P}$) has been plotted against

reduced temperature and pressure. This ratio $\left(\frac{f}{P}\right)$ is commonly termed the "fugacity coefficient" and these plots provide a very convenient method for obtaining the fugacity of a pure substance at any conditions of temperature and pressure.

For treatment of problems involving solutions it is convenient to define another thermodynamic property which is directly related to fugacity and hence also to free energy. This property, called activity, a , is defined as the ratio of the fugacity of a component in a given state to its fugacity in an arbitrarily defined standard state at the same temperature. Thus,

$$a = \left(\frac{f}{f^\circ} \right)_T \quad (6)$$

where

- a = activity
- f = fugacity in the given state
- f° = fugacity in the standard state at the same temperature and pressure which can be evaluated by Equation (5) under its own vapor pressure at the temperature, then corrected for pressure.

This correction for the effect of pressure on the fugacity of the liquid is derived from the same basic considerations as Equation (5) for gases. The expression is

$$\ln \frac{f_0}{f_P} = \frac{V_m (\pi - P)}{RT} \quad (7)$$

where

- f_P = fugacity of the pure liquid under its own vapor pressure at the temperature, T .
- V_m = molal volume of the liquid at the temperature, T , and pressure π
- π = total pressure of the system.
- P = vapor pressure of the pure liquid at the temperature, T .
- R = Gas Constant.

Combination of Equations (6) and (4) gives

$$RT \ln a = \bar{F} - \bar{F}^0 \quad (8)$$

where

\bar{F} = partial molal free energy in the given state at temperature T.

\bar{F}^0 = partial molal free energy in the standard state at the same temperature T.

In the case of liquid solutions it is convenient to define the standard state as the pure component at the temperature and pressure of the mixture. With this choice of standard state the activities become equal to the mole fractions, x , in mixtures which form ideal solutions, since f in Equation (6) can be replaced by xf^0 . It should be noted that this is a variable standard state since in the case of constant pressure vapor-liquid equilibrium, the temperature of the solution varies with composition, or when isothermal the pressure varies with composition. The effect of this variable standard state on activity should be studied.

The statement, that when ideal liquid solutions are formed, the activity equals the mole fraction, does not hold for non-ideal liquid solutions. To account for this G. N. Lewis²⁴ introduced the activity coefficient, γ , which when multiplied by the mole fraction, x , gives the activity. Thus

$$\gamma x = a = \left(\frac{f}{f^0} \right)_T \quad (9a)$$

or

$$\gamma = \frac{a}{x} = \frac{f}{x f^0} \quad (9b)$$

The standard state has already been defined and may be summed up in the following manner: A standard state of unit activity is often very convenient, and it is known that the behavior of a solution approaches

the ideal (γ solvent approaches unity) as the pure solvent is approached (x approaches unity). Hence the product, γx , or the activity also approaches unity, and the pure component at the temperature and pressure of the mixture yields a convenient standard state of unit activity.

For binary systems under conditions where the vapor phase may be treated as a perfect gas (low pressures) without much error and where the vapor phase may be assumed to represent an ideal solution, Equation (9b) reduces to the following for component 1:

$$\gamma_1 = \frac{P_1^*}{x_1 P_1^*} = \frac{y_1 \pi^*}{x_1 P_1^*} \quad (10)$$

where

x_1 = mole fraction of component 1 in the liquid phase.

y_1 = mole fraction of component 1 in the vapor phase.

P_1^* = partial pressure of component 1 at the temperature of the solution.

P_1^* = vapor pressure of component 1 at the temperature of the solution.

π^* = total pressure of the system.

The asterisk represents a pressure sufficiently low that the above assumptions will hold.

From Equations (3) and (8) one form of the Gibbs-Duhem equation for binary mixtures can be written

$$n_1 d \ln a_1 + n_2 d \ln a_2 = 0 \quad (11)$$

It is desirable for graphical manipulations to express this in terms of activity coefficients since they vary less with change in composition than do the activities. For a binary mixture the following development can be written

$$\begin{aligned}
X_1 + X_2 &= 1 \\
dX_1 + dX_2 &= 0 \\
\frac{X_1 dX_1}{X_1} + \frac{X_2 dX_2}{X_2} &= 0
\end{aligned} \tag{12}$$

Equation (11) can be written in the following equivalent form

$$X_1 d \ln a_1 + X_2 d \ln a_2 = 0$$

Now subtraction of Equation (12) from Equation (11) gives

$$X_1 d \ln \frac{a_1}{X_1} + X_2 d \ln \frac{a_2}{X_2} = 0$$

or

$$d \ln \gamma_1 = - \frac{X_2}{X_1} d \ln \gamma_2 \tag{13}$$

This form is more convenient for graphical integrations, but the following form is more convenient for checking thermodynamic consistency of vapor-liquid equilibrium data by use of the slopes of the usual activity coefficient versus mole fraction plots.

$$X_1 \frac{d \log \gamma_1}{dX_1} = - X_2 \frac{d \log \gamma_2}{dX_1} \tag{14}$$

B. DEVELOPMENT OF THE INTEGRATED FORMS OF THE GIBBS-DUHEM EQUATION.

These integrated forms, which are the expressions most commonly used to show the variation of activity coefficients with composition at conditions of constant temperature, are most conveniently derived by consideration of the free energy changes accompanying the formation of a solution from its components in their standard states. According to Hougen and Watson¹⁷ the free energy change of mixing, ΔF_M , is given by the following general equation where the standard state is taken as

the pure components at the temperature and pressure of the system:

$$\Delta F_M = \sum n_i \bar{F}_i - \sum n_i F_i^0 \quad (15)$$

where

$$\begin{aligned} \sum n_i \bar{F}_i &= n_1 \bar{F}_1 + n_2 \bar{F}_2 + \dots = \bar{F} \\ \sum n_i F_i^0 &= n_1 F_1^0 + n_2 F_2^0 + \dots = F^0 \end{aligned}$$

Combining Equations (15), (8), and (9b)

$$\Delta F_M = RT \sum n_i \ln \chi_i + RT \sum n_i \ln \gamma_i \quad (16)$$

where

$$\begin{aligned} \sum n_i \ln \chi_i &= n_1 \ln \chi_1 + n_2 \ln \chi_2 + \dots \\ \sum n_i \ln \gamma_i &= n_1 \ln \gamma_1 + n_2 \ln \gamma_2 + \dots \end{aligned}$$

For an ideal solution all activity coefficients are equal to unity and the term $RT \sum n_i \ln \gamma_i$ reduces to zero. This term was designated by Scatchard and Hamer³⁸ as the excess free energy, F^E , of the solution.

Thus, the free energy, F , of any solution may be written as

$$F = \sum n_i F_i^0 + RT \sum n_i \ln \chi_i + F^E \quad (17)$$

where

$$F^E = RT \sum n_i \ln \gamma_i \quad = \text{the excess free energy.}$$

The partial molal free energy of any component is obtained by differentiating Equation (17), thus for component 1,

$$\bar{F}_1 = \bar{F}_1^0 + RT \frac{\partial \sum n_i \ln \chi_i}{\partial n_1} + \frac{\partial F^E}{\partial n_1} \quad (18)$$

Expansion of the second term combined with Equation (12) gives

$$RT \frac{\partial \sum n_i \ln \chi_i}{\partial n_1} = RT \left[\ln \chi_1 + n_1 \frac{\partial \ln \chi_1}{\partial n_1} + n_2 \frac{\partial \ln \chi_2}{\partial n_1} + \dots \right] = RT \ln \chi_1 \quad (19)$$

Then,

$$\bar{F}_1 = \bar{F}_1^0 + RT \ln \chi_1 + \frac{\partial F^E}{\partial n_1} \quad (20)$$

By comparison of Equations (20) and (8) it may be seen that

$$RT \ln \gamma_1 = \frac{2F^E}{2n_1} \quad (21)$$

and

$$RT \ln \gamma_2 = \frac{2F^E}{2n_2} \quad (22)$$

Wohl⁵⁴ pointed out that the empirical equations which have been commonly used for correlation of activity coefficients represent special cases of the following equation for the excess free energy, F^E .

$$\frac{F^E}{RT(\sum q_i k_i)} = \sum_{ih} z_i z_h a_{ih} + \sum_{ihj} z_i z_h z_j a_{ihj} + \sum_{ihjl} z_i z_h z_j z_l a_{ihjl} \quad (23)$$

where

- x_i = mole fraction of component i.
- q_i = effective molal volume of component i.
- z_i = effective volume fraction of component i.
- $a_{ih}, \text{etc.}$ = empirical constants corresponding to the indicated groups of components in the summations.

Subscripts i, h, j, and l each may correspond to any component of the mixture in the terms of the indicated summations.

Equation (23) is designated a four suffix equation as characterized by the last summation term indicating interactions of groups of four molecules. If the last term is dropped there remains a three-suffix equation. Each additional summation introduces added constants to permit improved representation of increasingly complex relationships.

The relations which have been used in the past to correlate vapor-liquid equilibrium data have assumed that Equation (23) or some simpler form of Equation (23) is a satisfactory expression for the excess free energy, F^E , which is questionable. Therefore the value of such equations is doubtful except as an approximation.

The effective molal volume, q , in Equation (23) serves to relate the effective volume fractions, z , to the mole fractions, x , thus

$$Z_1 = \frac{x_1}{x_1 + q_2/q_1 x_2 + q_3/q_1 x_3 + \dots} \quad (24)$$

and

$$Z_2 = \frac{x_2 q_2/q_1}{x_1 + q_2/q_1 x_2 + q_3/q_1 x_3 + \dots} \quad (25)$$

Since Equations (21) and (22) are valid, thermodynamically consistent expressions for the logarithm of the activity coefficients at constant temperature can be obtained by differentiation of a suitable form of Equation (23). Wohl²⁴ did this for a binary system of components 1 and 2 using a three-suffix form of Equation (23) with the following equations being developed:

$$\log \gamma_1 = Z_2^2 [A + Z(B q_2/q_1 - A) Z_1] \quad (26)$$

$$\log \gamma_2 = Z_1^2 [B + Z(A q_2/q_1 - B) Z_2] \quad (27)$$

These equations contain three constants, A , B , and q_1/q_2 , which must be empirically determined for each system under consideration. By use of various assumptions regarding the ratio of the effective molal volumes, q_1/q_2 , the number of empirical constants may be reduced to two.

Margules²⁷ in effect assumed this ratio q_1/q_2 to be unity. With this assumption Equations (26) and (27) reduce to the Margules equations as modified by Carlson and Colburn⁶.

$$\log \gamma_1 = x_2^2 [A + Z(B-A)x_1] = (ZB-A)x_2^2 + Z(A-B)x_2^3 \quad (28)$$

$$\log \gamma_2 = x_1^2 [B + Z(A-B)x_2] = (ZA-B)x_1^2 + Z(B-A)x_1^3 \quad (29)$$

Scatchard³⁷ and his coworkers^{38, 39, 40} took the effective molal volumes as equal to the actual molal volumes of the pure components so

that q_1/q_2 equalled v_1/v_2 .

Van Laar^{50, 51} assumed the ratio q_1/q_2 equal to A/B and reduced equations (26) and (27) to the following forms as rearranged by Carlson and Colburn⁶:

$$\log r_1 = A z_2^2 = \frac{A x_2^2}{(A/B x_1 + x_2)^2} \quad (30)$$

$$\log r_2 = B z_1^2 = \frac{B x_1^2}{(x_1 + B/A x_2)^2} \quad (31)$$

which may be rearranged to a form suitable for solving for A and B directly.

$$A = \log r_1 \left[1 + \frac{x_2 \log r_2}{x_1 \log r_1} \right]^2 \quad (32)$$

$$B = \log r_2 \left[1 + \frac{x_1 \log r_1}{x_2 \log r_2} \right]^2 \quad (33)$$

The work of White⁵² suggested the rearrangement of these equations in the straight line form as follows:

$$(\log r_1)^{-1/2} = \frac{A^{1/2}}{B} \left(\frac{x_1}{x_2} \right) + \frac{1}{A^{1/2}} \quad (34)$$

$$(\log r_2)^{-1/2} = \frac{B^{1/2}}{A} \left(\frac{x_2}{x_1} \right) + \frac{1}{B^{1/2}} \quad (35)$$

Differentiation proves that equations (30) through (35) satisfy the general relation of Equation (14) provided A and B are considered as true constants. The result of this differentiation is as follows:

$$\left(\frac{\partial \log r_1}{\partial x_1} \right)_{x_1=0} = -\frac{2A^2}{B} \quad ; \quad \left(\frac{\partial \log r_2}{\partial x_2} \right)_{x_2=1} = 0$$

$$\left(\frac{\partial \log r_1}{\partial x_1} \right)_{x_1=1} = 0 \quad ; \quad \left(\frac{\partial \log r_2}{\partial x_2} \right)_{x_2=0} = -\frac{2B^2}{A}$$

However these "constants" are not constant even under the conditions for which the equation was derived as can be seen from Figures 1, 2, 3, 4, 5, 6, and 7. Figure 1 is a plot of the Van Laar constants A and B , which were calculated by use of Equations (32) and (33) on the isothermal data

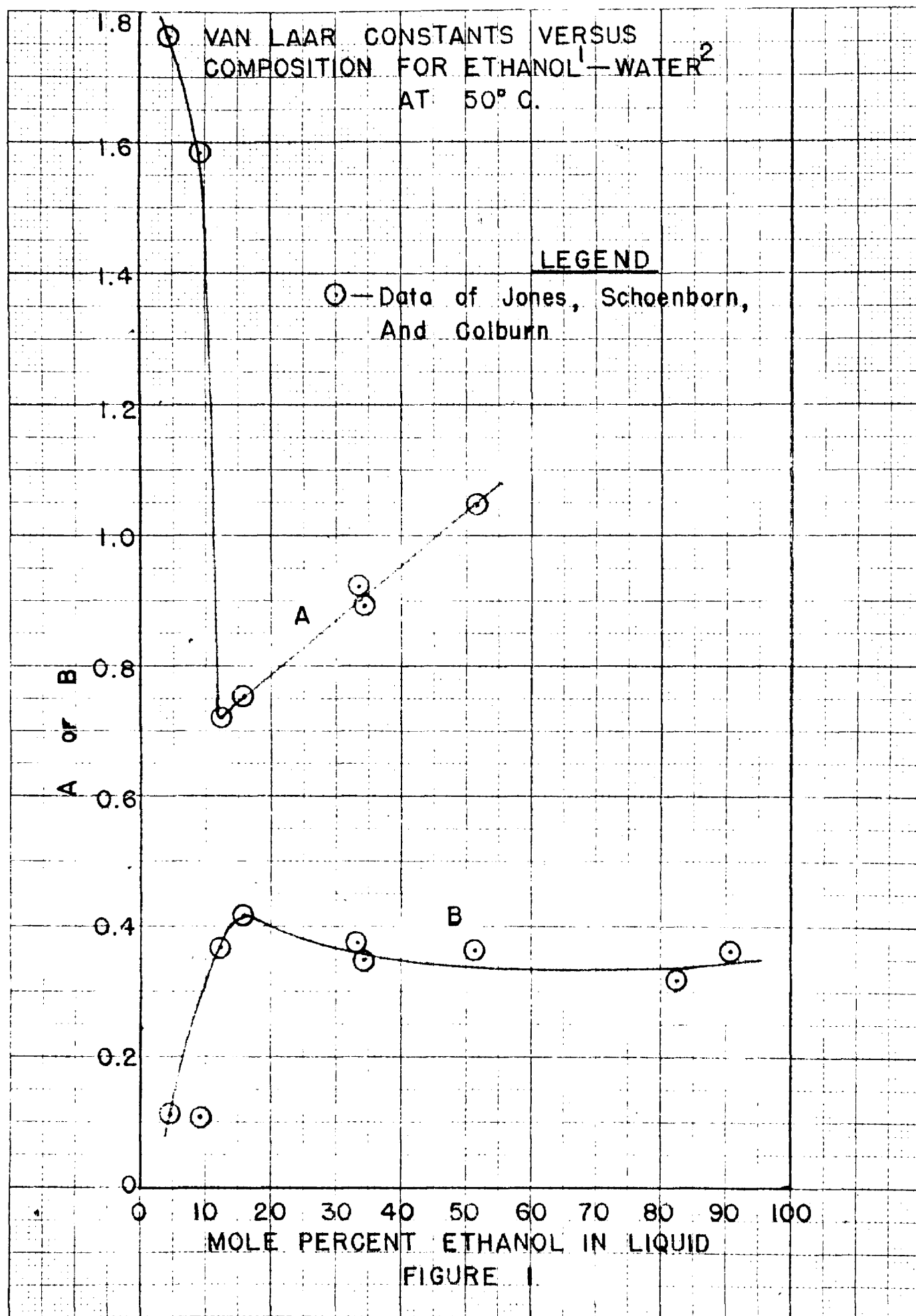


FIGURE 1.

ACTIVITY COEFFICIENT CURVES FOR ETHANOL¹—WATER² AT 50° C.

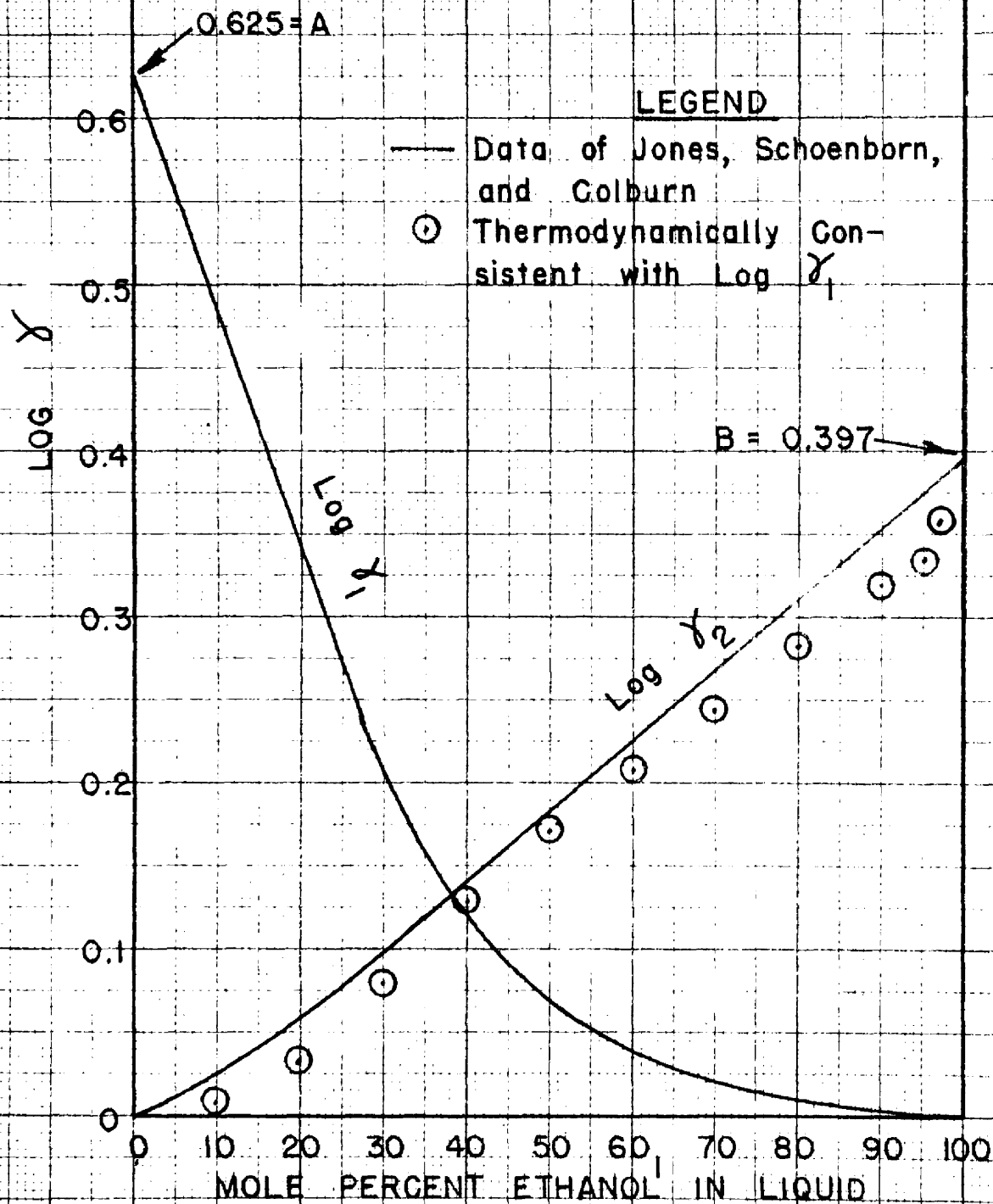


FIGURE 2

VAN LAAR CONSTANTS VERSUS
COMPOSITION FOR ETHANOL-WATER²
AT 760 mm. PRESSURE

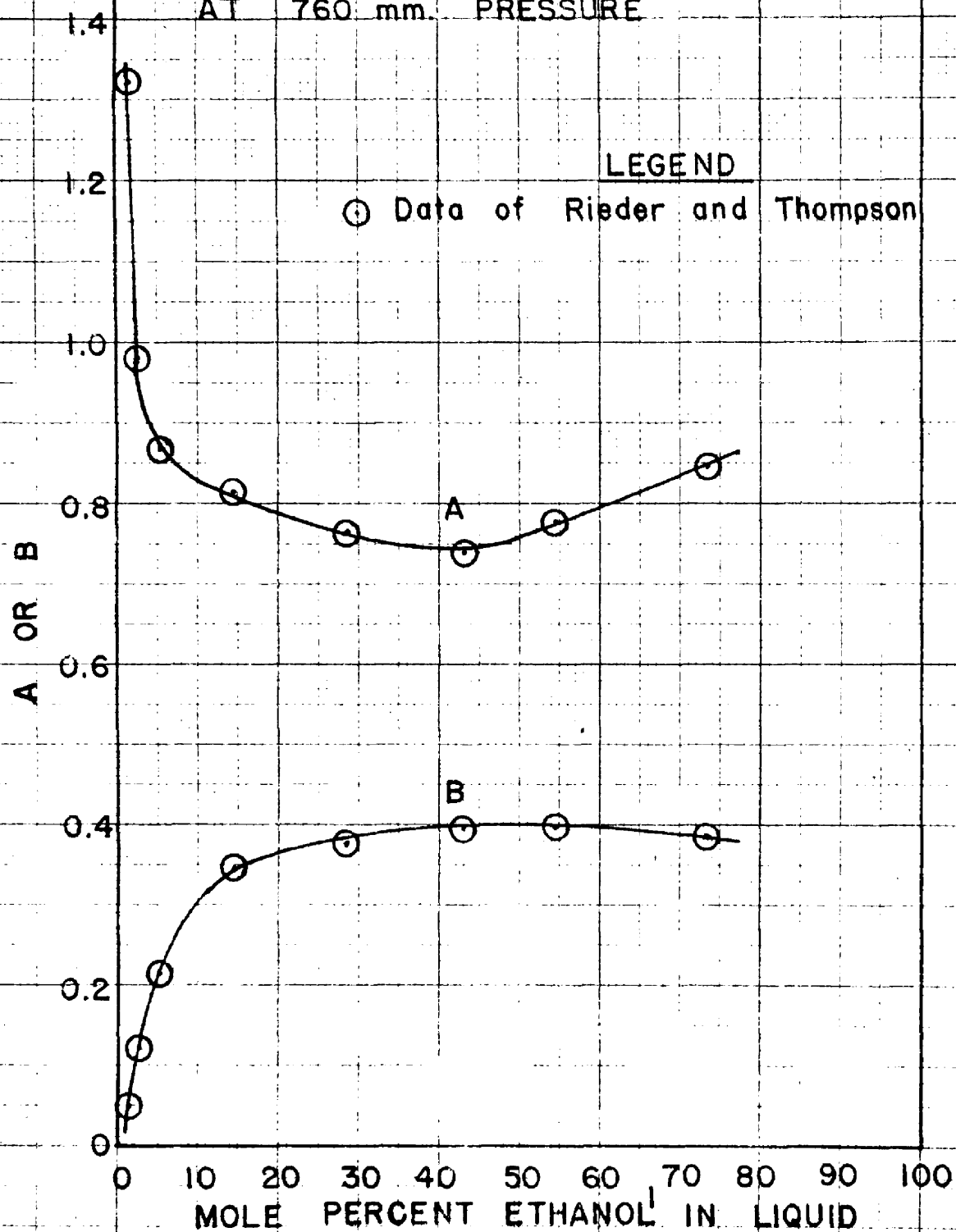


FIGURE 3

VAN LAAR CONSTANTS VERSUS
TEMPERATURE FOR ETHANOL¹—WATER²
AT 760 mm. PRESSURE

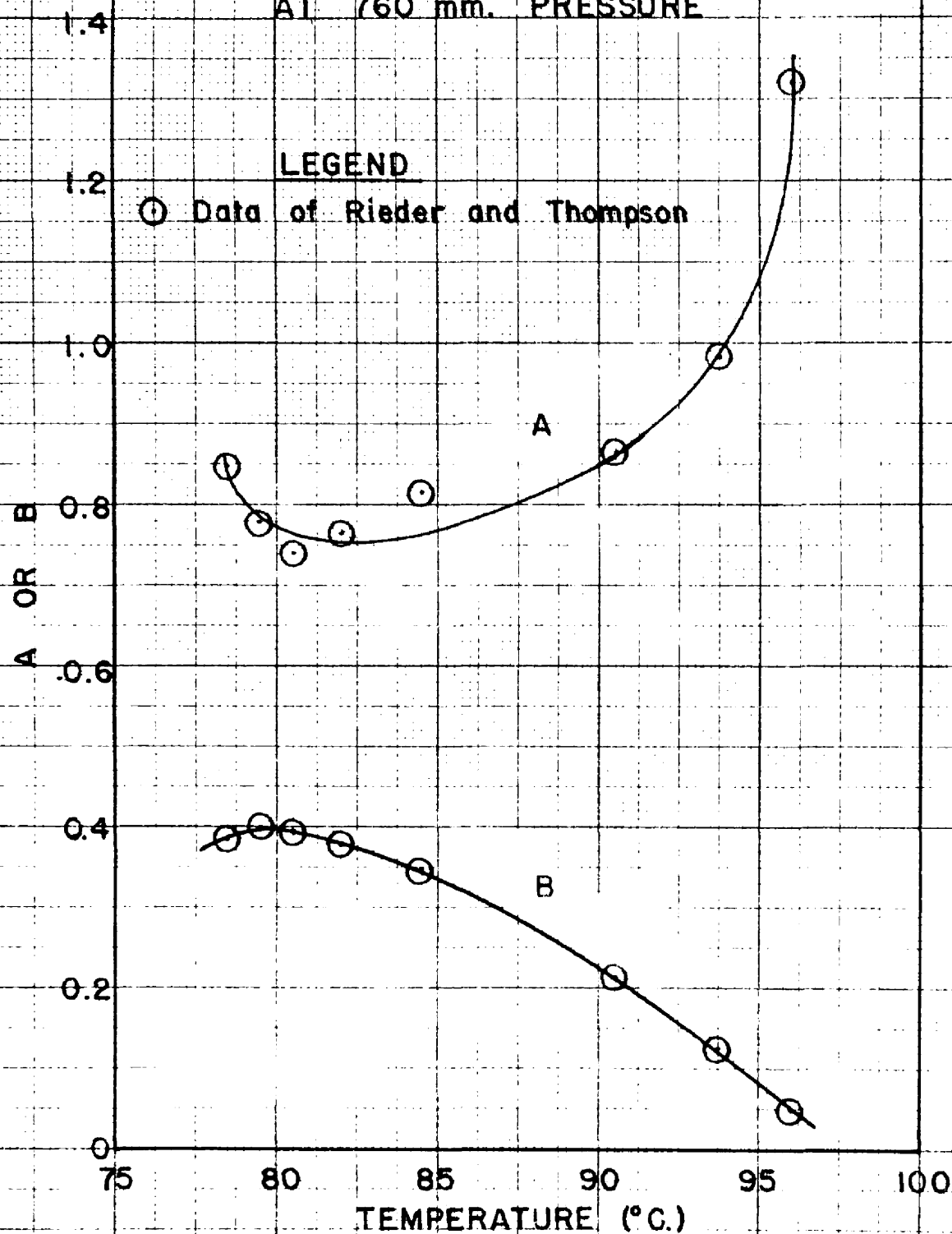


FIGURE 4

ACTIVITY COEFFICIENT CURVE FOR ETHANOL¹—WATER² AT 760 mm.

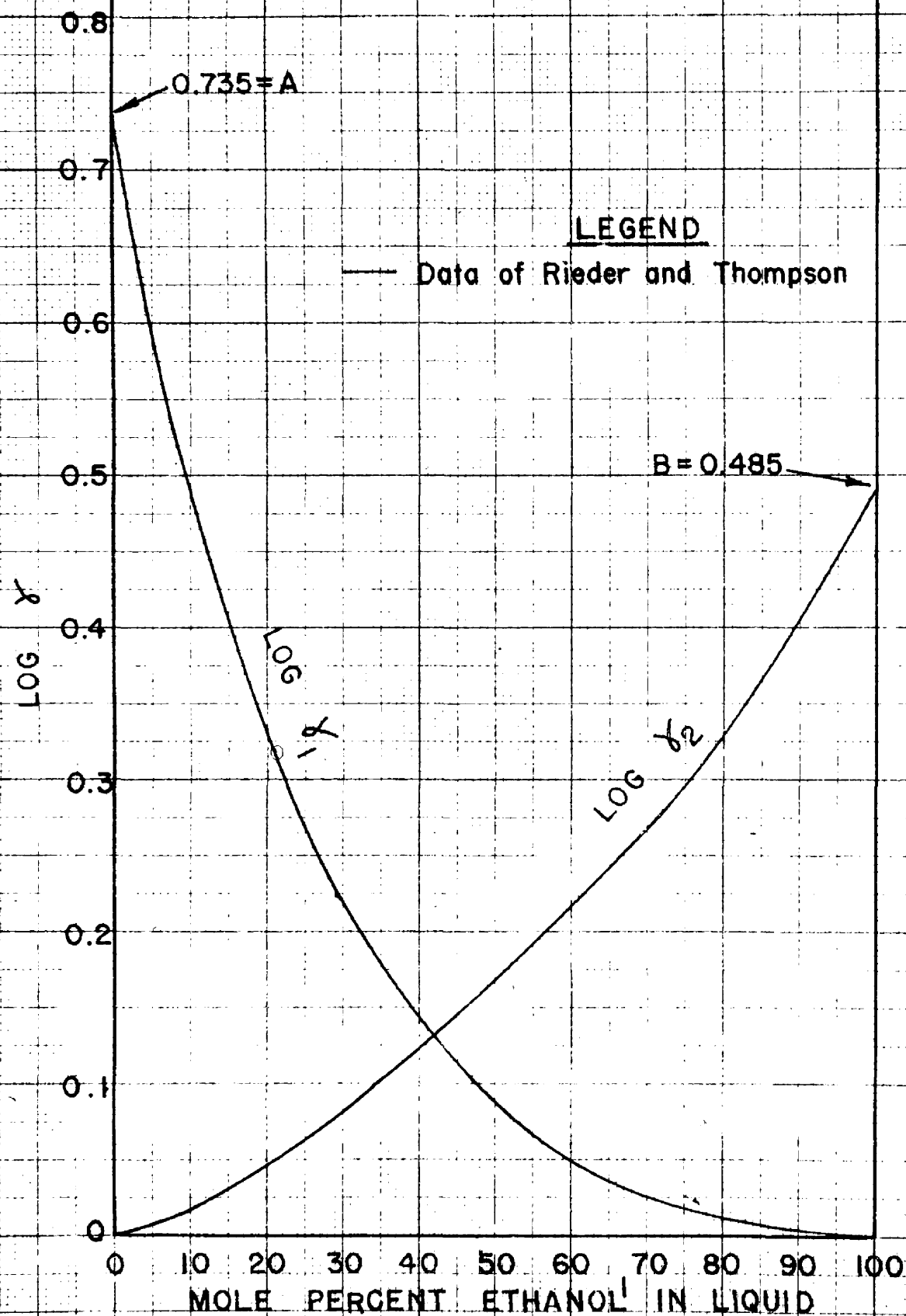


FIGURE 5

ACTIVITY COEFFICIENT CURVES FOR ETHANOL¹-CHLOROFORM² AT 45° C.

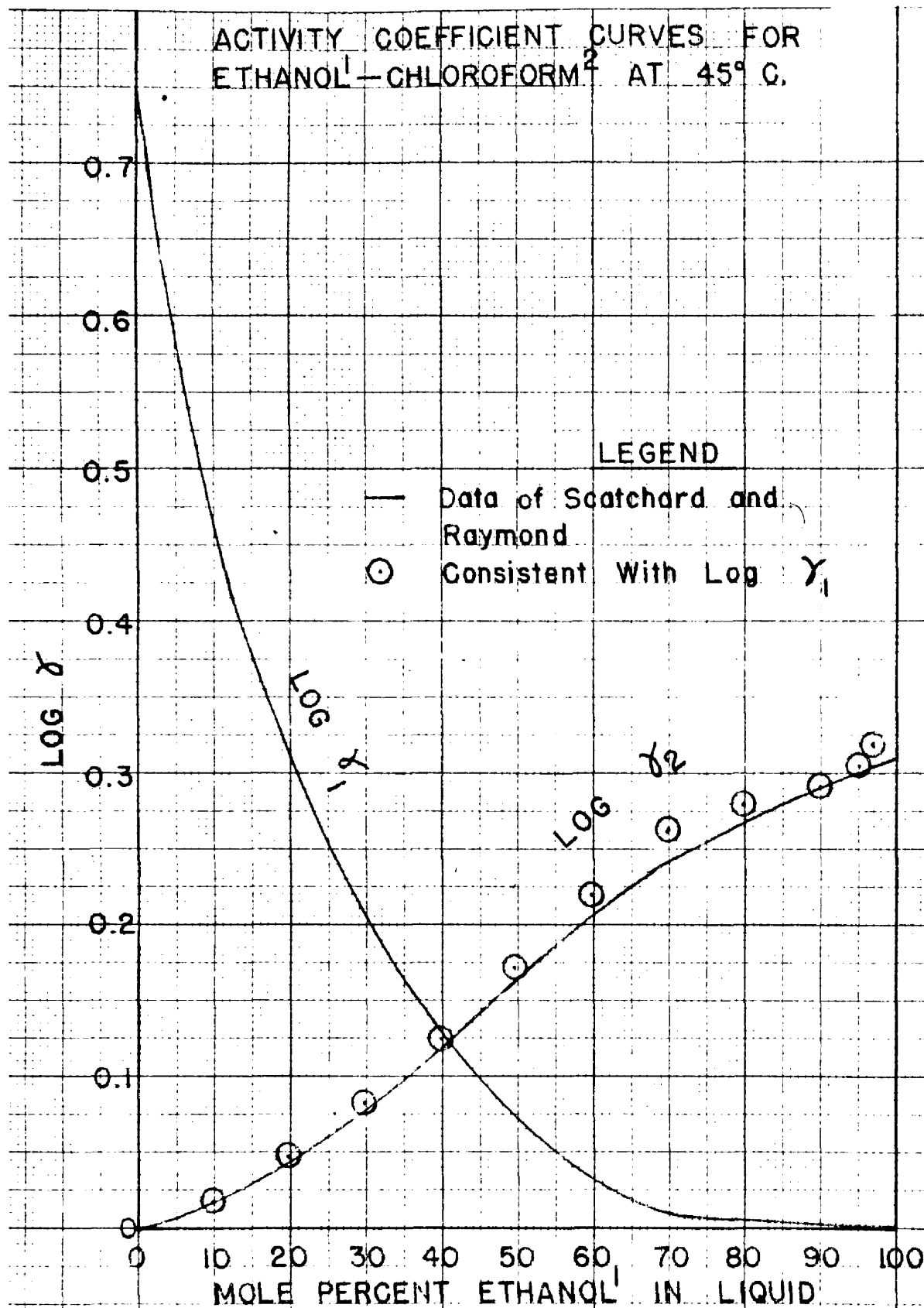
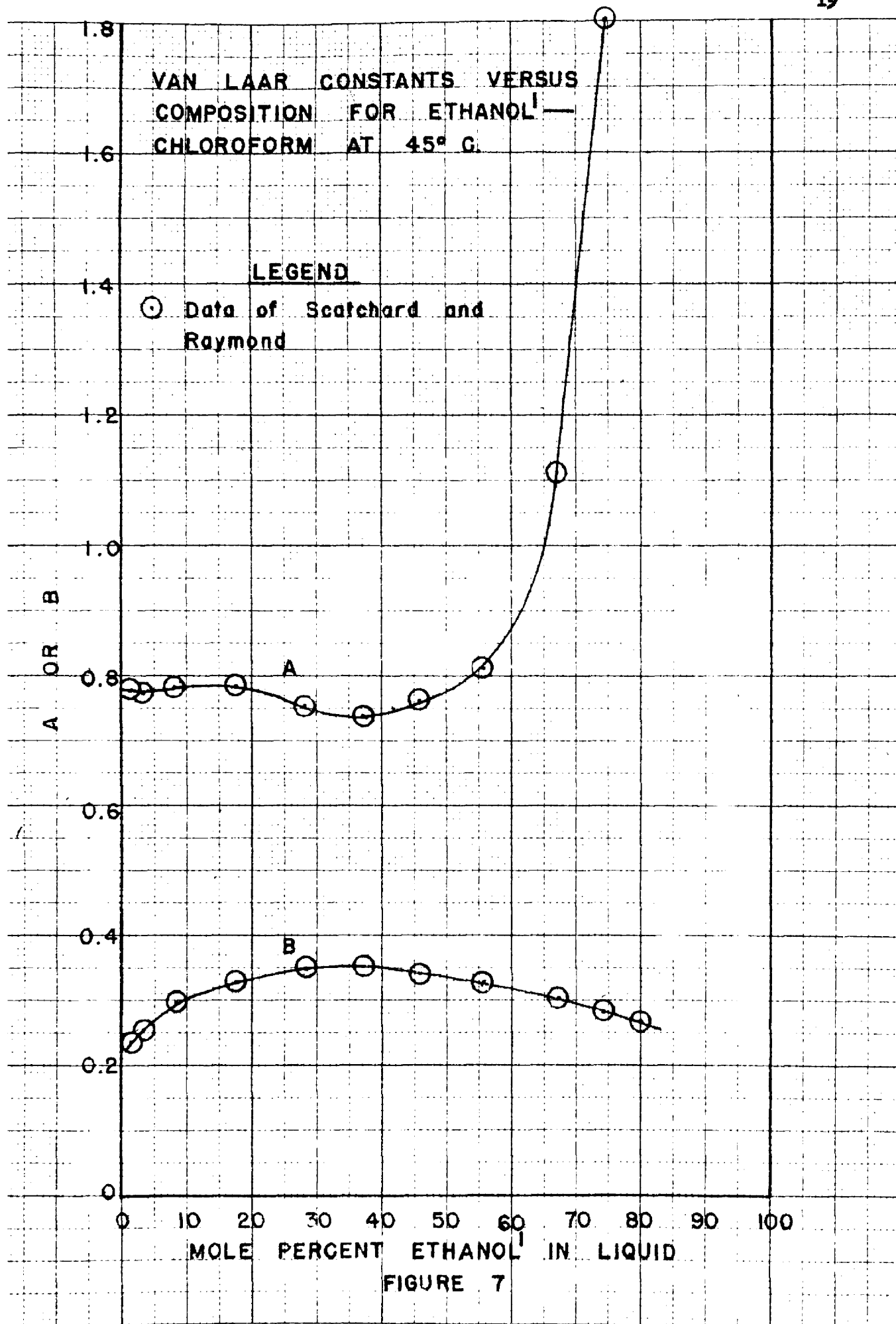


FIGURE 6



for Ethanol-Water of Jones, Schoenborn, and Colburn²² at 50° C., against mole percent Ethanol in the liquid. Figure 2 is a plot of logarithm of the activity coefficients against mole percent Ethanol in the liquid, and was inserted for purposes of comparison since Equations (30) and (31) show that $\log \gamma_1$ equals A at x_1 equal zero, and likewise $\log \gamma_2$ equals B at x_1 equal unity. The circles show what $\log \gamma_2$ should be if it were thermodynamically consistent with $\log \gamma_1$ according to the Gibbs-Duhem Equation. Figures 3 and 5 are similar plots for the constant pressure (760 millimeter) data of Rieder and Thompson³⁶ on the same system. The constants would be expected to vary here since the temperature varies from a low value of 78.15° C. to 100.00° C. In Figure 4 the constants are plotted against the temperature corresponding to the various liquid concentrations of Figure 3. Choice of any of the many possible values would lead to a poor data fit over some range of the concentrations which is undesirable, therefore these are approximations which should only be used in the absence of any but a minimum of experimental data. The highly precise data of Scatchard and Raymond⁴⁰ on Ethanol-Chloroform at 45° C. is shown in Figures 6 and 7. The circles show the data to be more thermodynamically consistent than the Ethanol-Water data, but the variations of the Van Laar constants is still evident.

If the validity of the Van Laar type equations is accepted, vapor-liquid equilibrium data can be calculated over the entire concentration range from a knowledge of one point. It is apparent from examination of Equation (1) that at the azeotropic point where $x = y$, the activity coefficients can be evaluated from a knowledge of the vapor pressure of the particular components at the azeotropic temperature together with the total

pressure. Using Equations (28) and (29) or (32) and (33) the constants A and B can be evaluated from a minimum of data. This method is quoted by Hougen and Watson¹⁷ as giving fair results when the azeotropic point lies between 0.25 and 0.75 mole fraction.

Kurt Wohl^{18,4} reviewed the foregoing methods and equations and has made recommendations as to which equation gives best results for various types of systems. His recommendations are as follows:

It is demonstrated that the usual Margules equation will be quantitatively useful mainly for systems of relatively small dissymmetry for which it is about equivalent with the usual Van Laar equation. The latter holds for many systems up to somewhat higher degrees of dissymmetry. When it does not fit the data it is suggested to use the three-suffix Scotchard and Hamer equation or, with special advantage in certain cases the four-suffix Van Laar equation. In cases of still higher dissymmetry in which the curve for the activity coefficient with the lower end value shows a maximum or a very flat course in the neighborhood of its end value, the three-suffix ϕ -equation may be applied. Still more useful will be the four-suffix Margules equation.

Benedict and his coworkers³ used an equation of the same type as Equation (23) together with curve fitting of experimental P-V-T data by the method of least squares to evaluate certain constants of the binary systems and then used these to evaluate ternary data composed of the three binary mixtures. They claimed that this circumvented the inaccurate assumptions of the Van Laar type equations.

Their expression relating the activity coefficient of any component to the vapor-liquid equilibrium compositions for the same component is a modification of Equation (9) based on the theory that the second coefficient of the virial equation of state is sufficient to express the deviations from the perfect gas laws. His equation is

$$\gamma_1 = \frac{\phi_1 \pi}{x_1 P_1 e^{\frac{(\pi - P_1)(\phi_1 - B_1)}{RT}}} \quad (36)$$

where v_1 is the molal volume of the liquid component 1 at the temperature and pressure of the solution, and B_1 is the second virial coefficient of the virial equation of state

$$PV = RT \left(1 + \frac{B}{V} + \frac{C}{V^2} + \dots \right) \quad (37)$$

where B and C are the virial coefficients and are functions of temperature. The additional term of Equation (35) corrects for the non-ideality of the gaseous phase and the effects of pressure on the liquid.

C. EFFECT OF TEMPERATURE ON ACTIVITY COEFFICIENTS

The equations developed by White⁵² from considerations of the Van der Waals equation of state for mixtures of gases included a temperature factor and are valid for low pressures only, if at all, since the Van der Waals equation of state is not adequate to express the behavior of most systems. His equations are

$$T \log \gamma_1 = \left[\frac{\frac{a_{21}}{b_1^{1.5}}}{\frac{x_1}{x_2} + \frac{b_2}{b_1}} \right]^2 \quad (38)$$

$$T \log \gamma_2 = \left[\frac{\frac{a_{12}}{b_2^{1.5}}}{\frac{x_2}{x_1} + \frac{b_1}{b_2}} \right]^2 \quad (39)$$

where constants "a" and "b" are the constants of the Van der Waals equation, $\left(P + \frac{a}{V^2} \right) (V - b) = RT$. By inspection it can be seen that these equations are equivalent to the usual Van Laar equations, if the temperature is constant. His equations are probably superior to the usual Van Laar equations for constant pressure data at low pressures since the temperature factor is taken into consideration. Theoretically it should be

possible to calculate these constants from the critical constants of the pure components, but according to White these methods are not reliable. In addition, the terms " a_{12} " and " a_{21} " are not sufficiently defined except that they are the Van der Waals constants for the mixture.

Partial differentiation of Equation (9b) with respect to temperature at constant composition yields

$$\left(\frac{\partial \ln \gamma_1}{\partial T}\right)_{X_1} = \left(\frac{\partial \ln f_1}{\partial T}\right)_{X_1} - \left(\frac{\partial \ln f_1^0}{\partial T}\right)_{X_1} \quad (41)$$

The change of fugacity with temperature and hence the right hand side of Equation (41) can be related to heat quantities by the method of Lewis and Randall²⁵ which yields an expression for the variation of activity coefficients with temperature.

$$\frac{\partial \ln \gamma_1}{\partial T} = \frac{(H_1^* - \bar{H}_1) - (H_1^* - H_1^0)}{RT^2} = - \frac{(\bar{H}_1 - H_1^0)}{RT^2} \quad (42)$$

where

H_1^* is the molal enthalpy of component 1 at the temperature of the solution but at a pressure sufficiently low that it behaves as an ideal gas.

\bar{H}_1 is the partial molal enthalpy of component 1 in the solution and at the temperature of the solution with respect to the same reference state as the molal enthalpy of the gas, H_1^* .

H_1^0 is the partial molal enthalpy of pure component 1 or at a state of infinite dilution with respect to component 2 referred to the same reference state as the molal enthalpy of the gas, H_1^* .

$(\bar{H}_1 - H_1^0)$ is the partial molal enthalpy relative to the pure components at the temperature of the solution or the differential heat of solution.

The differential heat of solution is described as that quantity of heat involved when one mole of the component is added to such a large quantity

of the solution that the overall concentration remains essentially constant. According to Hougou and Watson¹⁷ the use of Equation (42) for calculating the effects of temperature is complicated by the fact that values of $(H_1 - H_1^0)$ vary considerably with temperature and are rarely known over any extensive range.

Jones, Scheenborn, and Colburn²² attempted to compare the theoretical effect of temperature as defined by Equation (42) to the experimentally determined deviations of activity coefficients or more specifically to Van Laar constants with temperature for the system Ethanol-Water. The results were inconclusive partly due to the narrow temperature range (50° C. to 60° C.) studied and partly due to the lack of reliable heat of solution data. In reality it seems more logical to determine heat of solution data from activity coefficient data since the latter are more easily and reliably determined.

Among the more recent attempts at correlation of the effects of temperature on activity coefficients is that of Berg and McKinnis⁴ who developed a purely empirical relation in straight line form at constant composition

$$\left[\log \gamma \right]_x = K \frac{(1 - T_R)^{0.43}}{T_R} \quad (43)$$

where

K is an empirical constant.

T_R is the reduced temperature of the solution, T/T_c solution.

A plot of $\log \gamma$ at constant composition versus $\frac{(1 - T_R)^{0.43}}{T_R}$ should be a straight line with a slope of K and an intercept of zero. This intercept will be zero because at the critical point of a solution the

properties of liquid and vapor are indistinguishable giving an activity coefficient of unity whose logarithm is zero. At the same time the T_R function is zero because T_R is unity at the critical point. However when this function was tested on experimental data only one of the systems presented by the authors gave a straight line in accordance with Equation (41). It is believed that if the temperature range of this system was extended to the lower temperatures it would show curvature also. Obviously a correlation of this type is not very beneficial if extrapolation over a relatively wide range of temperatures is not possible without extensive experimental data.

Mertes and Colburn²⁸ called the term $\frac{1}{C} \frac{(\pi - P_1)(T_c - T_1)}{RT}$ of the Benedict equation " Z_1 ", a correction factor. Scheibel⁴¹ presented an empirical method of calculating values of Z as a function of the vapor pressure, critical pressure, and critical temperature of the pure component and the total pressure on the system. The equation is

$$\ln Z_1 = \frac{P_1 - \pi}{P_c} \left[f(T_R) - \frac{0.197}{T_R} + 0.012 + \frac{0.400}{T_R^2} + \frac{0.146}{T_R^{4.27}} \right] \quad (44)$$

where P_1 is the vapor pressure of component 1, π is the total pressure, P_c is the critical pressure of component 1, and T_R is the reduced temperature T/T_c for component 1. It is somewhat involved so a nomograph was presented for rapid evaluation. This correction is important at higher pressures, but is also significant when differences between the boiling points of the components of the mixture are large so that one or more of the components will be present in the liquid at a temperature considerably different from its own boiling point.

An approximate method for estimating the effect of temperature on azeotropes is given by Carlson and Colburn⁶. It is assumed that the ratio of activity coefficients γ_1/γ_2 is independent of temperature at a given concentration. Then from Equation (10) at the azeotropic concentration where $x_1 = y_1$,

$$\left(\frac{\gamma_1}{\gamma_2}\right)_{a_3} = \frac{P_2^*}{P_1^*} \quad (45)$$

Then by plotting γ_1/γ_2 against x_1 from data at a known temperature and on the same scale as γ_1/γ_2 plot P_2^*/P_1^* against temperature, the azeotropic concentration can be found that will give the same value for the ratio γ_1/γ_2 as P_2^*/P_1^* at any temperature desired.

The following empirical equation may then be used to estimate the total pressure corresponding to the azeotropic concentration estimated by the preceding method:

$$P_{a_3} = P_{a_3}' \frac{(x_1 P_1 + x_2 P_2)}{(x_1' P_1' + x_2' P_2')} \quad (46)$$

where

P_{az}, P_1, P_2 --vapor pressures of the azeotrope, component 1, and component 2 at temperature t .

P_{az}', P_1', P_2' --vapor pressures of the azeotrope, component 1, and component 2 at the temperature t' .

x_1, x_2 --mole fractions of components 1 and 2 in the azeotrope at temperature t .

x_1', x_2' --mole fractions of components 1 and 2 in the azeotrope at temperature t' .

From the azeotrope compositions and pressures estimated in this manner corresponding constants for the Van Laar equation may be gotten from Equations (32) and (33). In this way activity coefficient and

vapor-liquid compositions may be estimated over limited ranges of temperatures and pressures. This method has not been sufficiently explored to estimate the errors involved, but they would seem to be many and serious in view of the assumptions involved. Inspection of experimental data from the literature shows that γ_1/γ_2 at constant composition is not independent of temperature. However, if Equation (45) were modified using Equation (36), it can be seen that

$$\left(\frac{\gamma_1}{\gamma_2}\right)_{a_3} = \left(\frac{P_2}{P_1}\right)_{a_3} \left(\frac{Z_2}{Z_1}\right)_{a_3}. \quad (47)$$

An extension of this idea to the method of Carlson and Colburn just presented might be of value in estimating more correctly the effect of temperature on azeotropes.

D. OTHER CORRELATIONS

Gilmont and co-workers²⁵ presented a method of correlating vapor-liquid equilibrium data by relating the relative volatility,

$$\alpha_{12} = \frac{y_1 x_2}{x_1 y_2}$$

to composition by use of an empirically determined power series. Their claim is that this method eliminates the necessity of knowledge of total pressure for isothermal data or boiling points for constant pressure data. Whatever virtues the method might possess are overshadowed by the fact that it is purely empirical, tedious, and it departs from the fundamental equilibrium concepts.

Redlich and Kister³⁵ in a review of the thermodynamics of non-electrolyte solutions developed a method of algebraic representation of

activity coefficient data based on the excess free energy, F^E , of Seatchard as defined by Equation (17). For one mole of mixture, the following can be written:

$$\frac{F^E}{2.303 RT} = x_1 \log \gamma_1 + (1-x_1) \log \gamma_2 \quad (48)$$

If the left side of Equation (48) is termed Q and differentiated with respect to x_1 , one obtains

$$\frac{dQ}{dx_1} = \log \frac{\gamma_1}{\gamma_2} \quad (49)$$

Since according to Equation (48) Q equals zero at x_1 equal zero or unity

$$\int_0^1 dQ = \int_0^1 \log \frac{\gamma_1}{\gamma_2} dx_1 = 0 \quad (50)$$

The authors then developed suitable power series of mole fractions of the more volatile component to represent the data and satisfy the foregoing requirements. An extension of this method to ternary systems was presented.

This method permits smoothing of experimental data when calculated in the form $\log \frac{\gamma_1}{\gamma_2}$ since in accordance with Equation (50) the positive and negative areas of a plot of $\log \frac{\gamma_1}{\gamma_2}$ versus x_1 must be equal.

The power series is again an empirical method and a digression from the fundamental thermodynamic relations involved.

E. CONCLUSIONS

In the foregoing discussion it has been shown that the methods used in the past to correlate vapor-liquid equilibrium data have some serious limitations brought about by unjustified assumptions in development of the methods, applications under conditions where they are not valid, or

complete obscuring of the subject by purely empirical methods which are useless without extensive experimental data. In no case has a broadly applicable method been presented to accurately relate the variations encountered in studies of non-ideal liquid solutions with properties easily determined.

It appears to the author that it would be better to confine the considerations of the subject to the original fundamental relationships and use these directly rather than use the numerous empirical methods presented which have overstressed the idea of referring everything to the ideal system by use of correction factors.

The following equation is proposed for correlation of activity coefficients and vapor-liquid equilibrium. The component parts of the equation are not new ideas, but the arrangement of the equation and the method of application is different and more direct than the methods previously presented.

Equation (9b) can be written for each component of a binary mixture as follows:

$$\gamma_1 = \frac{f_1}{\chi_1 f_1^0}$$

$$\gamma_2 = \frac{f_2}{\chi_2 f_2^0}$$

The fugacities f_1 , f_1^0 , f_2 , and f_2^0 can be evaluated from a knowledge of the total pressure of the system, temperature of the system, and properties of the pure components as outlined by Hougen and Watson¹⁷.

The evaluation of these fugacities involves the assumption that the fugacity coefficient as determined from reduced temperature and pressure

generalized charts is correct.

The fugacity of each component f_1 , or f_2 , in solution is given by

$$\begin{aligned} f_1 &= \sqrt{\pi_1} \pi y_1 \\ f_2 &= \sqrt{\pi_2} \pi y_2 \end{aligned} \quad (51)$$

where

$\sqrt{\pi}$ - the fugacity coefficient of each component evaluated from the generalized charts of Hougen and Watson at reduced temperatures corresponding to the temperature of the solution and reduced pressure corresponding to the total pressure, π .

π - total pressure.

y - the mole fraction of each component in the vapor which is in equilibrium with the liquid of interest.

By use of Equation (7) the fugacity, f_0 , for each component as a pure liquid at the temperature and pressure of the solution can be evaluated. Equation (7) can be rearranged to the form

$$\begin{aligned} f_1^0 &= f_{P_1} e^{\frac{V_{m_1}(\pi - P_1)}{RT}} \\ f_2^0 &= f_{P_2} e^{\frac{V_{m_2}(\pi - P_2)}{RT}} \end{aligned} \quad (52)$$

where all terms were previously defined. The fugacity of the pure liquid under its own vapor pressure at the temperature of the system, f_p , is evaluated by use of the fugacity coefficient as read from the generalized chart at a reduced temperature corresponding to the temperature of the solution and a reduced pressure corresponding to the vapor pressure of the pure component at that temperature. Then

$$f_{P_1} = \sqrt{P_1} P_1 \quad (53)$$

Substitution of all these values in Equation (9b) gives

$$\gamma_1 = \frac{\sqrt{\pi_1} \pi y_1}{x_1 f_{P_1} e^{\frac{V_{m_1}(\pi - P_1)}{RT}}} \quad (54)$$

$$\gamma_2 = \frac{\sqrt{\pi_2} \pi y_2}{x_2 f_{P_2} e^{\frac{V_{m_2}(\pi - P_2)}{RT}}}$$

and dividing γ_1 by γ_2 yields

$$\frac{\gamma_1}{\gamma_2} = \frac{y_1 x_2 f_{P_2} \sqrt{\pi_1} e^{\frac{V_{m_2}(\pi - P_2)}{RT}}}{y_2 x_1 f_{P_1} \sqrt{\pi_2} e^{\frac{V_{m_1}(\pi - P_1)}{RT}}} \quad (55)$$

Taking the logarithm of both sides and grouping like terms

$$\log \frac{\gamma_1}{\gamma_2} = \log \frac{y_1 x_2}{y_2 x_1} + \log \frac{f_{P_2}}{f_{P_1}} + \log \frac{\sqrt{\pi_1}}{\sqrt{\pi_2}} + \frac{V_{m_2}(\pi - P_2)}{2.303 RT} - \frac{V_{m_1}(\pi - P_1)}{2.303 RT} \quad (56)$$

The following observations can be made about Equation (56):

(1) $\log \frac{\gamma_1}{\gamma_2}$ becomes equal to $\log \gamma_1$ at $x_1 = 0$, since γ_2 is unity at that point, and similarly $\log \frac{\gamma_1}{\gamma_2} = -\log \gamma_2$ at $x_1 = 1.0$.

(2) At some value of x_1 , $\gamma_1 = \gamma_2$ and $\log \frac{\gamma_1}{\gamma_2} = 0$.

(3) At the azeotropic point $x_1 = y_1$ and $x_2 = y_2$, hence

$$\log \frac{y_1 x_2}{x_1 y_2} = 0 \text{ at that points.}$$

(4) It should be noted that $\frac{y_1 x_2}{x_1 y_2}$ is the relative volatility, α

and the limit of $\log \frac{y_1 x_2}{x_1 y_2}$ as x_1 approaches zero is of the

indeterminate form $\log \frac{0}{0}$.

According to L'Hospital's Rule

$$\lim_{\substack{x_1 \rightarrow 0 \\ y_1 \rightarrow 0}} \log \frac{y_1 x_2}{y_2 x_1} = \lim_{\substack{x_1 \rightarrow 0 \\ y_1 \rightarrow 0}} \log \frac{d \left[\frac{y_1 x_2}{y_2 x_1} \right]}{d x_1}$$

if it exists.

Hence

$$\lim_{\substack{x_1 \rightarrow 0 \\ y_1 \rightarrow 0}} \log \frac{y_1 x_2}{x_1 y_2} = \lim_{\substack{x_1 \rightarrow 0 \\ y_1 \rightarrow 0}} \log \frac{\frac{d y_1}{d x_1} - x_1 \frac{d y_1}{d x_1} - y_1}{1 - y_1 - x_1 \frac{d y_1}{d x_1}}$$

making the substitution $x_2 = (1-x_1)$ and $y_2 = (1-y_1)$.

By Henry's Law for dilute solutions at or very near $x_1 = 0$.

$$y_1 = K x_1$$

$$\left(\frac{d y_1}{d x_1} \right)_{x_1=0} = K$$

This value, K , is the slope of the x - y diagram at $x_1 = 0$. Substitution gives

$$\lim_{\substack{x_1 \rightarrow 0 \\ y_1 \rightarrow 0}} \log \frac{y_1 x_2}{x_1 y_2} = \lim_{\substack{x_1 \rightarrow 0 \\ y_1 \rightarrow 0}} \log \frac{K - K x_1 - y_1}{1 - K x_1 - y_1} = \log K$$

A line with a slope equal to this limit drawn through $x_1 = 0$ should be used as a guide to the approach of the equilibrium curve to the zero point on the x - y diagram.

(5) According to the development of Redlich and Kister

$$\int_0^1 \log \frac{\delta_1}{\delta_2} = 0$$

(6) All the terms on the right side of the equation except

$\log \frac{y_1 x_2}{x_1 y_2}$ can be calculated from a knowledge of the properties of the pure component coupled with knowledge of the temperature and total pressure of the system.

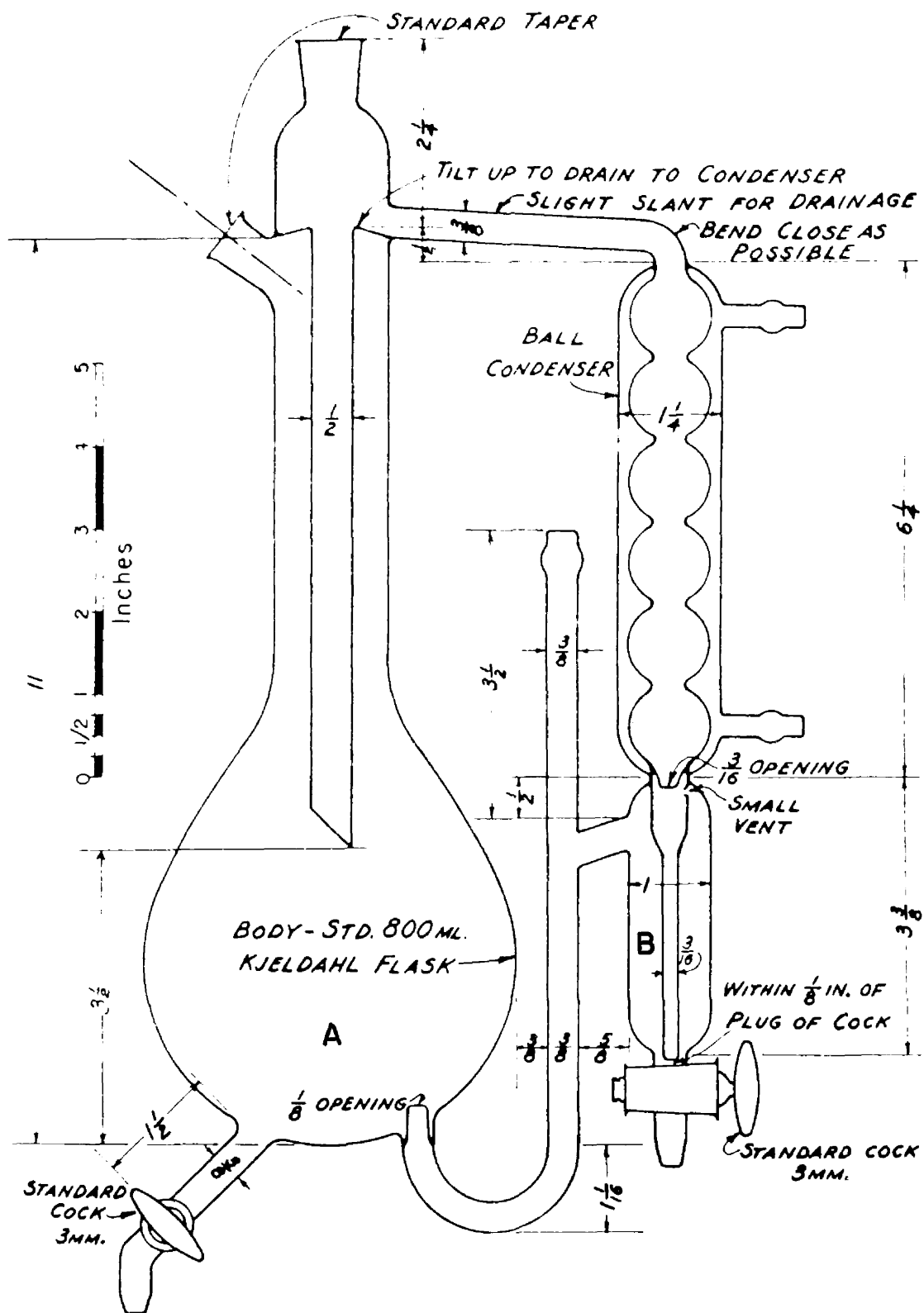
CHAPTER III

AN EQUILIBRIUM STILL FOR PARTIALLY MISCIBLE LIQUIDS

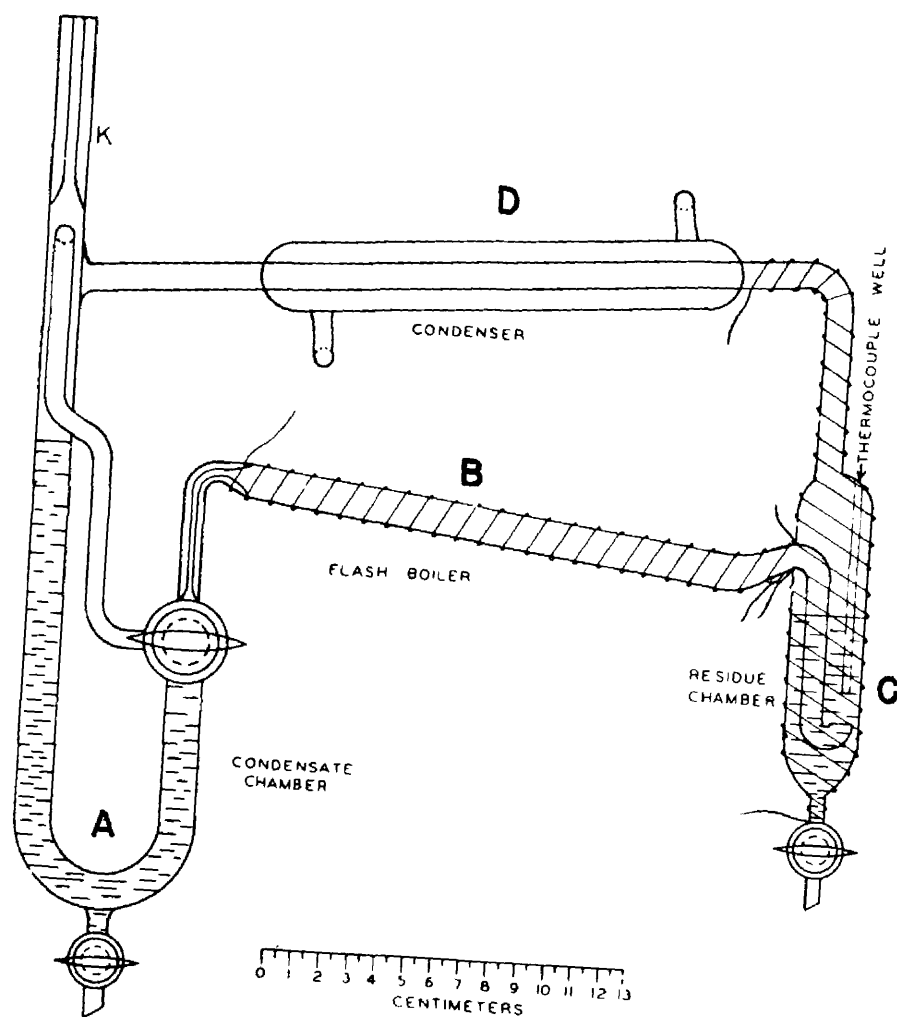
A. RESUME¹ OF PREVIOUS DESIGNS

The object of all vapor-liquid equilibrium stills is to obtain for analysis sufficient samples of vapor and liquid which are in equilibrium. Making such determinations is not easy and to obtain reliable values requires a highly developed laboratory technique. There are several methods for experimentally determining vapor-liquid equilibria, but the most widely used and generally most satisfactory method is by circulating the vapor through a system and repeatedly contacting it with the liquid. Circulating type stills fall into two categories: (a) those in which the vapor is generated from the boiling liquid and subsequently condensed and returned as liquid to the body of the boiling liquid, or (b) those in which the vapor is generated elsewhere in the system and subsequently contacted in the vapor state with the liquid, then recirculated.

Those stills that fall into category (a) are best illustrated by the well-known Othmer still which is shown schematically in Figure 8. This type of recirculating still has two serious drawbacks in that the vapor leaving the surface of the liquid (A) may not be in equilibrium with the main body of the liquid in the still. Also since the liquid being returned from the condensate trap (B) is different in composition from the liquid in the boiler, it might flash due to its lower boiling point unless mixing is instantaneous.



OTHMER STILL
FIGURE 8



JONES, SCHOENBORN, AND COLBURN STILL

FIGURE 9

The still of Jones, Schoenborn, and Colburn²² was one of the first of the type defined by Category (b). This still is schematically shown in Figure 9 where a liquid representing the composition of the vapor flows from the condensed vapor receiver (A) to the flash vaporizer (B) where it is totally vaporized before bubbling through the liquid in chamber (C). The vapors are then condensed in condenser (D) and recirculated. This type still seems to satisfactorily circumvent the undesirable characteristics of category (a), but care must be exercised to prevent superheating of the vapor bubbling through the liquid, refluxing after it leaves the liquid, and entrainment of the liquid with the vapor passing through.

There are two major difficulties encountered in studies of partially miscible systems in addition to those usually inherent in equilibrium stills. The first is that the vapor from any but the most dilute samples will, on condensing, form an immiscible mixture. Therefore the recirculation type of apparatus has not been used in the past for immiscible mixtures, since the condensate on separating into two layers cannot be returned to the still with the two liquid layers in proper proportion. While a stirrer might be utilized there may be some question with the usual types of stirrers as to whether or not mixing was thorough enough to cause the heterogeneous mixture to act like a homogeneous phase. Tests conducted by this investigator under circumstances very similar to those encountered in equilibrium stills, showed that the two phases could not be satisfactorily circulated after even the most thorough agitation with laboratory type stirrers.

Stockhardt and Hull⁴⁷ eliminated recirculation merely by distilling off small quantities from a large quantity of a mixture of known composition after first refluxing in a tilting condenser arrangement, but this method involves slight errors caused by differential condenser hold-up, and in addition encounters the second major difficulty discussed below.

The second undesirable characteristic offered by these partially miscible systems lies in the great difference in composition between the vapor and liquid in the miscible region and the small concentrations of the dilute component in the liquid. For example in the miscible region of *n*-butanol in water, Figure 16, which extends to about two mole percent *n*-butanol, the vapor is from fifteen to thirty times as rich in *n*-Butanol as the liquid. Therefore, if an equilibrium study is undertaken where a liquid sample is distilled, its composition with respect to the dilute component will change very rapidly and arrival at the desired steady state conditions in the still is virtually impossible.

The still proposed by Smith and Bonner⁴⁴ with minor variations such as a magnetic agitator, and fixed sample take-off device seems essentially the same in principle as that of Stockhardt and Hull and with the same inherent errors. They found the vapor evolved from the boiling liquid to be appreciably superheated, so the boiling points reported were taken on an ebulliometer independent of the vapor-liquid equilibrium determinations.

Colburn, Schoenborn, and Shilling⁷ proposed a still where vapor was generated from separate boilers of pure components and mixed in the vapor state to form a mixture of the desired composition. The amounts of vapor generated from each boiler was controlled by the heat input to each.

This vapor was bubbled through the liquid which changed to the equilibrium composition. The vapor was condensed on leaving and analyzed. This still set-up is not advantageous regardless of the accuracy of the results obtained because of the large consumption of reagents which are very difficult and expensive to obtain in any quantity in a sufficiently pure state for vapor-liquid equilibrium measurements.

Norman²⁹ presented a modification of this design whereby two streams of solution were mixed in any predetermined ratio and totally vaporized giving a vapor of a certain concentration depending on the ratio in which the two solutions were charged. As in the still of Colburn, Schoenborn, and Shilling the vapor was bubbled through the liquid and subsequently condensed. This has the disadvantage of being a batch operation where the liquid has only a limited time in which to come to equilibrium. However, it has the advantage of not requiring great quantities of pure reagents as the resulting condensed vapor even if it is partially miscible can be reused as feed solution.

The still of Colburn, Schoenborn, and Shilling as well as that of Norman had a very good thermal insulation feature. They utilized a jacket surrounding the liquid equilibrium chamber through which the vapor feed must pass before entering the liquid chamber. This gives automatic insulation at approximately the correct temperature since any heat loss will merely condense some of the vapor which is easily removed or re-vaporized. This also prevents appreciable superheating of the vapors entering the liquid chamber.

B. DESIGN OF THE NEW TYPE OF STILL

Since all the stills previously proposed for determination of vapor-liquid equilibrium data of partially miscible systems have certain limitations and disadvantages as previously mentioned as well as not being of a suitable design to permit work at pressures greater than slightly above atmospheric, it was thought to be of considerable importance to improve on these designs. The nature of this investigation was such that a still capable of operating at pressures considerably above atmospheric was desired so that a wide range of temperatures could be included in the investigation.

Griswold, Andres, and Klein¹⁵ presented a high pressure recirculation type still for miscible mixtures whereby the pressure in the still was controlled by the rate of heat input and the rate of coolant circulation in the condensers. This new still resembles their design only in that the materials of construction are the same, it is a recirculation type still, and the rate of coolant circulation to the condenser is intended to control the pressure within the still.

Figure 10 is a detailed drawing of the new design, and Figures 11 and 12 show the external appearance of the original design. The most important differences in this still and any still proposed thus far are: (1) It is a recirculation still of the type described under category (b), utilizing a centrifugal pump with a large by-pass line as an agitation chamber and as a condensed vapor receiver which should give complete mixing. (2) It combines the good features of the Colburn, Schoenborn, and Shilling type and Norman type stills with the very important advantages of continuous operation over any period of time desired with use of a

VAPOR-LIQUID EQUILIBRIUM STILL
FOR IMMISCIBLE LIQUIDS

DRAWN BY: GRR SCALE: 1/2" = 1" FEBRUARY 10, 1950

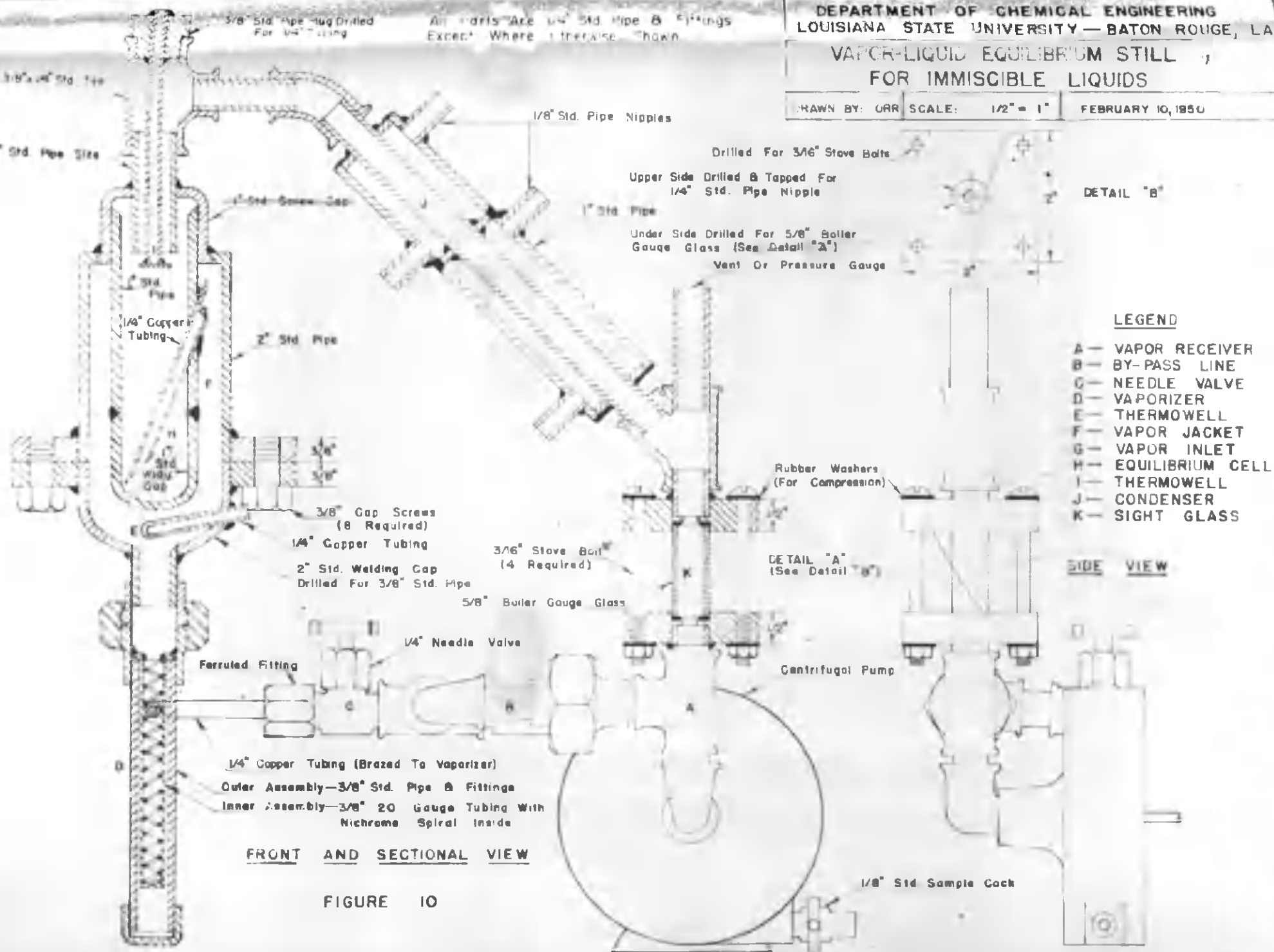
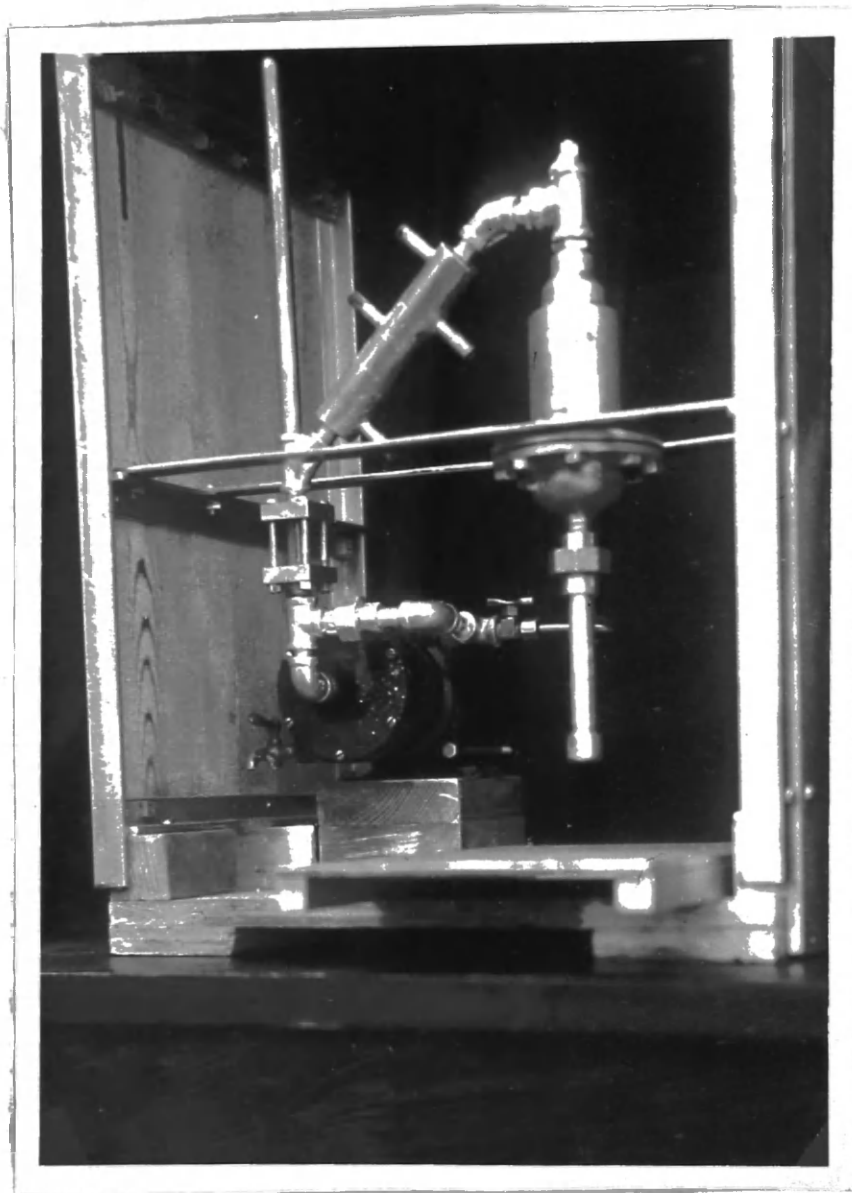


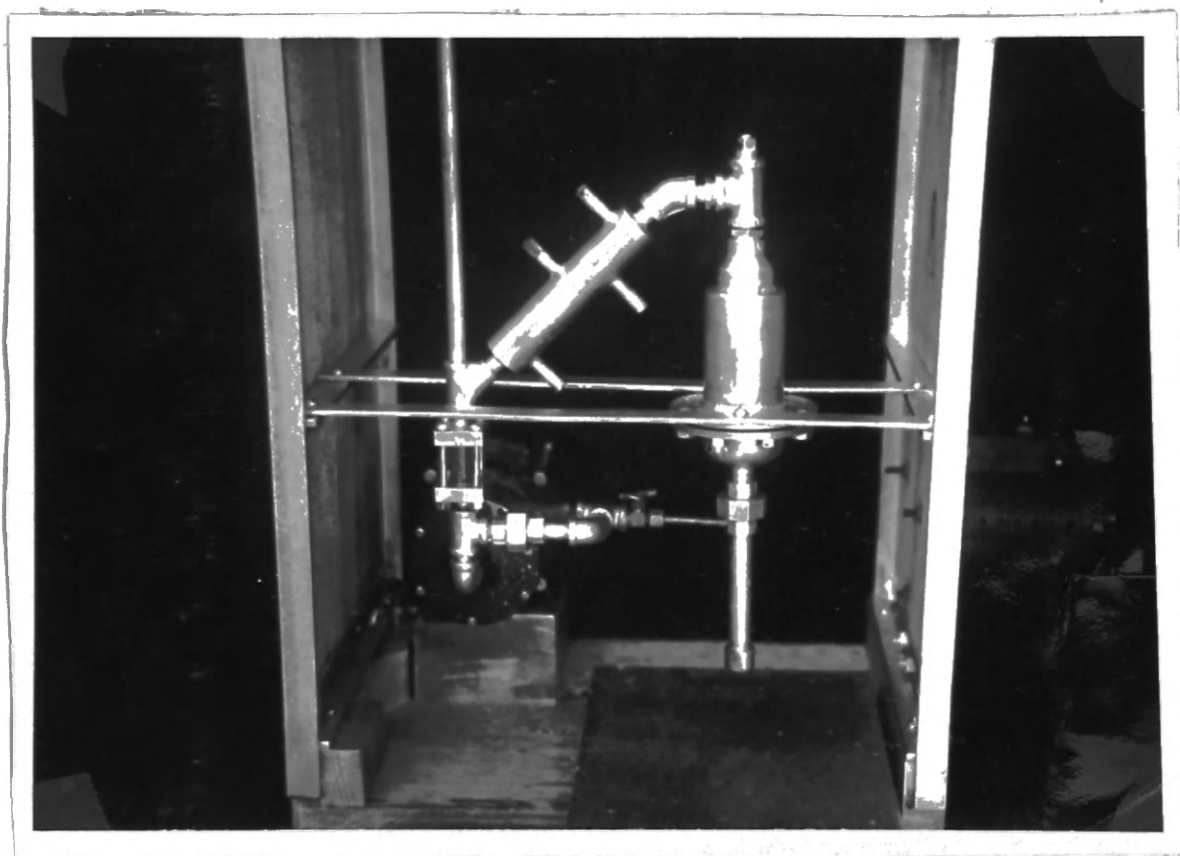
FIGURE 10



OBLIQUE VIEW OF ORIGINAL DESIGN

FIGURE 11





FRONT VIEW OF ORIGINAL DESIGN

FIGURE 12

definite small quantity of reagents.

The condensed vapor receiver (A) is a bronze centrifugal pump with explosion proof motor manufactured by the Eastern Centrifugal Pump Company. This particular pump is equipped with a packing gland specially designed by the pump manufacturer to permit pumping of alcohols. The materials handled during this investigation are primarily alcohols and water, the only exception being n-hexane. A mechanical seal was used at first, but failed due to lack of sufficient liquid head to keep the seal lubricated and cooled. A relatively large by-pass line (B) is used on the pump to permit continuous circulation and agitation of the condensed heterogeneous vapor while the desired quantity is withdrawn and fed to the total vaporizer (D) through the needle valve (C). This needle valve constitutes a major control device during the operation of the still.

The vaporizer is constructed of three-eighths inch standard pipe and fittings with a section of twenty gauge three-eighths inch copper tubing forming a concentric cylinder inside thus forcing the incoming liquid downward around the hot wall, where it is vaporized. The vapor rises through the center of the tubing where the nichrome spiral picks up superheat from the vapor and transfers it back to the cold entering liquid through the tubing wall. The heat is furnished by resistance ribbon externally wound through which a controlled current is passed. The current is controlled with a "Variac" controller. As the vapor leaves the vaporizer its temperature is measured by thermocouple (E) before passing through the adiabatic jacket feature (F) to enter the liquid chamber (H) by bubbling in through tube (G).

As the vapor bubbles through the liquid there is material transfer until such time as the liquid and vapor compositions have come to the equilibrium values. The temperature of the equilibrium vapor leaving the liquid is measured by the thermocouple (I) before passing to the condenser section (J). Both thermocouple (E) and (I) are specially calibrated copper-constantan couples connected by a double pole, double throw switch to common leads which are connected to a Leeds and Northrup, Type "K" potentiometer capable of determining voltages to 0.00001 volts. Both cold junctions were immersed in a melting ice bath as a reference point.

The condensed vapor then passes back to the condensed vapor receiver. The sight glass (K) is provided to observe the operation of the still. During the atmospheric pressure runs the still was vented through a condenser connected to the Y above the sight glass as shown in Figure 10. The vent condenser was used to prevent vapor losses from the still. During pressure runs a pressure gauge and vent replaced the condenser as seen in Figure 13.

This particular model was constructed of standard pipe size, schedule 40 iron pipe and fittings wherever possible. Copper tubing and ferruled fittings found application in the feed tube from the needle valve to the vaporizer, thermocouple wells, inside tube of the vaporizer, and inlet to the liquid chamber. The sight glass is five-eighths inch boiler gauge glass mounted in special flanges as shown in details "A" and "B" in Figure 10.

Corrosion presented some problem, but this factor could be eliminated by proper choice of metals of construction depending on the type of system

to be studied. Stainless steel would probably be satisfactory for most systems. A cheaper construction with a silver plated interior might also be expected to be satisfactory.

Any nonvolatile material that might have been left in the vapor receiver had a tendency to be deposited in the vaporizer by the pump and was taken out of either of the samples to be analyzed. This permitted sufficiently good analyses to get reliable data on the systems studied.

Assembly of the equilibrium chamber body is possible by a flange assembly welded to the outer jacket and machined so as to form a smooth pressure and leak tight joint with a suitable solvent resistant gasket. The flanges are joined by eight three-eighths inch cap screws. The inner equilibrium chamber is easily inserted by screwing into the cap at the top of the vapor jacket. Thermowell (I) is easily removed for charging or sampling.

This construction is of a simple and rugged nature which is a distinctly desirable characteristic for equilibrium stills since most are of some intricate glass design and must be prepared by an experienced glass blower. Since the material used is metal the usual problem of breakage is not a major one.

C. OPERATING PROCEDURE AND CHARACTERISTICS

The operating procedure and characteristics are included since the development of the still was not considered complete until it was shown that its mechanical operation was satisfactory and that it would give reliable data on both miscible and immiscible liquid systems.

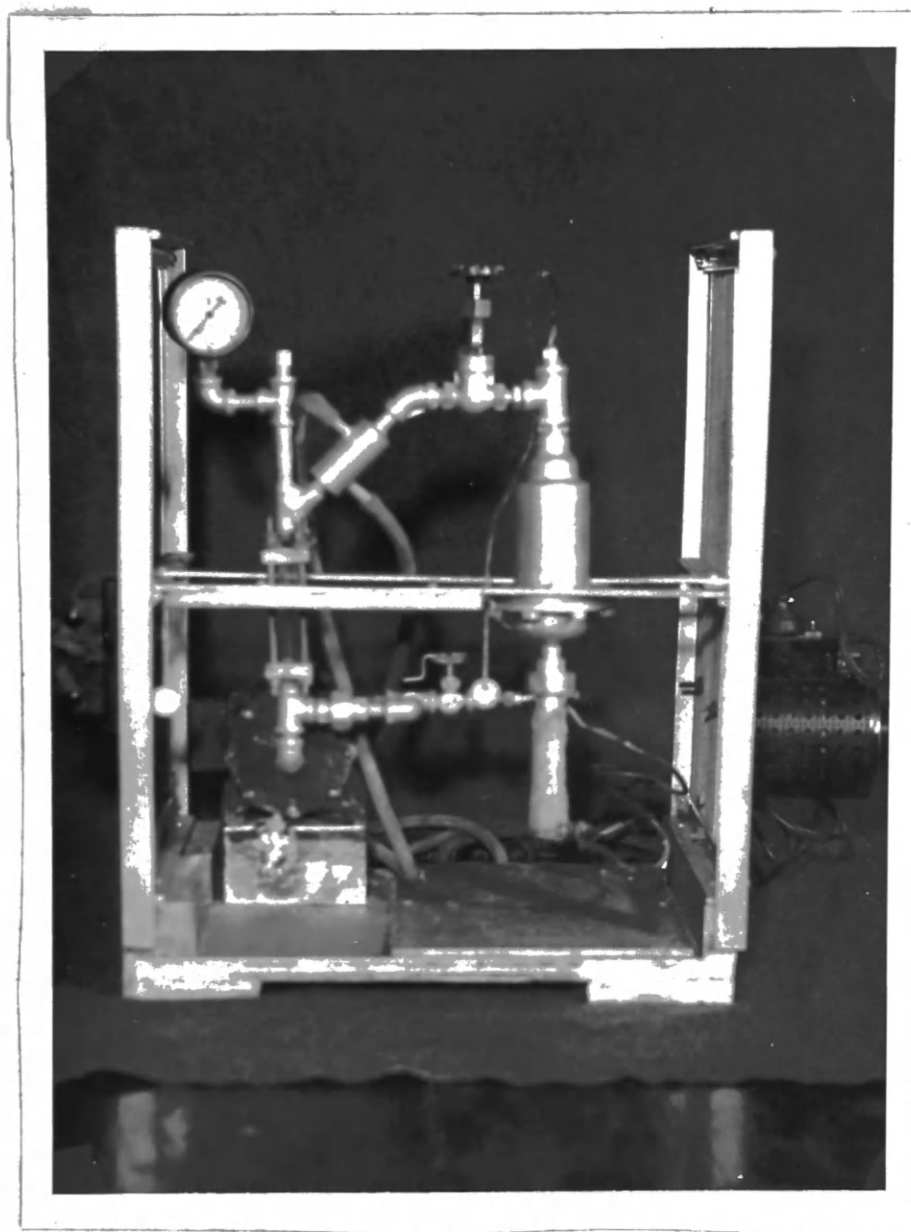
To set the still in operation for the runs at atmospheric pressure a sample of the mixture to be studied was charged to the condensed vapor receiver in a quantity sufficient to bring the level into the sight glass with the needle valve closed and the pump running. Similarly a suitable sample was charged to the liquid chamber by removing the thermowell (I). Current was then applied to the vaporizer until it became sufficiently hot to vaporize any feed from the condensed vapor receiver. The coolant flow was started to the condenser section and the needle valve opened one quarter to one half turn and subsequently adjusted to hold the level in the vapor receiver approximately constant. This level will change slightly until such time as equilibrium is attained, and there is not further material transfer as the vapor passes through the liquid sample.

The temperatures at points E and I were checked and the current to the heater regulated so that the temperature at point E was never higher than at point I, but so that all material entering was still completely vaporized as indicated by a constant level in the condensed vapor receiver. Once these simple adjustments were made the still was allowed to operate until constancy of the temperature at point I indicated there was no further change in composition of the mixture in the equilibrium chamber. An additional period of operation was allowed to be sure equilibrium was reached. At this time the temperatures were read and recorded and the samples were withdrawn for analysis. If the operation was on partially miscible liquids and in the range of concentration where the liquid separated into two phases it was necessary to analyze only the vapor sample since the vapor corresponding to any two phase liquid sample should be the same.

For the runs above atmospheric pressure it was found necessary to modify the apparatus slightly as shown in Figures 13 and 14 by inserting a one-quarter inch gate valve (L) just after the liquid chamber in the vapor line so that the two samples could be isolated after a run. This was necessitated when the liquid sample was found to flash into the condensed vapor receiver on reduction of the pressure previous to withdrawing the samples at the end of the run. This valve was added at the expense of the condenser section which was much larger than necessary in the original design. As a result of this change it was necessary to increase the length of the sight glass. The substitution of the pressure gauge and vent for the condenser at the vent point for the atmospheric work had been anticipated.

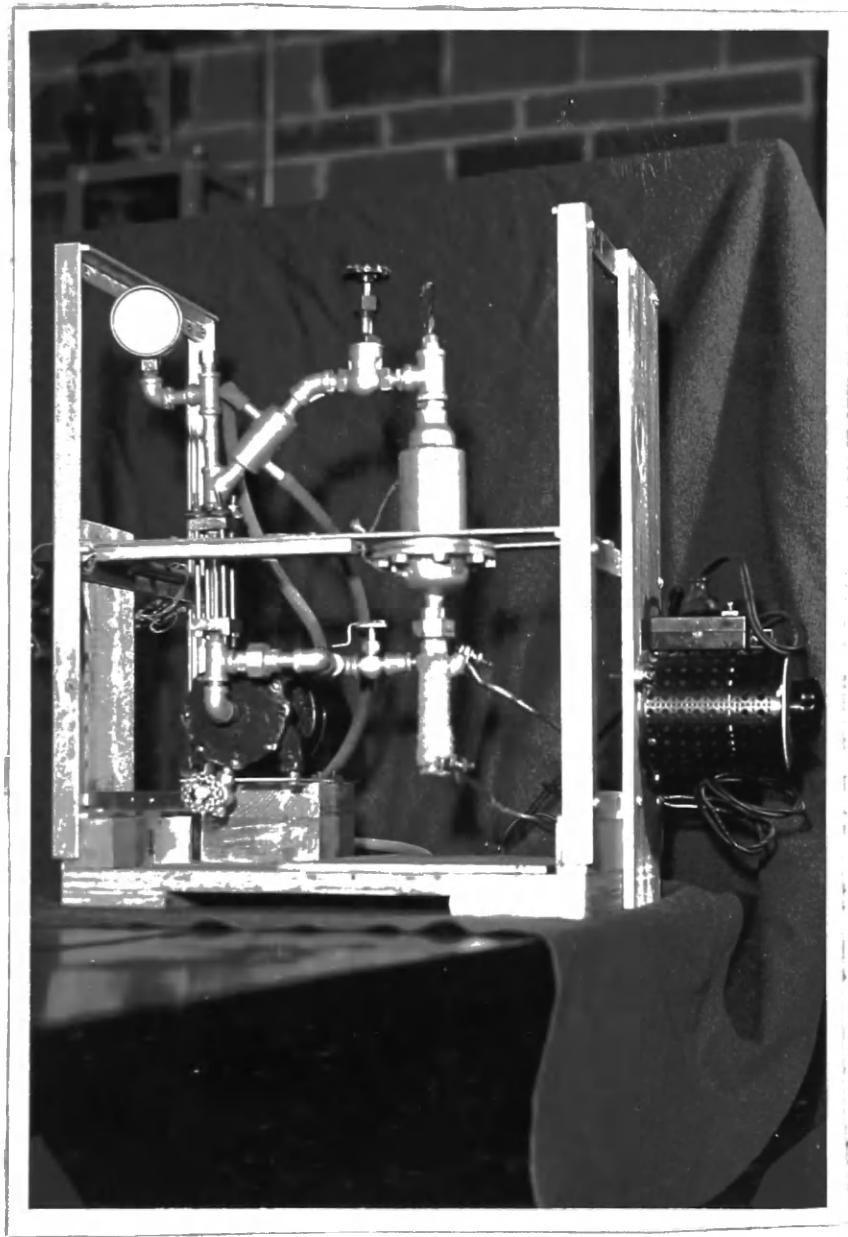
It was also found necessary to cool the contents of the pump a slight degree to eliminate vapor locking at the pump intake. This was done by the crude but effective method of wrapping a towel wet with cold water around the by-pass line and pump intake line.

Operation was begun exactly as for atmospheric operation with the vent open. When the still was operating satisfactorily under atmospheric pressure the condenser coolant was stopped. In this manner the still was filled with vapor forcing the air out through the vent. When vapor had escaped for a short while the vent was closed and the pressure allowed to build up to the desired value by proper adjustment of the current input to the vaporizer and rate of circulation from the condensed vapor receiver. When the pressure reached the desired value the coolant was again started and the rate of circulation adjusted to maintain this value. The rate of condensation of the vapors filling the still controlled the



FRONT VIEW OF MODIFIED STILL

FIGURE 13



OBLIQUE VIEW OF MODIFIED STILL

FIGURE 14

pressure within the still. This method of pressure control is advantageous over pressurizing with an inert gas since the pressure-temperature relations are more likely to be correct and the solubility of inert gas increases with increased pressure.

The coolant was water maintained at a temperature slightly lower than room temperature by a refrigerating type constant temperature bath. The water was pumped by a centrifugal pump giving constant flow and regulation of the flow was by a screw clamp choke on the line to the condenser.

The criteria for equilibrium were the same as for the atmospheric run, at which time the needle valve (O) and the gate valve (L) were simultaneously closed and the power to the vaporizer removed. This action isolated the two samples. When they had cooled sufficiently to reduce the pressure, the samples were removed as before for analysis.

D. PROOF OF THE EQUILIBRIUM STILL

Although the still was specifically designed to handle partially miscible systems it should work equally as well on miscible systems. To test the performance of the still, the miscible system Ethanol-Water was chosen as representative with results of many investigations being available in the literature. The most recent of these is that of Rieder and Thompson³⁶ whose data at atmospheric pressure check with that previously determined. They present smoothed values based on their own data. These values are represented by the solid line of Figure 15 for comparison with the experimental points obtained on the still being tested. By reference to Figure 15 and Table I it can be readily seen the agreement is good throughout the concentration range.

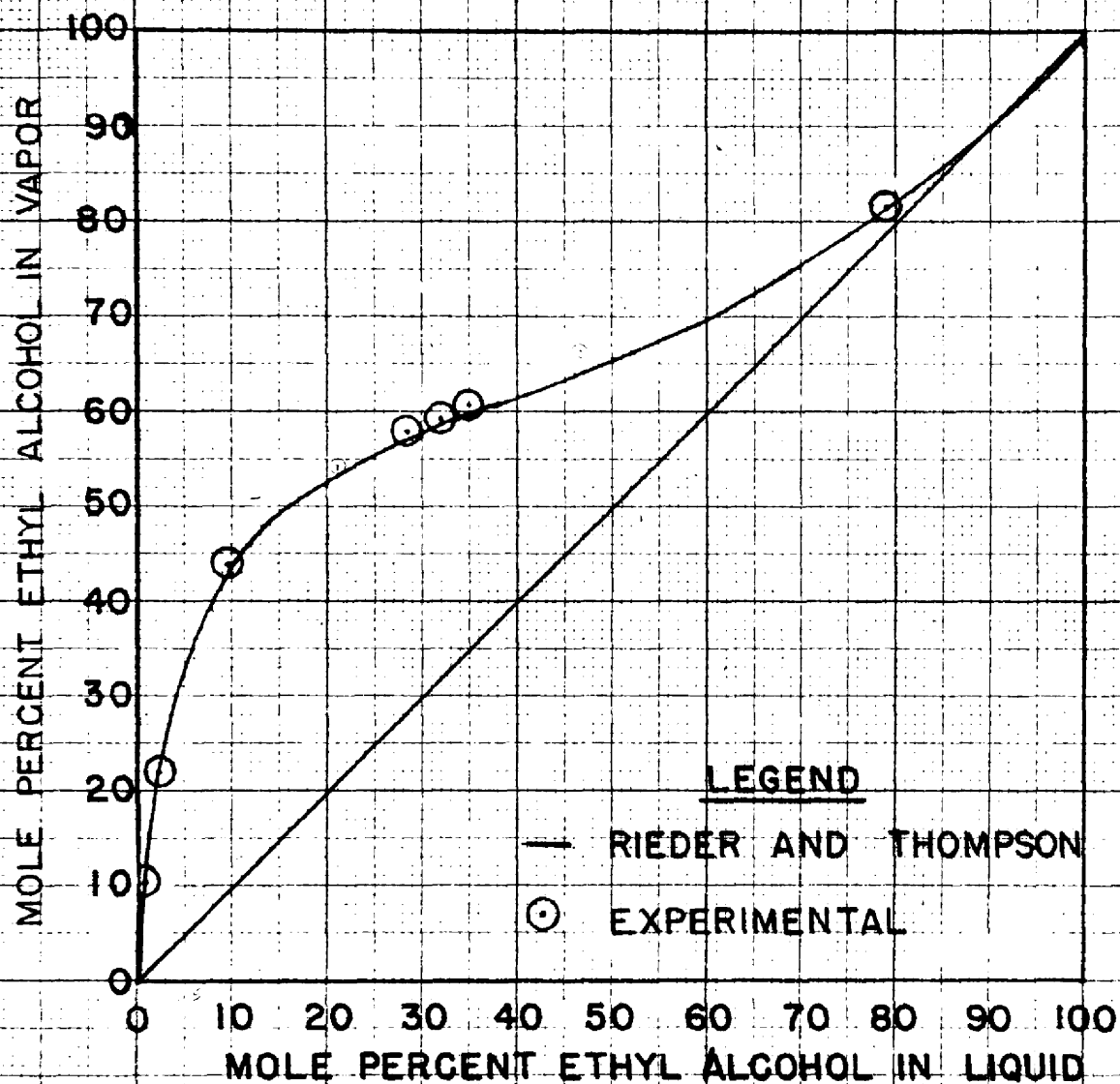


FIGURE 15

VAPOR-LIQUID EQUILIBRIUM DIAGRAM FOR
ETHANOL-WATER AT 760 mm. PRESSURE

TABLE I
EXPERIMENTAL DATA ON ETHYL ALCOHOL-WATER AT ATMOSPHERIC PRESSURE

<u>Temperature (° C.)</u>	<u>Mole Percent Ethanol</u>	
	<u>Liquid</u>	<u>Vapor</u>
97.7	0.60	10.5
94.5	2.26	22.1
87.0	9.5	44.0
81.8	28.3	58.3
81.5	32.0	59.5
81.0	35.0	60.7
78.4	79.0	81.3

The n-Butyl Alcohol-Water system, which has been the subject of investigation by Stockhardt and Hull⁴⁷ and more recently by Smith and Bommer⁴⁴, was chosen as being representative of the partially miscible systems. Their data are shown in Figure 16 and Tables III and IV and compared with the data from the new still as shown in Table II and Figures 16, 17, and 18. As can be seen, the agreement is very good throughout the region for which the apparatus was designed--that region where the vapor and liquid separate into two phases.

The deviations noted in the range of high concentration of n-Butanol will be explained later by a statistical analysis, and it is firmly believed this deviation is not attributable to the equilibrium still but to the method of analysis as will be discussed later.

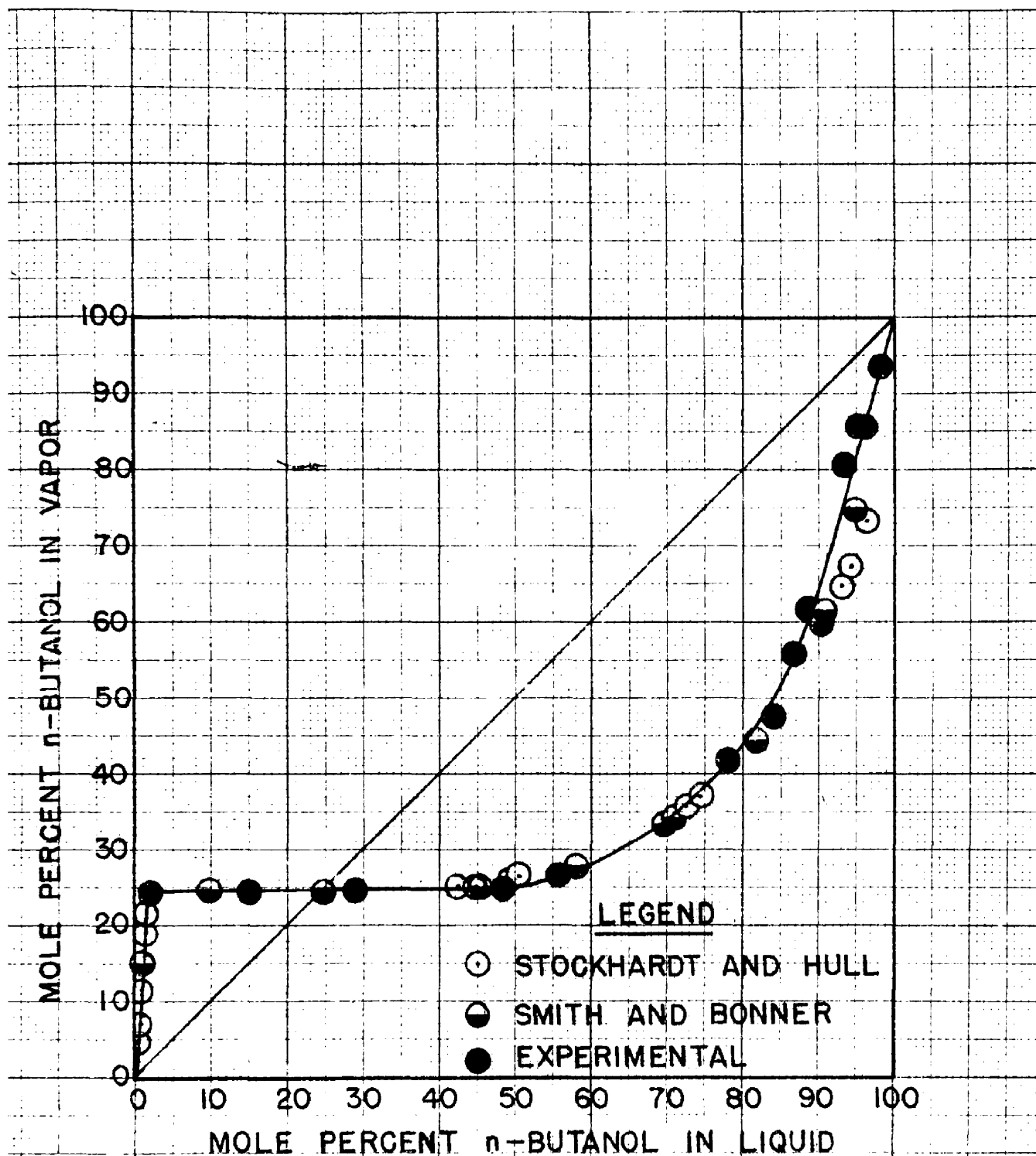
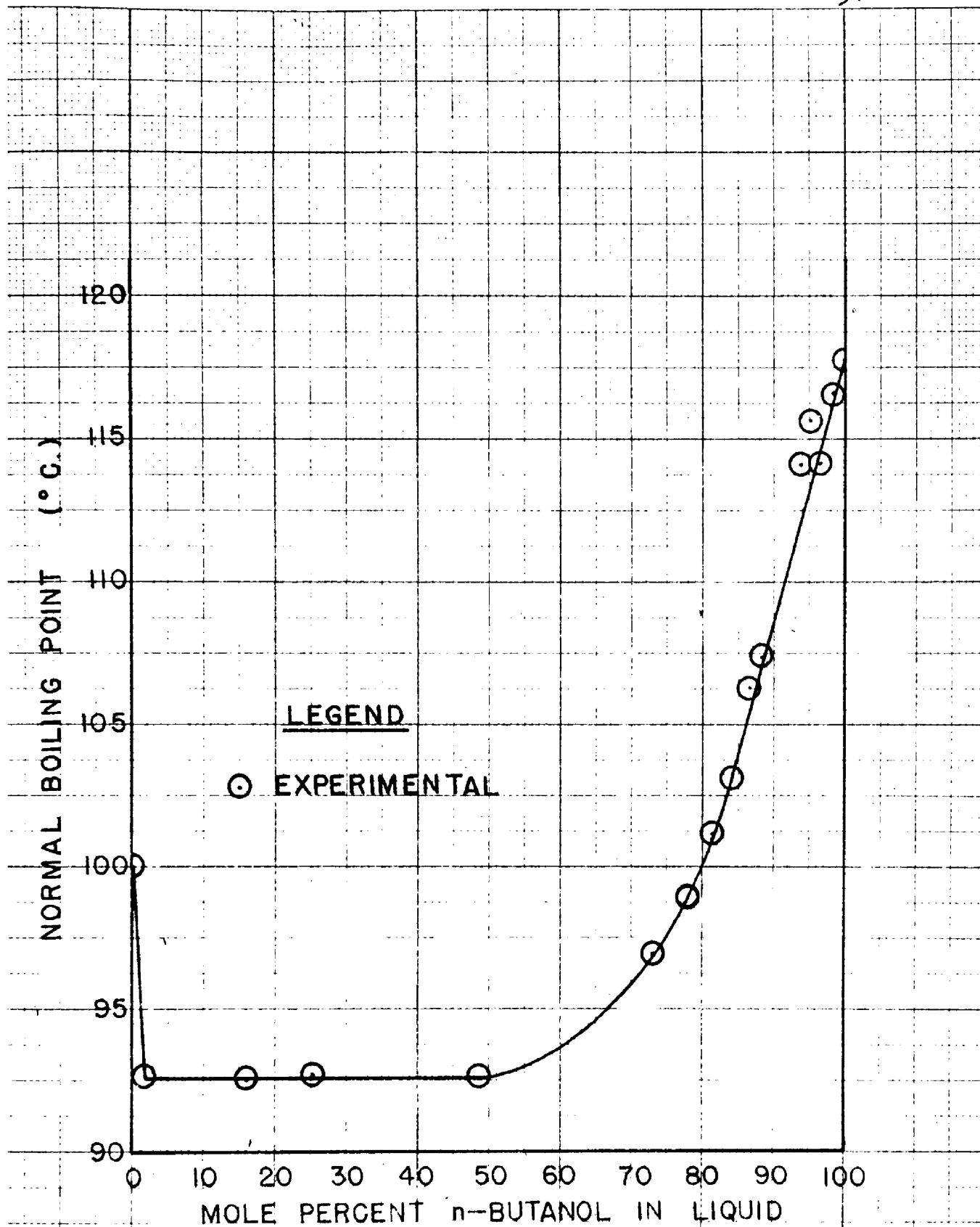


FIGURE 16

VAPOR-LIQUID EQUILIBRIUM FOR
n-BUTANOL-WATER AT 760mm. PRESSURE



BOILING POINT DIAGRAM
FOR
n-BUTANOL—WATER
FIGURE 17

TABLE II
EXPERIMENTAL DATA ON n-BUTANOL¹--WATER AT ATMOSPHERIC PRESSURE

Temp.	<u>Mole Percent n-Butanol¹</u>					
(° C.)	<u>Liquid</u>	<u>Vapor</u>	<u>γ_1</u>	<u>Log γ_1</u>	<u>γ_2</u>	<u>Log γ_2</u>
98.0	0.59	13.2	45.70	1.6599	0.925	-----
92.6	1.91	24.75	34.33	1.5357	1.007	0.0030
92.5	16.05	24.4	3.845	0.5849	1.184	0.0734
92.7	25.3	25.1	2.540	0.4048	1.332	0.1245
92.6*	26.36	24.92	2.385	0.3775	1.336	0.1258
92.6*	29.10	24.7	2.148	0.3320	1.395	0.1446
92.6	48.80	24.75	1.344	0.1284	1.930	0.2856
93.2	55.7	26.8	1.228	0.0892	2.020	0.3054
96.9	73.0	37.3	1.100	0.0414	2.582	0.4120
98.9	78.0	41.9	1.079	0.0330	2.752	0.4397
101.2	81.2	45.7	1.089	0.0370	2.775	0.4433
103.1	84.0	47.2	1.019	0.0082	2.921	0.4655
106.3	86.5	55.9	1.065	0.0273	2.695	0.4306
107.4	88.5	61.5	1.034	0.0141	2.583	0.4121
107.8	89.2	60.9	1.011	0.0048	2.695	0.4306
111.9*	93.7	80.5	1.097	0.0402	2.086	0.3193
113.3*	95.1	85.4	1.091	0.0378	1.905	0.2799
114.2	96.6	85.3	1.009	0.0039	2.674	0.4272
116.6	98.1	93.5	0.996	-----	1.973	0.2951

¹--Component 1

*--These values read from a plot of the other values.

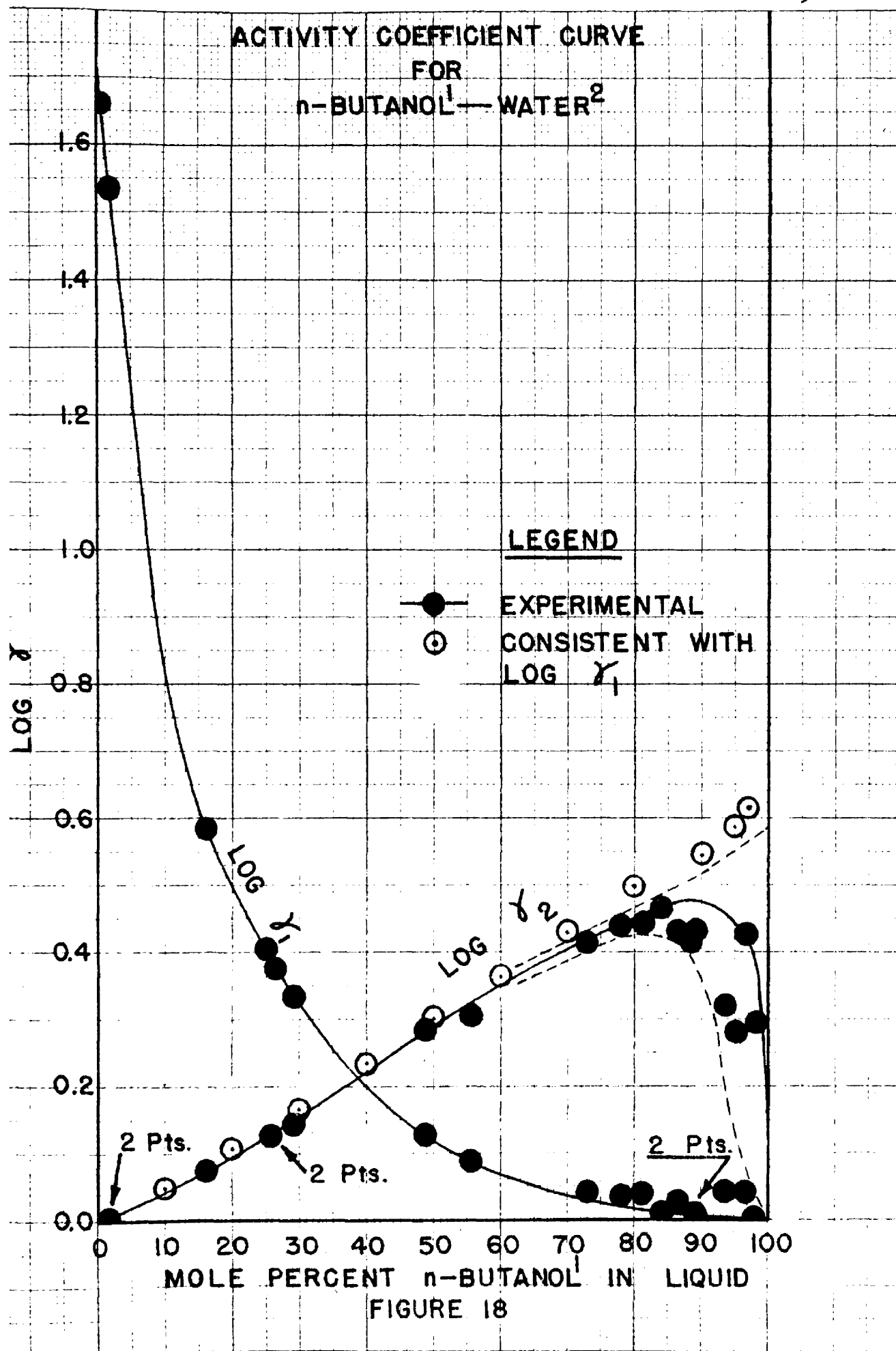


FIGURE 18

TABLE III
 DATA OF STOCKHARDT AND HULL⁴⁷ ON n-BUTANOL¹--WATER AT
 ATMOSPHERIC PRESSURE

Temp. (° C.)	<u>Mele Percent n--Butanol</u>		γ_1	Log γ_1	γ_2	Log γ_2
	<u>Liquid</u>	<u>Vapor</u>				
98.4	0.20	4.90	51.0	1.7076	1.000	0
96.8	0.60	11.60	43.2	1.6355	1.000	0
93.7	1.20	19.20	40.5	1.6075	1.029	0.0124
93.0	2.00	24.40	32.0	1.5052	0.995	-----
92.8	42.30	25.0	1.564	0.1942	1.705	0.2317
92.9	44.8	25.0	1.476	0.1691	1.784	0.2514
93.5	50.4	26.4	1.343	0.1281	1.880	0.2742
96.3	69.5	33.8	1.120	0.0492	2.475	0.3936
96.7	70.8	34.5	1.088	0.0366	2.545	0.4057
97.9	74.3	37.1	1.067	0.0282	2.630	0.4200
108.8	93.0	64.8	1.013	0.0056	3.700	0.5682
109.6	94.5	67.7	1.003	0.0013	4.250	0.6284
111.5	96.1	73.3	1.000	0	4.660	0.6684

1--Component 1.

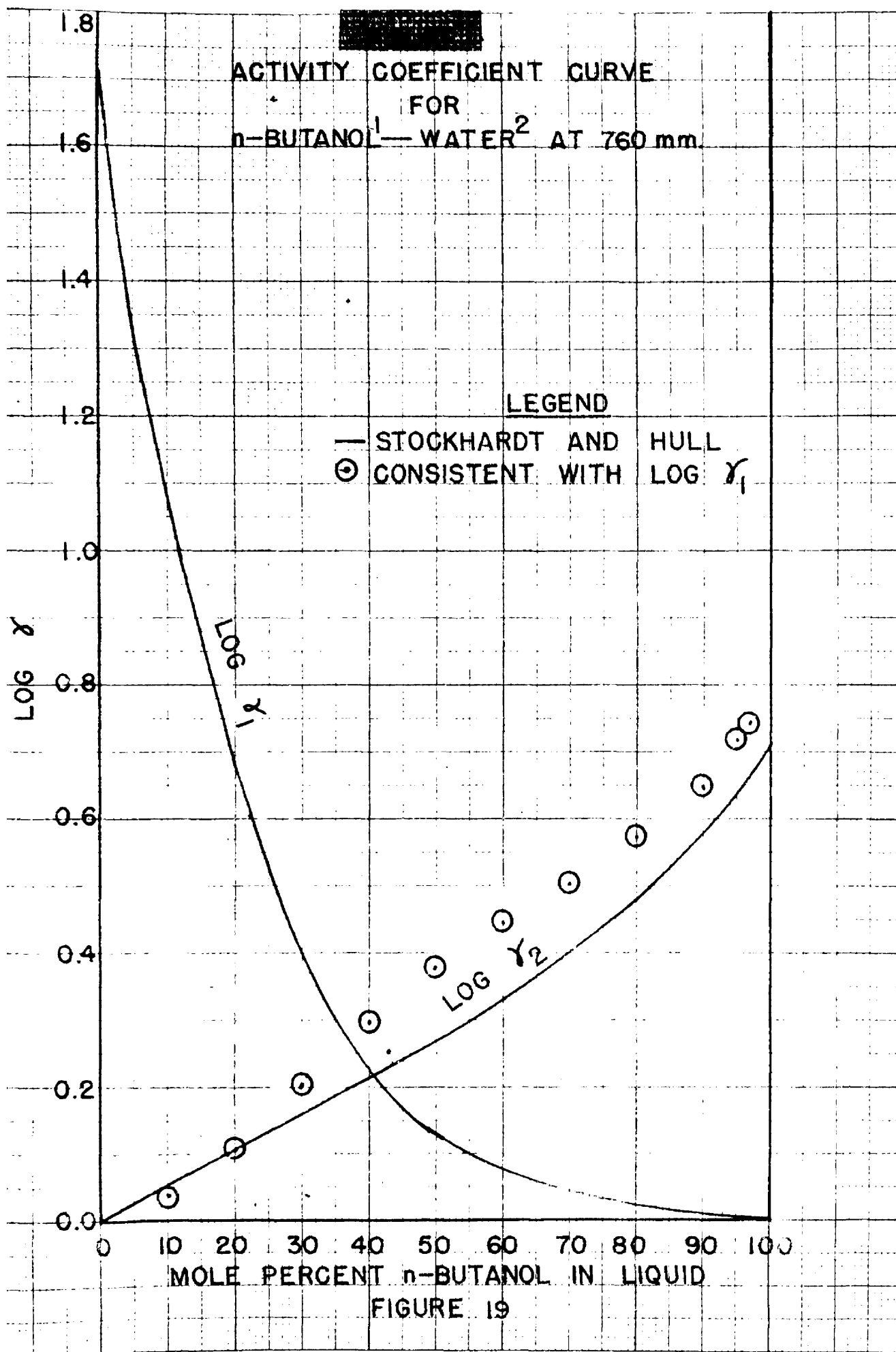


FIGURE 19

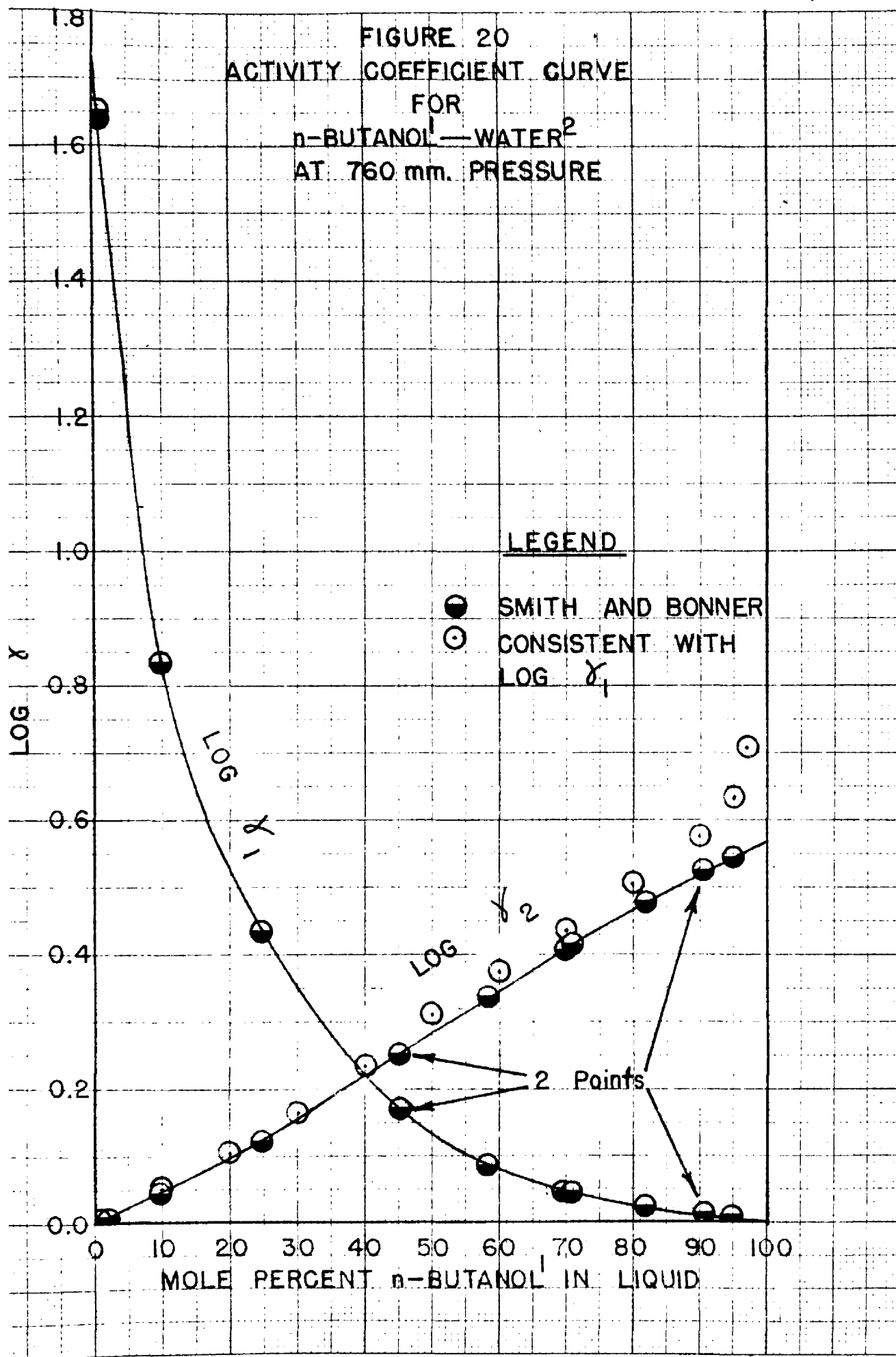


TABLE IV
 DATA OF SMITH AND BONNER⁴⁴ ON n-BUTANOL¹--WATER
 AT ATMOSPHERIC PRESSURE

Temp. (° C.)	<u>Mole Percent n-Butanol</u>		γ_1	Log γ_1	γ_2	Log γ_2
	<u>Liquid</u>	<u>Vapor</u>				
110.95	95.0	74.7	1.020	0.0086	3.494	0.5433
106.85	90.8	61.2	1.028	0.0120	3.352	0.5253
106.40	90.3	59.8	1.028	0.0120	3.342	0.5240
100.85	81.9	44.4	1.052	0.0220	3.010	0.4786
96.65	70.9	34.0	1.108	0.0445	2.585	0.4125
96.35	69.7	33.4	1.121	0.0496	2.535	0.4040
94.00	58.3	27.6	1.222	0.0871	2.179	0.3383
93.02	45.4	25.0	1.482	0.1708	1.789	0.2526
93.00	45.0	24.7	1.476	0.1691	1.783	0.2512
92.70	24.8	24.6	2.708	0.4326	1.321	0.1209
92.70	9.9	24.6	6.783	0.8314	1.103	0.0426
92.70	9.8	24.6	6.852	0.8358	1.102	0.0422
92.80	2.0	24.0	32.640	1.5137	1.019	0.0082
92.85	1.9	23.7	33.810	1.5291	1.020	0.0086
95.40	0.9	16.1	43.560	1.6391	1.010	0.0043
95.80	0.8	15.0	44.820	1.6515	1.007	0.0030

¹--Component 1.

The results of a thermodynamic consistency test on the data of Stockhardt and Hull (Table III) by graphical integration of Equation (15) of Chapter II are shown in Figure 19 where the circles show what $\log \gamma_2$ should be in order to be thermodynamically consistent with $\log \gamma_1$. This test shows their data to be inconsistent and therefore incorrect.

Similar tests were carried out on the data of Smith and Bonner (Table IV) with results as shown in Figure 20. Their data are satisfactory up to approximately 80 mole percent n-Butanol where deviation begins. Their equilibrium still is believed to be the source of their deviation since they analyzed for water content by Karl Fischer reagent, a very precise and accurate method.

Figure 18 and Table II show the results of similar tests on the data obtained on the new still. Again the data are satisfactory up to approximately 80 mole percent n-Butanol, where deviation is noted. This deviation can be attributed to the analytical method which was by density measurement in the miscible range (48.8 to 100 mole percent).

A statistical analysis was performed on this analytical method under optimum conditions. The tests were of such a nature as to give the maximum precision obtainable with the existing equipment, taking into consideration the preparation of solutions, measuring their densities, reading the compositions from a plot of density versus composition, and any other hidden factors involved. This statistical analysis showed that with all other factors being equal any analysis could be duplicated within 0.32 mole percent 67 percent of the time, within 0.635 mole percent 95 percent of the time, and within 0.96 mole percent 99.7 percent of the time. On the x-y diagram where each individual point is the result of two such

analyses, each of the above figures should be multiplied by the square root of two to get the allowable limit for each case.

These precision limits together with an assumed $\pm 0.1^\circ \text{C.}$ temperature variation were transformed into the corresponding limits of the activity coefficients and the resulting confidence limits for $\log \gamma_2$ versus composition are shown by the dashed lines in Figure 18. These confidence limits show that all the deviation of the activity coefficient curves from that expected could have been caused by the analytical method used. It is concluded therefore that the equilibrium still operates satisfactorily, and that no major portion of the variation observed is due to the failure of the still to operate properly. It should be noted that although the data give a smooth curve when plotted on the x-y diagram, the activity coefficient plots may become very erratic over the same range.

The Ethyl Acetate--Water System was studied briefly, but due to corrosion of the still only the immiscible range was completed. This data is shown in Table V and Figure 21 and compared with the values predicted by Winsauer⁵³ from solubility data with the Van Laar equations. The samples were analyzed by separating and weighing the phases at a constant temperature.

TABLE V

EXPERIMENTAL DATA ON ETHYL ACETATE-WATER AT 760 mm. PRESSURE

<u>Temperature ($^\circ \text{C.}$)</u>	<u>Mole Percent Ethyl Acetate</u>	
	<u>Liquid</u>	<u>Vapor</u>
71.5	1.36	73.0
71.5	77.40	73.0
76.0	1.03	71.8

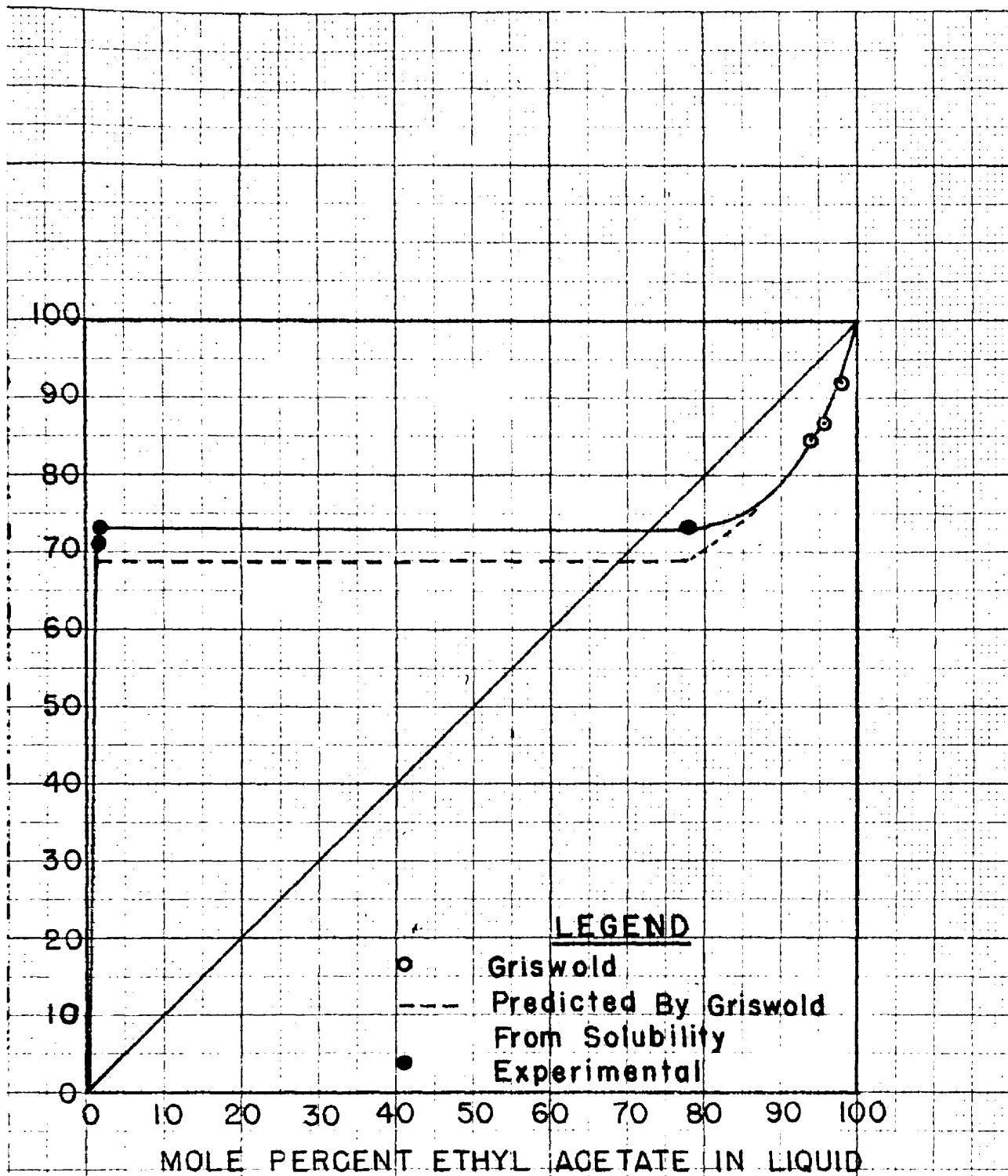


FIGURE 21

VAPOR-LIQUID EQUILIBRIUM DIAGRAM FOR
ETHYL ACETATE-WATER AT 760 mm. PRESSURE

E. REAGENTS

The reagents used in all tests were of analytical reagent grade redistilled in a four foot laboratory column packed with stainless steel helices. The middle fractions distilling at the correct temperature were taken as the pure material in most cases, but in some cases were redistilled to give physical properties commensurate with literature values. The water came from the laboratory distilled water supply.

Table VI is a tabulation of the physical properties of the reagents used.

TABLE VI
PHYSICAL PROPERTIES OF REAGENTS

<u>Reagent</u>	$n_D^{25^\circ C}$		Sp. Gr. $25^\circ C$	
	<u>Present</u>	<u>Literature</u>	<u>Present</u>	<u>Literature</u>
Water	1.3325	1.33252	<u>Standard</u>	0.99707
Ethyl Alcohol	1.3594	1.35912	0.78496	0.78510
Ethyl Acetate	1.3700	1.3701	0.8947	0.8950
n-Butyl Alcohol	1.3974	1.3973	0.8055	0.80525

All plots of the physical properties versus composition used for analysis were made up from data on the actual materials used rather than the literature values.

F. CONCLUSION

It has been shown that this new equilibrium still will give reliable values for vapor-liquid equilibria and in addition possesses the very important characteristics of continuous operation on a definite small quantity of reagents in the miscible or immiscible range of composition at pressures varying from below atmospheric to pressures considerably above atmospheric.

In addition to being versatile the still is rugged, simple to construct, easy to operate, and easily cleaned.

These features make the still superior to any unit thus far proposed for the general study of vapor-liquid equilibrium. Although this still does not solve all the problems involved, the approach is somewhat different and will perhaps stimulate further development of the ideas presented.

CHAPTER IV

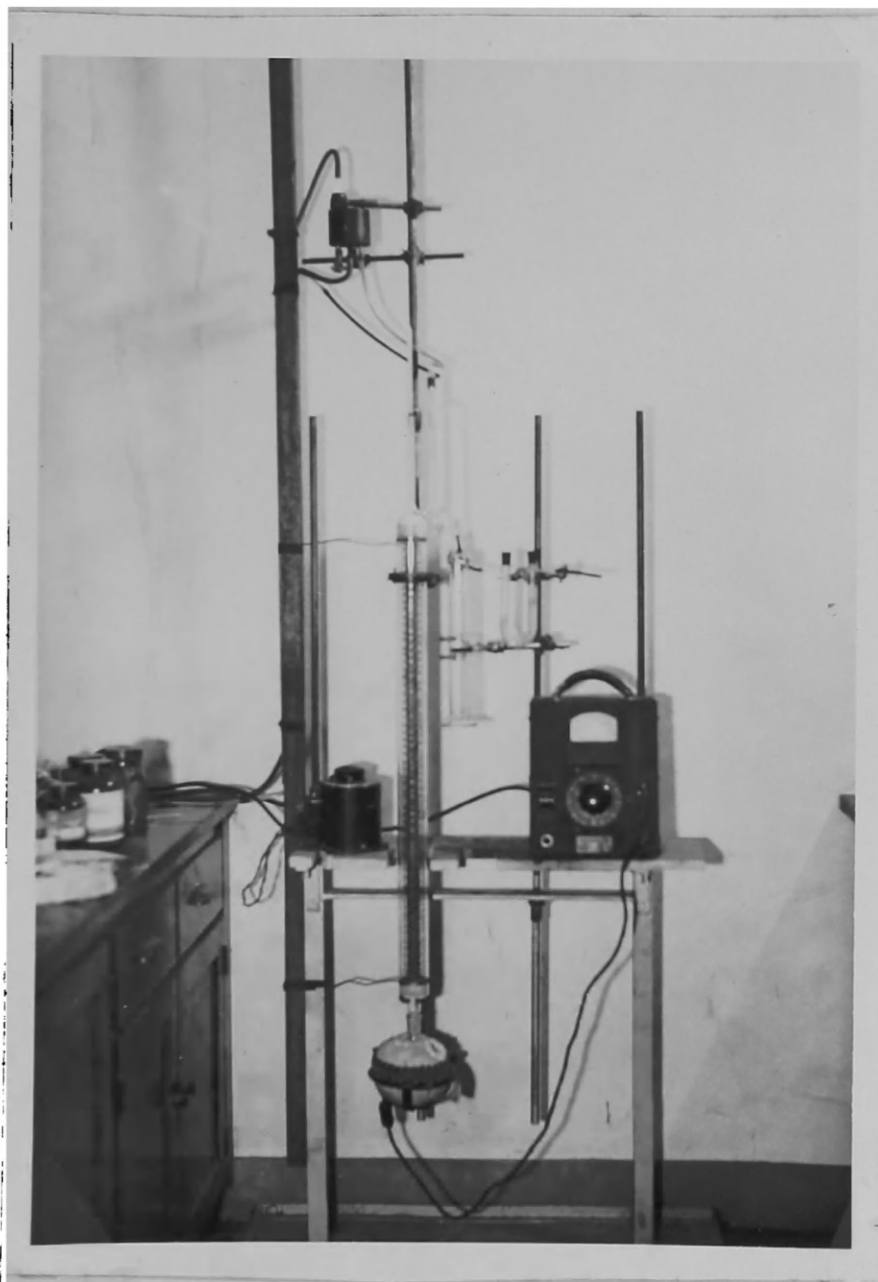
EXPERIMENTAL DATA

Study of the variation of activity coefficients with pressure and temperature would be greatly facilitated by the availability of reliable data over a relatively wide range of pressures. Such data has been obtained on a binary system which has become industrially important with the advent of the synthetic fuels program. Ethanol and n-Hexane appear as products in this synthesis along with a host of other chemicals most of which form azeotropes with each other bringing about difficulties in separation by distillation.

In addition data were determined on the binary systems Ethanol-Water, Ethyl Acetate-Water, and n-Butanol-Water as previously presented in Chapter III.

The Ethanol used in the investigation was absolute alcohol sold by U. S. Industrial Chemicals, Inc., which was fractionated in a four foot laboratory column packed with stainless steel helices (Figure 22) to yield cuts having physical properties in line with published values. The material used had a refractive index (n_D^{25}) of 1.3594 and a specific gravity (d_4^{25}) of 0.78496.

Technical grade n-Hexane, containing approximately 4 mole percent impurities, chiefly methylcyclopentane, was purchased from The Phillips Petroleum Co., Bartlesville, Oklahoma, and subsequently purified by batchwise extractive distillation with aniline in the laboratory column. (Figure 22). Aniline has been previously used as a separating agent



LABORATORY DISTILLING COLUMN

FIGURE 22

for these two compounds by a countercurrent extractive distillation in large columns but has not been recommended as a laboratory method. The first attempts at separation were by extraction with aniline in a separatory funnel and subsequent distillation of the hydrocarbon layer. This effected no separation. It has been reported¹⁹ that these compounds form an azeotrope boiling at a temperature close to that of pure n-Hexane. It is entirely possible that when the aniline is present in the still pot, it exerts a selective solvent action for the methylocyclopentane (B. P. 71.8° C.) sufficient to change its volatility characteristics with respect to that of n-Hexane (B. P. 68.75° C.) to such an extent that the azeotrope is broken and a separation is effected. The n-Hexane used had a refractive index (n_D^{25}) of 1.3723 and a specific gravity (d_4^{25}) of 0.65501.

Analysis of the various samples was by measuring refractive index and by use of a refractive index versus composition plot obtained by making up solutions of known composition and reading their refractive indices. The refractometer was maintained at 25.0° C. by combination of a heating and refrigerating type constant temperature bath and could be read to ± 0.0001 .

A statistical analysis was carried out to ascertain the precision of the analytical method used. This test was performed by reading the refractive indices of several solutions of known composition under the same conditions that the analyses on the experimental work were performed. For example, readings on any one of these known solutions were made in the morning, afternoon, and at night and on different days. In this way it was assumed that the many random variations that might affect such a determination would be included. A minimum of six such readings were

made on each of five solutions whose concentrations ranged from pure n-Hexane to pure Ethanol.

Statistical analysis of these precision tests showed an average standard deviation, σ , of 0.8 weight percent and that the precision of the determinations did not vary significantly over the entire range. However when this was converted to precision in terms of mole percent, a uniform increase from 0.4 mole percent equivalent to the average standard deviation in weight percent at pure Ethanol to 1.49 mole percent equivalent to the average standard deviation in weight percent at pure n-Hexane was found. This increase is due entirely to the differences in molecular weight of the two components.

For the purpose of setting up confidence limits about experimental data, each of these values should be multiplied by 3.0 to get limits inside which 99.7 percent of the data should fall to be entirely satisfactory and multiplied by 1.96 to get limits inside which 95 percent of the data should fall to be entirely satisfactory. When the standard deviation is used without a multiplier, 67 percent of the data should fall within the limits. In the case of an x-y diagram where each point is the result of two such determinations, each of the above values should be multiplied by the square root of two to get the appropriate limits. This depends to some extent on the shape of the curve.

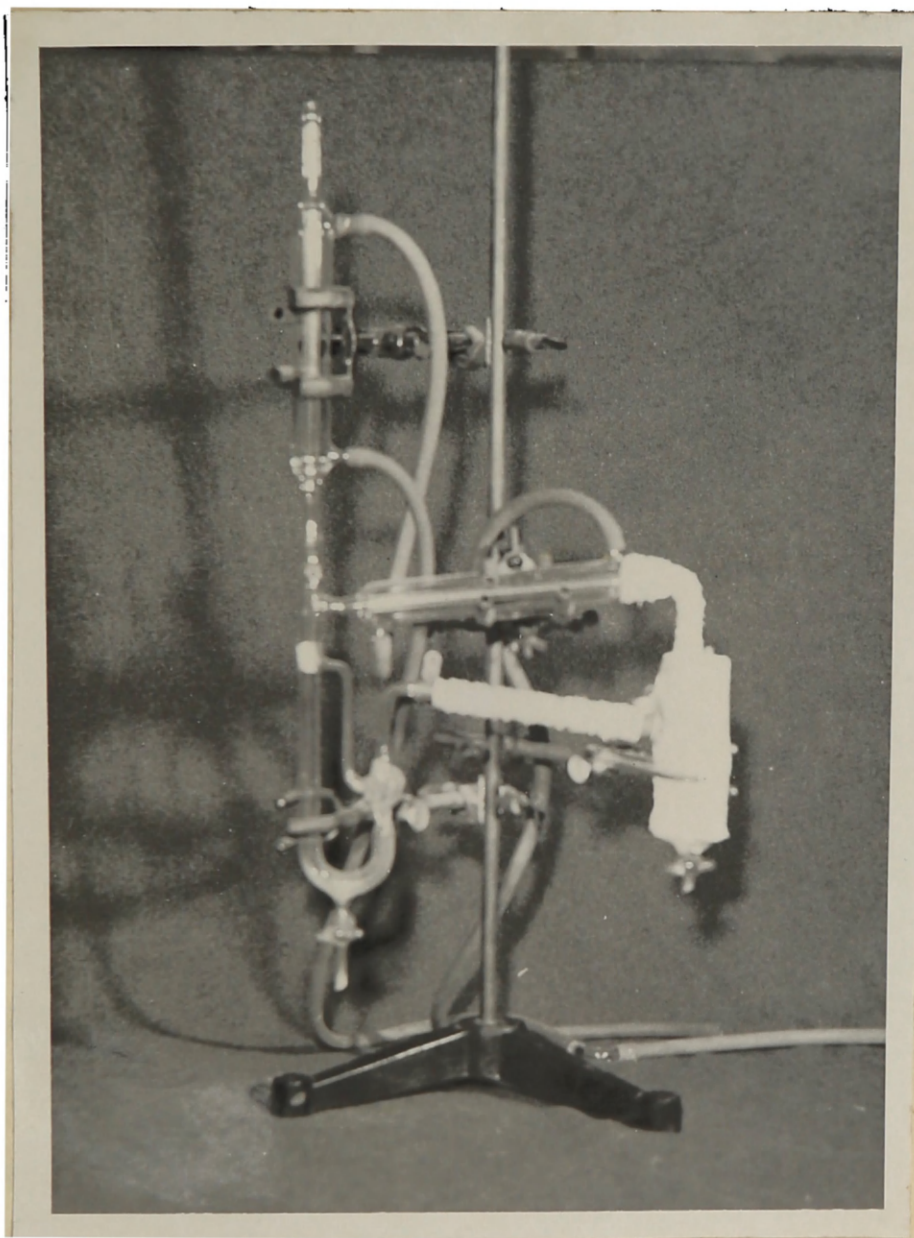
At first glance these values seem rather high, but the tests were performed with the same degree of care as the experimental determinations and considerable importance is attached to them. Such tests could probably explain much of the poor data that has been published. Such information might prevent investigators from making claims about their data that are

not wholly justified.

This information permits setting up confidence limits on experimental data or any data derived from this experimental data. To the knowledge of the author only one investigator⁴⁶ has published data with confidence limits, and these were gotten by assuming a reasonable deviation. Statistical analyses are tedious and difficult to perform correctly, but the information derived from such tests is ample reward for the labor. No experimental data should be considered complete until such tests have been performed.

The experimental data at 250 mm., 393 mm., and 760 mm. was obtained on a glass still of the Jones, Schoenborn, and Colburn type as shown in Figure 23. The data at the higher pressures was determined using the new type of still as described in detail in Chapter III. The development of the equilibrium still made possible the investigations over a range of pressures sufficient to show the effect of pressure on vapor-liquid equilibrium data on liquid activity coefficients. This data is shown in Tables VII-XIII and Figures 24-44.

The confidence limits are illustrated in Figures 27 and 29. The limits plotted are the 2 σ or 95 percent limits as previously explained.



JONES, SCHOENBORN, AND COLBURN STILL

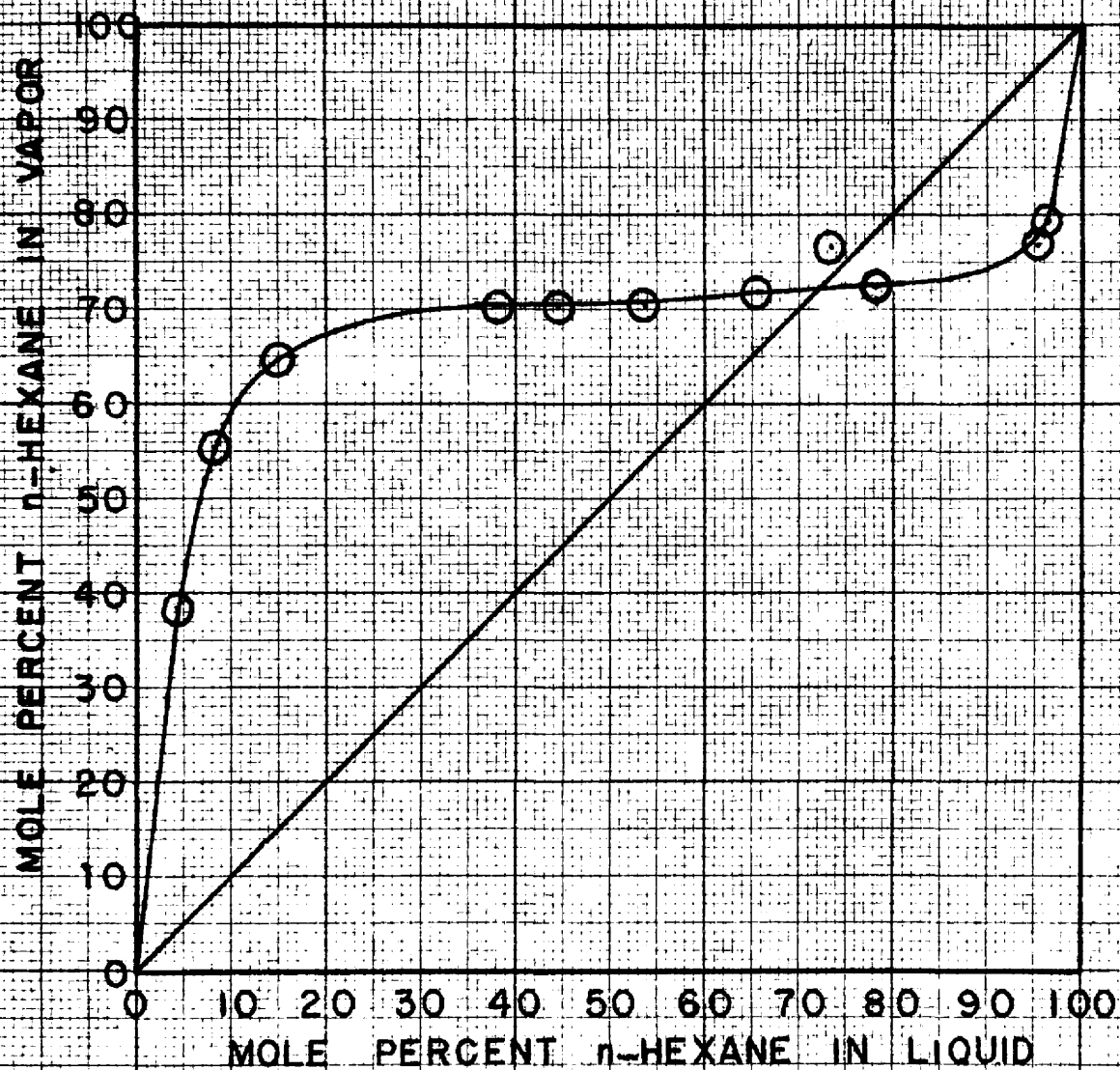
FIGURE 23

TABLE VII
EXPERIMENTAL DATA FOR n-HEXANE¹-ETHANOL² AT 250 mm. Hg.

TOTAL PRESSURE				
	<u>MOLE PERCENT n-HEXANE¹</u>			
<u>TEMPERATURE</u> <u>°C.</u>	<u>LIQUID</u>	<u>VAPOR</u>	<u>LOG γ_1</u>	<u>LOG γ_2</u>
41.8	4.5	38.3	.8508	.0379
38.1	8.4	55.4	.8072	.0196
34.5	15.0	64.8	.6852	.0150
31.7	38.4	70.2	.5589	.1479
31.7	44.5	70.2	.2949	.1947
31.5	52.1	71.9	.2371	.2368
30.5	53.8	70.2	.2115	.2881
31.2	65.8	71.9	.1323	.3882
30.9	78.4	72.7	.0629	.5731
32.1	95.4	76.7	---	1.1627
32.4	96.3	79.3	---	1.1886

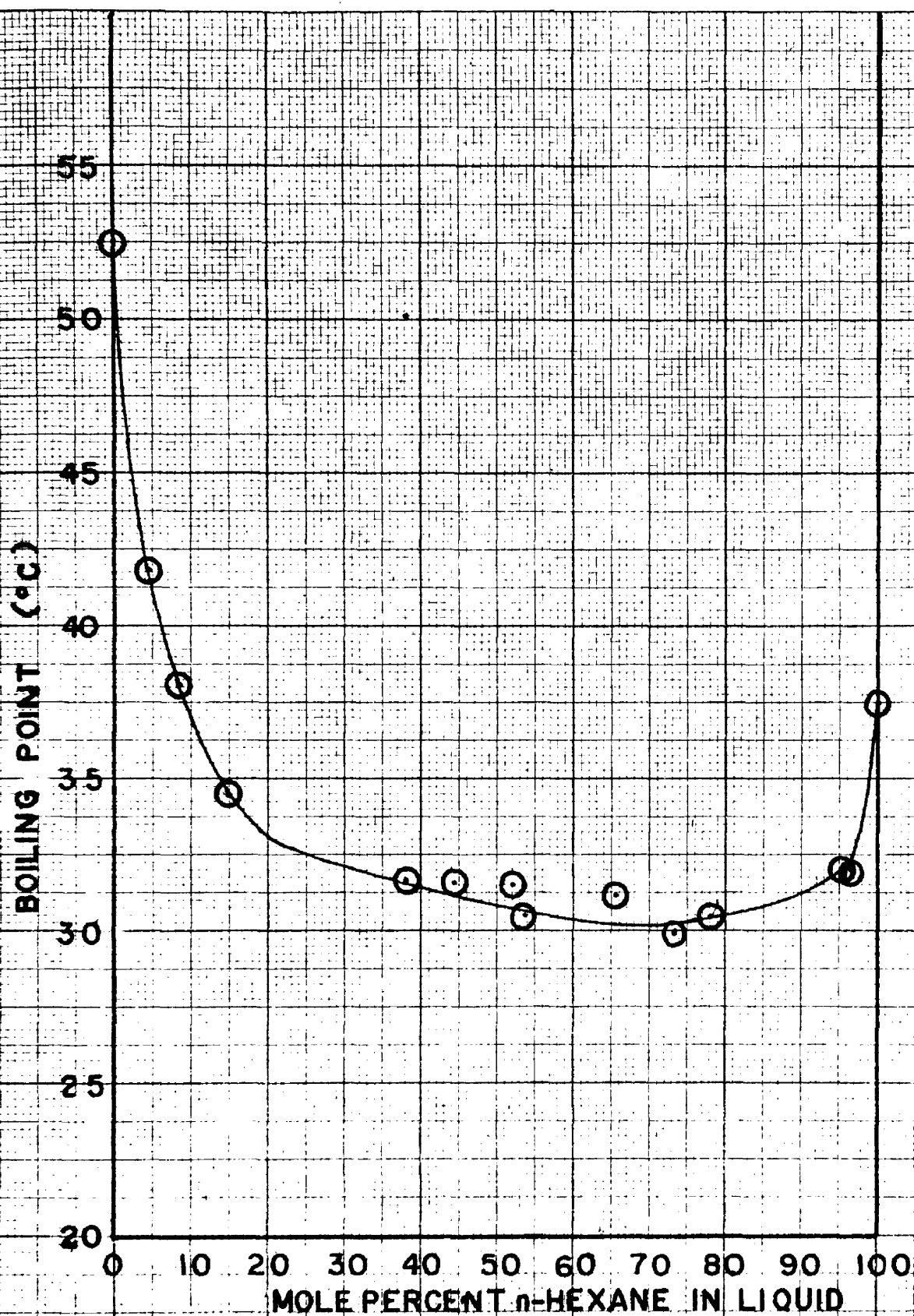
1--Component 1

2--Component 2



VAPOR—LIQUID EQUILIBRIUM DIAGRAM
FOR
n-HEXANE¹—ETHANOL² AT 250 mm. Hg.

FIGURE 24



BOILING POINT DIAGRAM
FOR
n-HEXANE—ETHANOL AT 250mm. Hg.
FIGURE 25

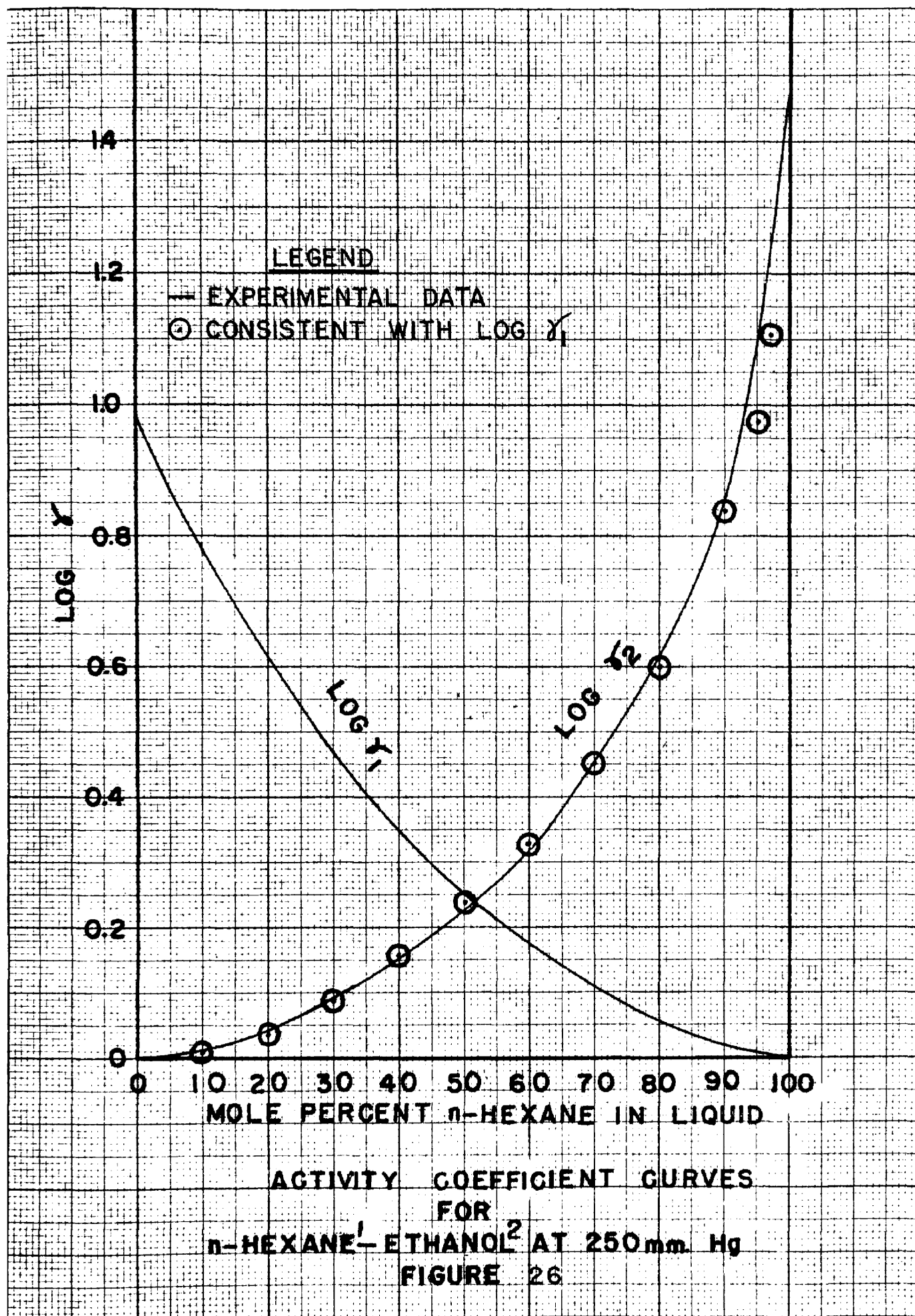
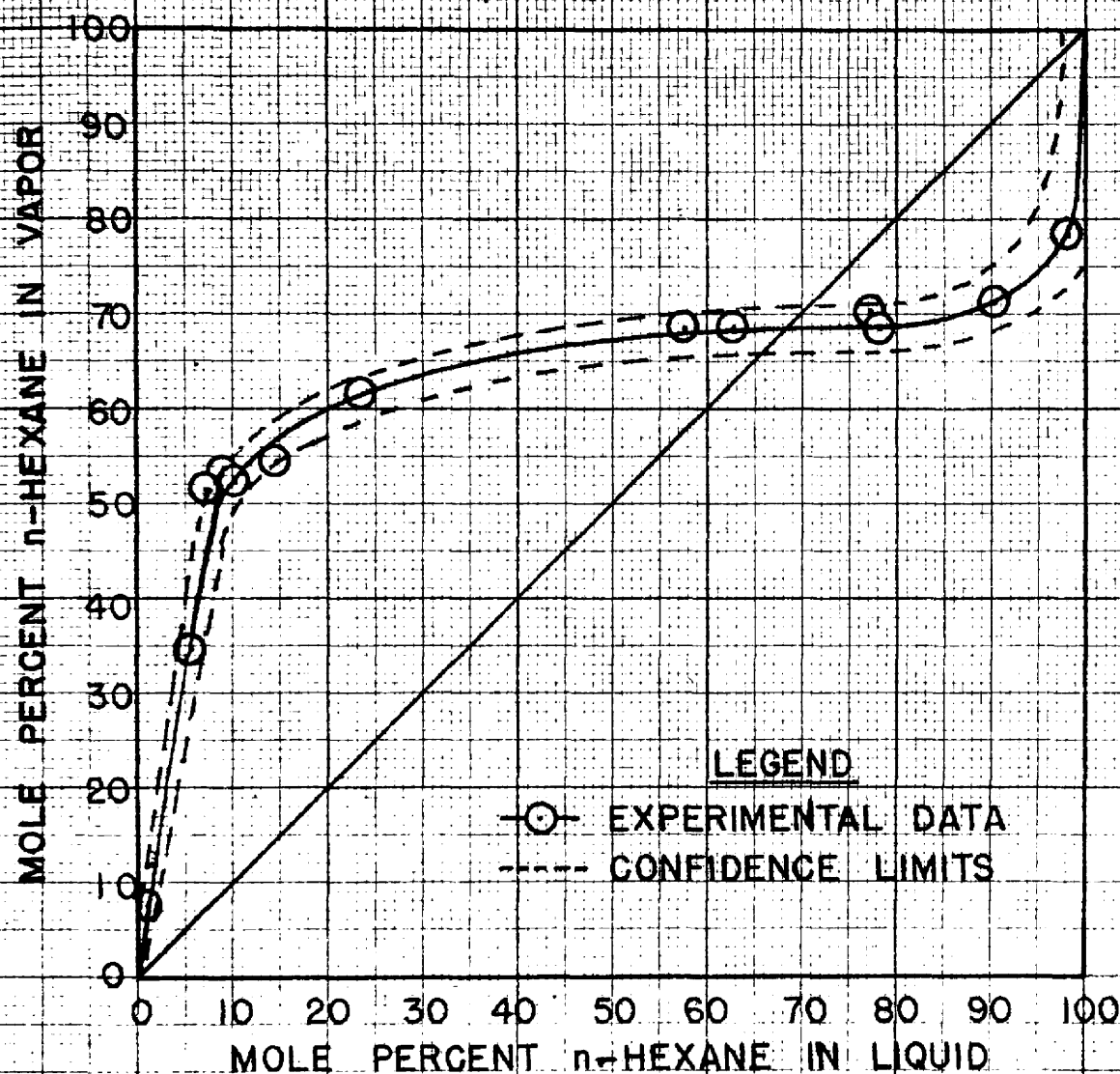


TABLE VIII
 EXPERIMENTAL DATA FOR n-HEXANE¹-ETHANOL² AT 393 mm. Hg.
 TOTAL PRESSURE

TEMPERATURE °C.	<u>MOLE PERCENT HEXANE</u>		<u>LOG γ_1</u>	<u>LOG γ_2</u>
	<u>LIQUID</u>	<u>VAPOR</u>		
58.1	1.0	7.7	.7444	
50.3	5.6	34.3	.7666	.0809
47.9	7.2	51.4	.8740	.0081
46.0	9.0	53.0	.8166	.0402
46.0	10.1	52.2	.7600	.0537
44.5	14.8	54.5	.6355	.0913
42.5	23.9	62.1	.5205	.0813
41.1	57.9	68.8	.2038	.3089
41.4	62.9	68.8	.1635	.3608
41.5	77.4	70.2	.0806	.5501
41.6	78.4	68.8	.0652	.5916
42.2	90.2	71.1	.0095	.8842
42.4	98.2	78.4	.0022	1.4811

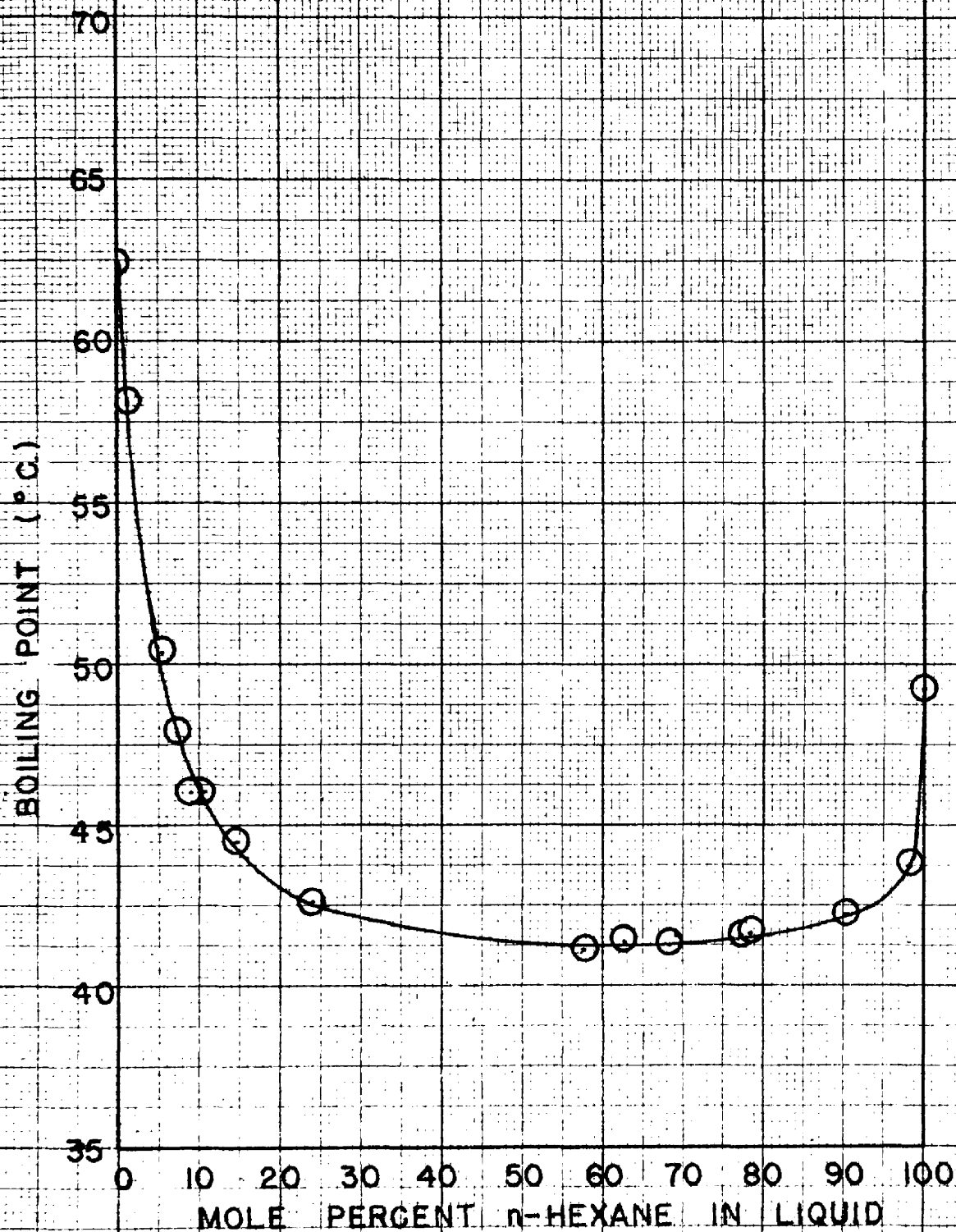
1--Component 1

2--Component 2



VAPOR-LIQUID EQUILIBRIUM DIAGRAM
FOR
n-HEXANE¹—ETHANOL² AT 393 mm. Hg.

FIGURE 27



BOILING POINT DIAGRAM
FOR
n-HEXANE¹—ETHANOL² AT 393 mm. Hg
FIGURE 28

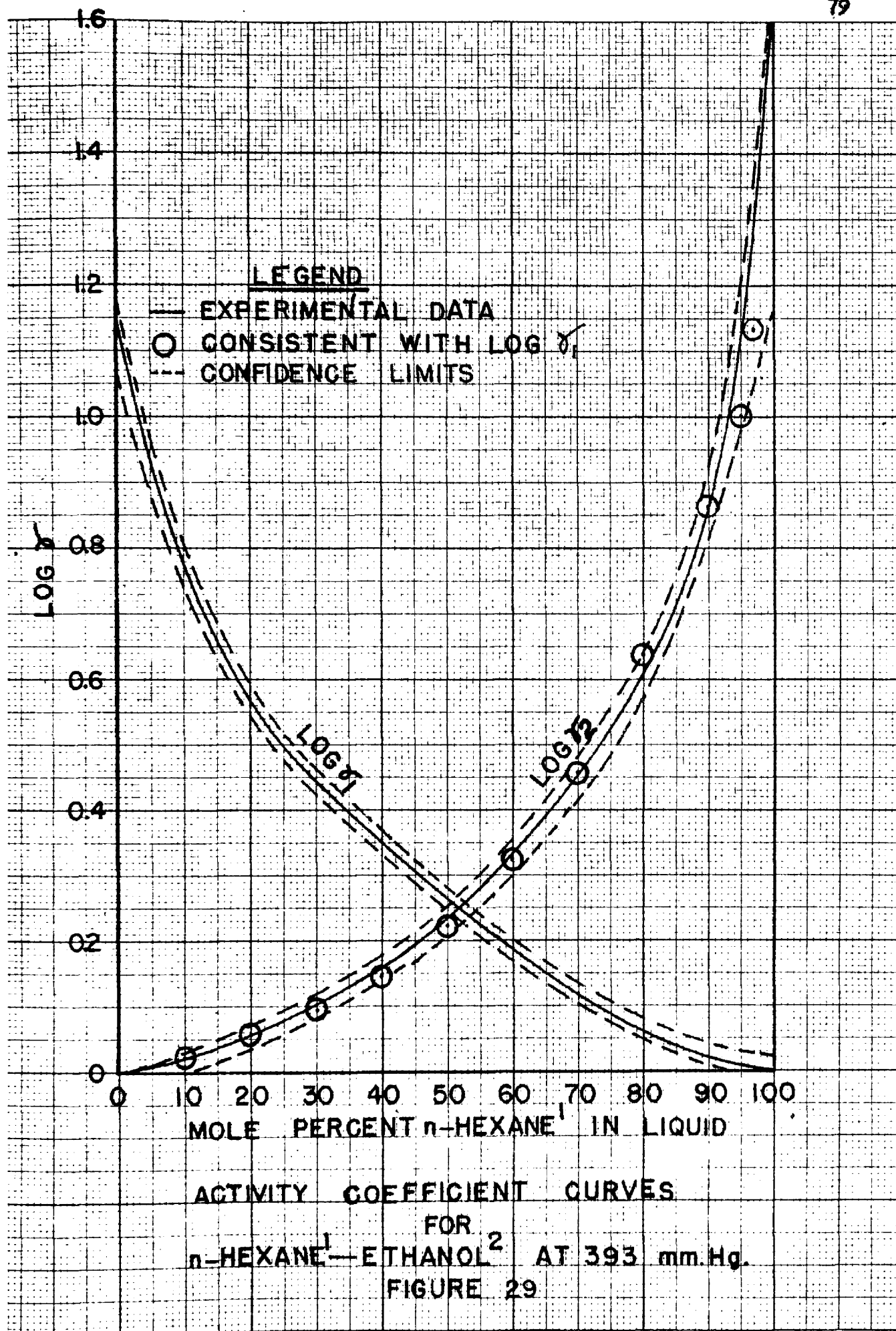
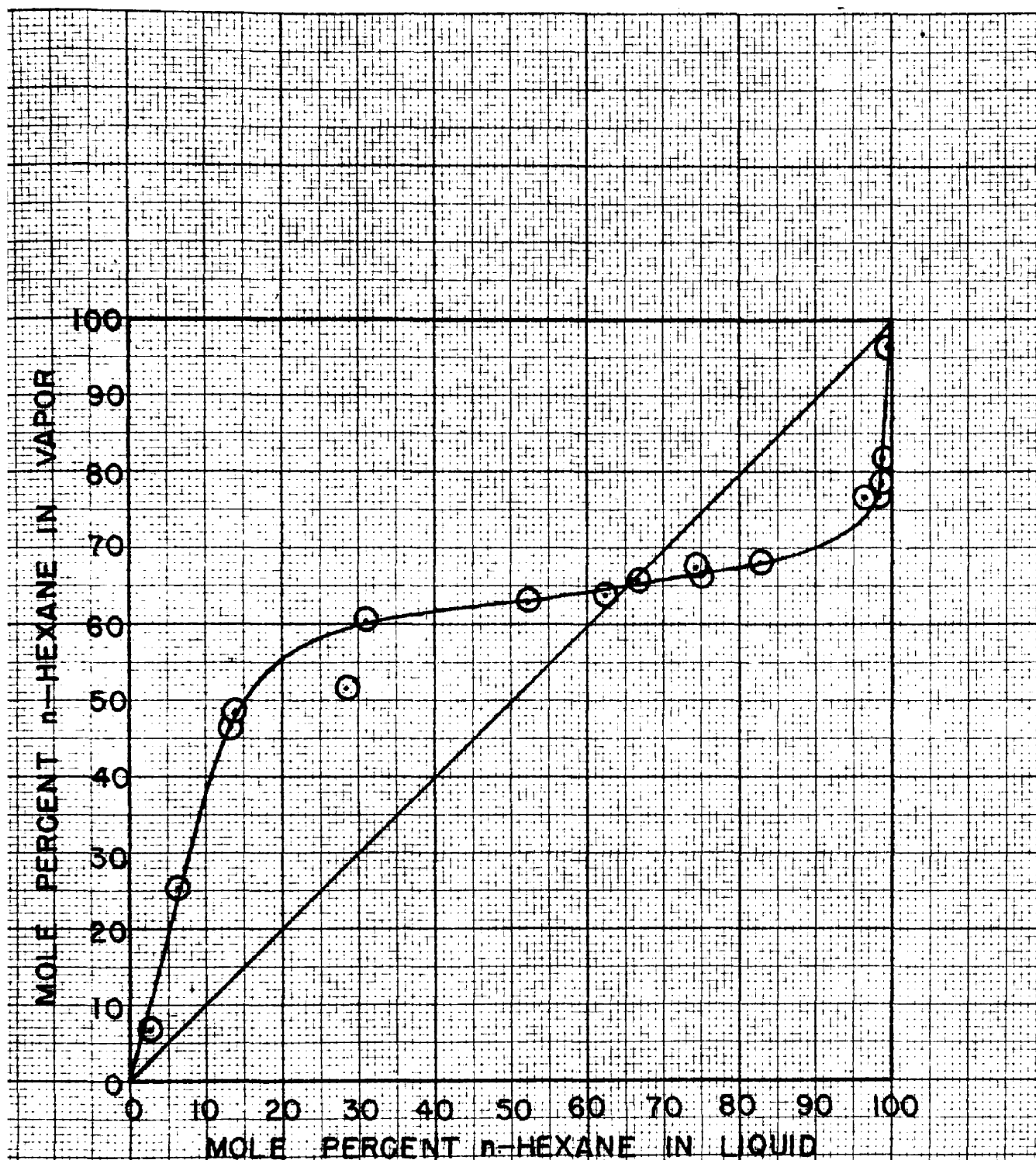


TABLE IX
EXPERIMENTAL DATA FOR n-HEXANE¹-ETHANOL² AT 760 mm. Hg.

TOTAL PRESSURE				
<u>MOLE PERCENT n-HEXANE¹</u>				
<u>TEMPERATURE</u> <u>°C.</u>	<u>LIQUID</u>	<u>VAPOR</u>	<u>LOG γ_1</u>	<u>LOG γ_2</u>
75.4	2.5	6.9	.3541	.6298
63.7	6.4	25.2	.6589	.1614
63.0	13.1	46.2	.6222	.0645
62.5	13.7	48.4	.6294	.0584
59.6	28.2	51.5	.3865	.1697
59.6	30.9	60.4	.4141	.0934
58.2	52.1	62.9	.2248	.2543
58.2	62.2	63.9	.1550	.3454
58.2	66.6	65.7	.1567	.3747
58.3	74.2	67.5	.1014	.4602
58.6	75.1	66.6	.0864	.6010
58.8	82.6	68.8	.0546	.6085
60.0	96.3	76.7	.0187	1.1310
61.0	98.2	76.7	-----	1.4108
62.2	98.9	78.4	.0047	1.5065
62.1	99.0	81.8	.0043	1.5490
63.4	99.4	96.3	.0294	1.0453

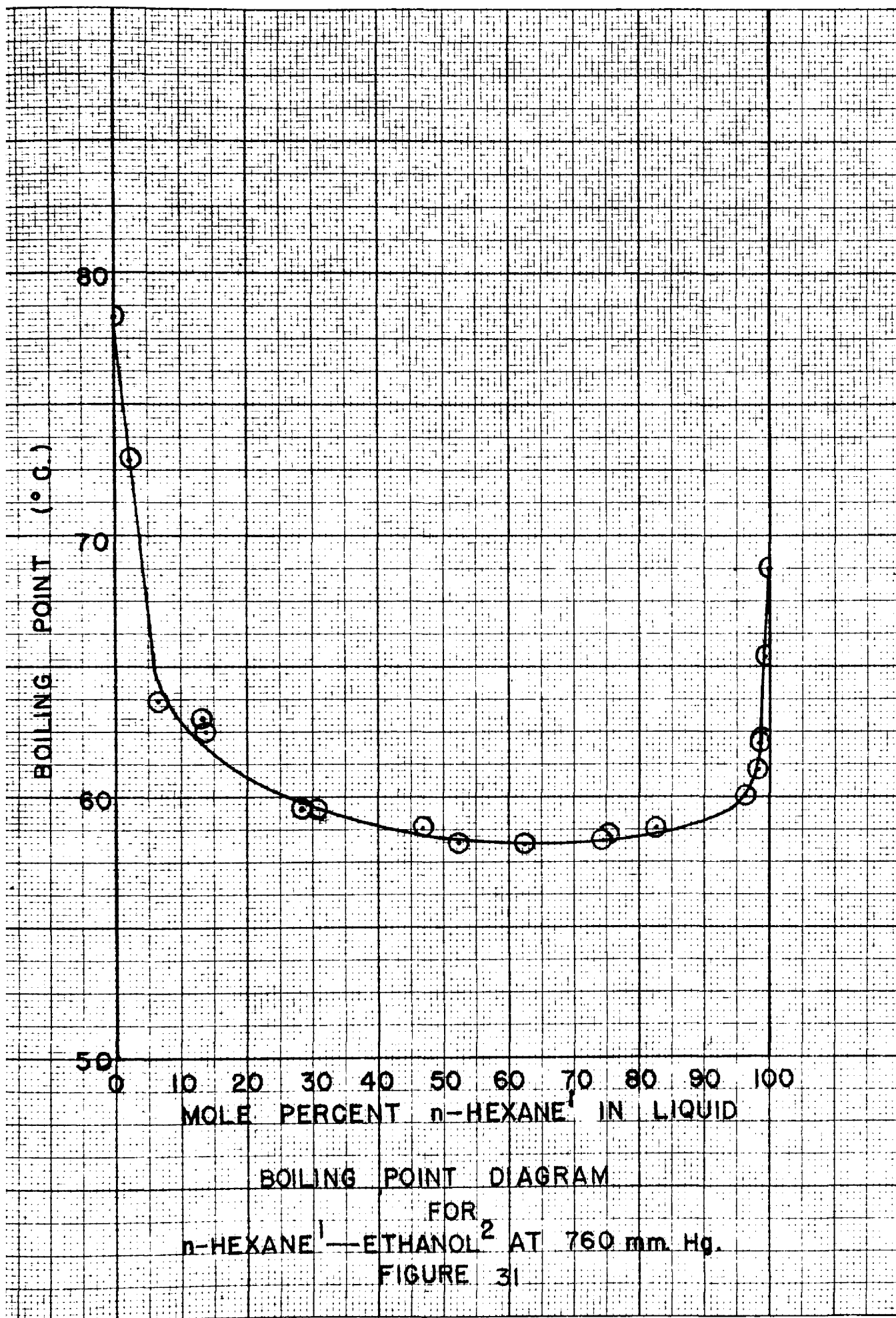
1--Component 1

2--Component 2



VAPOR-LIQUID EQUILIBRIUM DIAGRAM
FOR
n-HEXANE¹-ETHANOL² AT 760 mm. Hg.

FIGURE 30



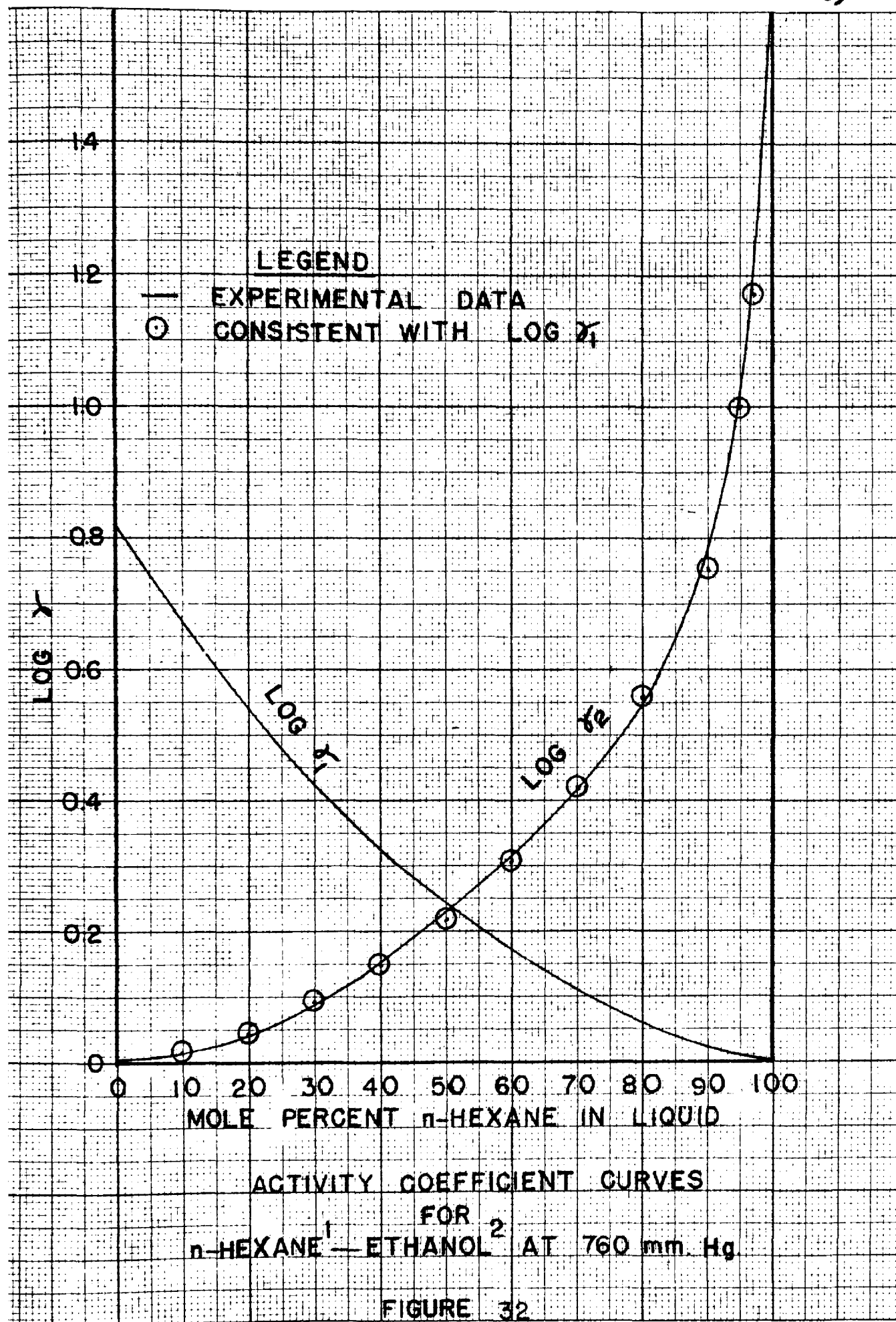


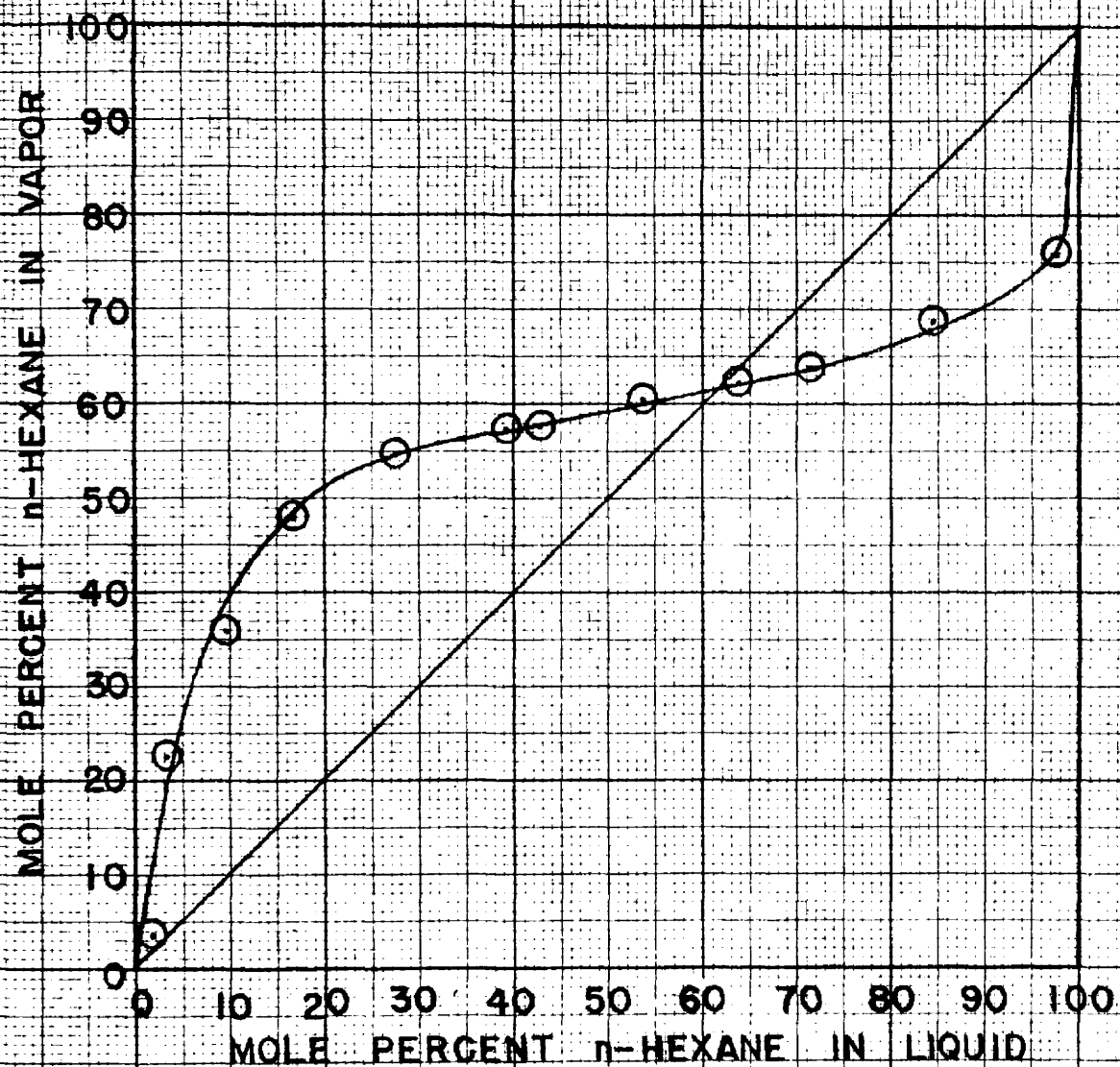
TABLE X
EXPERIMENTAL DATA ON n -HEXANE¹-ETHANOL² AT 1270 mm. Hg.
TOTAL PRESSURE

TEMPERATURE °C.	MOLE PERCENT n -HEXANE		LOG γ_1	LOG γ_2
	LIQUID	VAPOR		
87.5*	1.9	3.3	.1717	-----
85.6	3.1	22.6	.8756	-----
79.7	9.5	35.9	.6580	.0481
76.2	16.7	48.0	.5775	.0457
74.0	27.3	54.4	.4503	.0903
73.9	39.2	57.1	.3117	.1399
73.5	42.8	57.7	.2831	.1667
73.1	53.8	60.4	.2092	.2383
73.5	63.9	62.0	.1399	.3191
73.5	71.1	63.9	.1069	.3945
75.3	84.4	68.8	.0457	.5711
78.3	97.6	75.9	-----	1.2227

1--Component 1

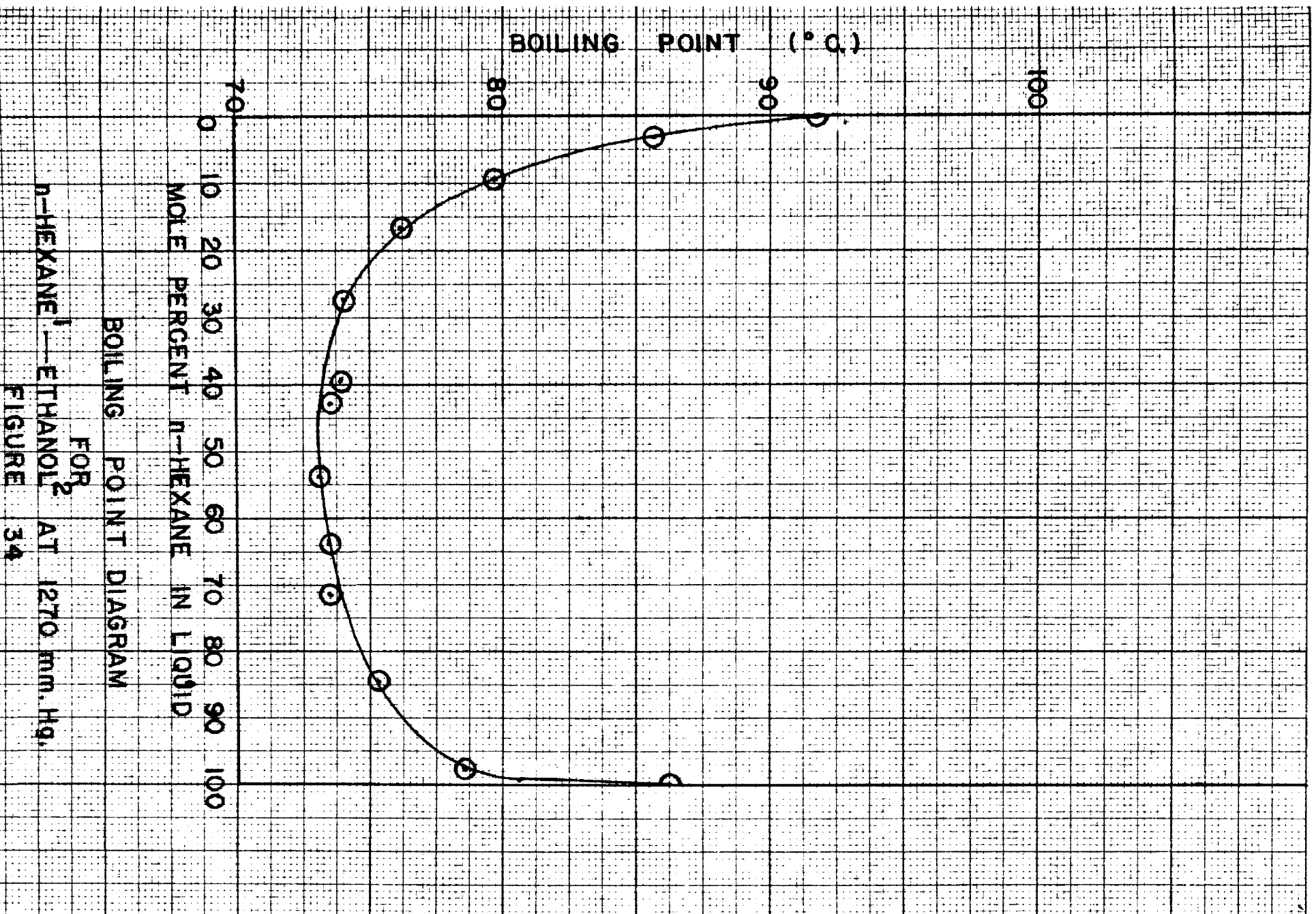
2--Component 2

*--Read from plot of other values.



VAPOR—LIQUID EQUILIBRIUM DIAGRAM
FOR
n-HEXANE¹—ETHANOL² AT 1270 mm. Hg.

FIGURE 33



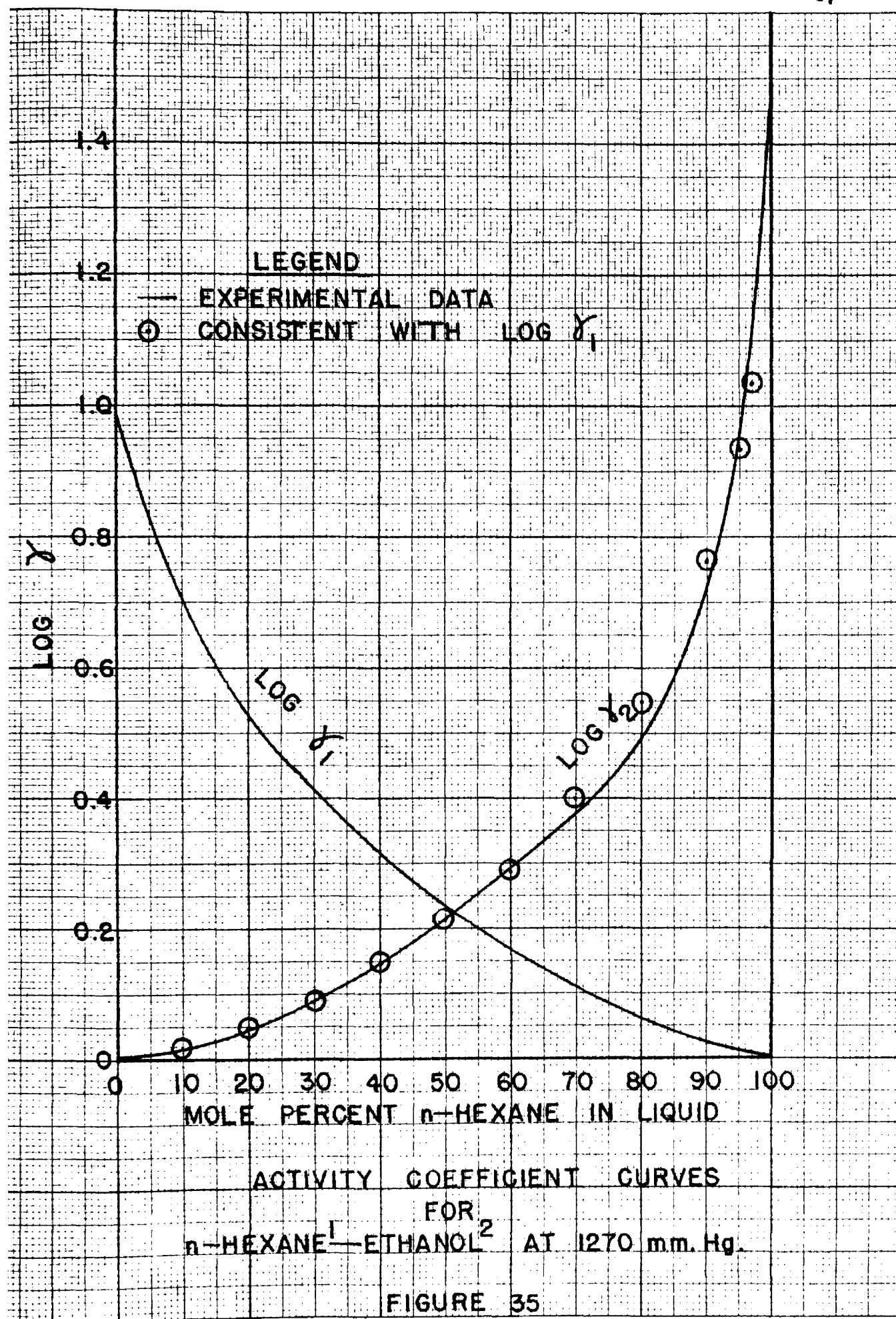


TABLE XI
EXPERIMENTAL DATA ON n-HEXANE¹-ETHANOL² AT 1545 mm. Hg.

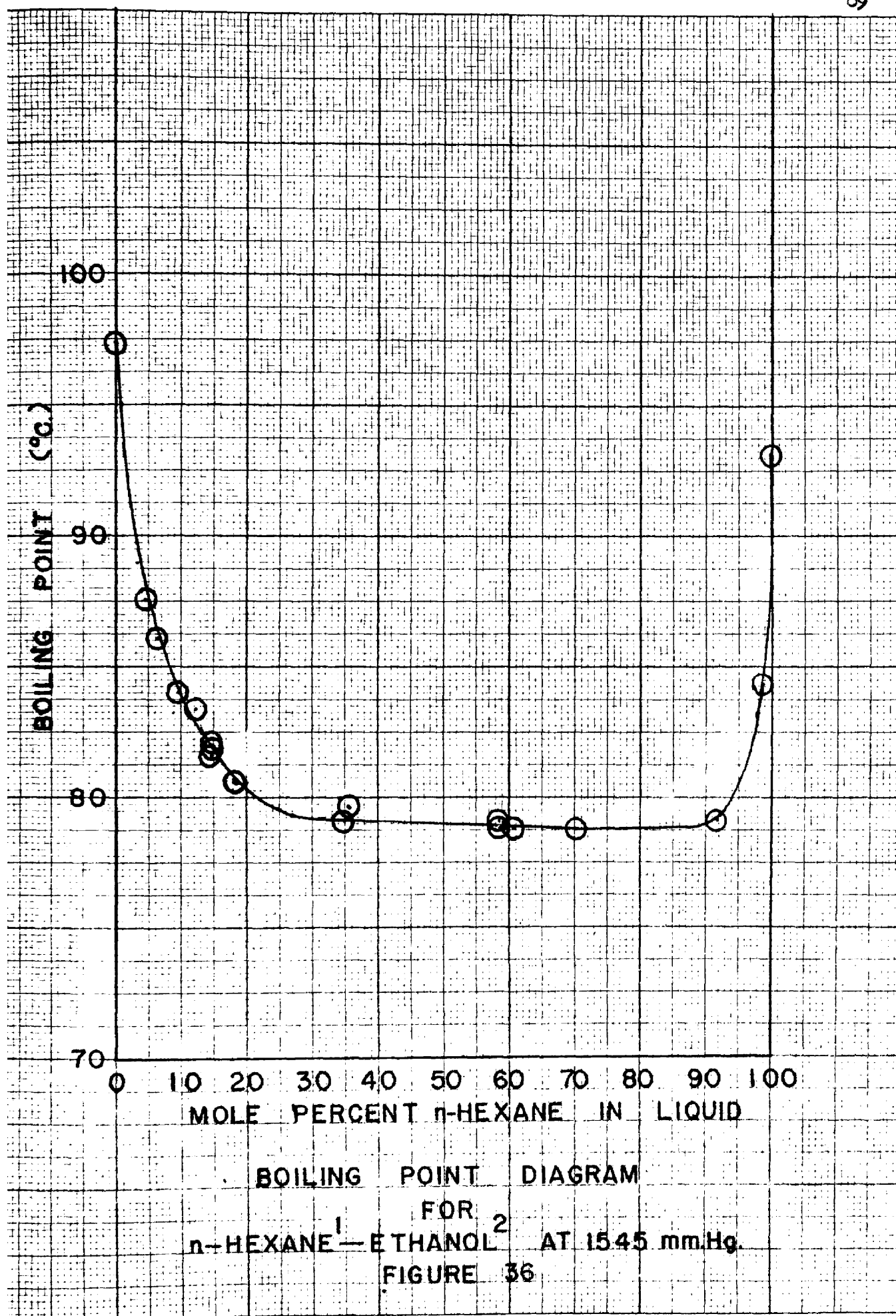
TOTAL PRESSURE

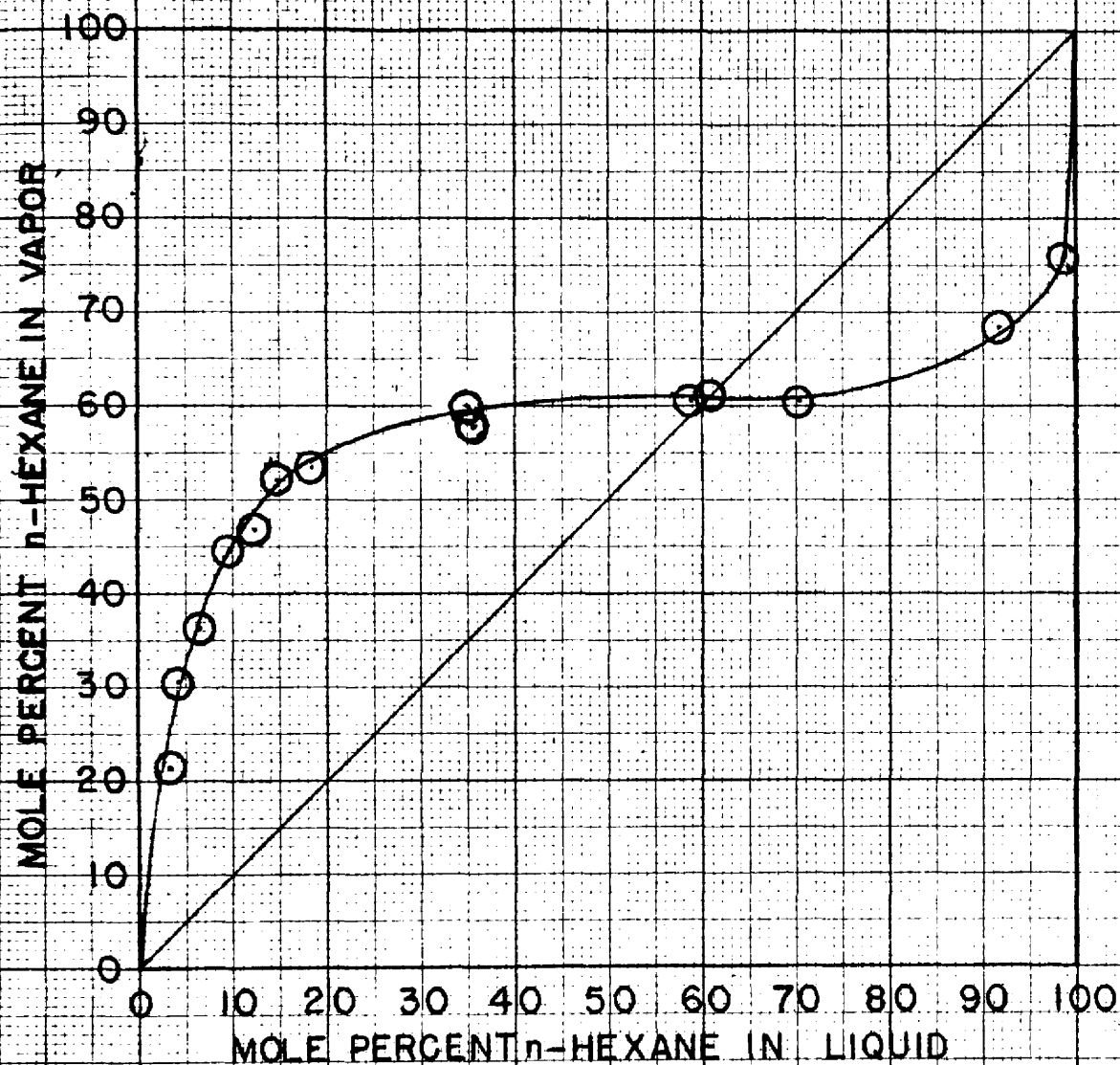
TEMPERATURE °C.	MOLE PERCENT n-HEXANE ¹		LOG γ_1	LOG γ_2
	LIQUID	VAPOR		
89.0*	3.2	21.2	.8774	.0406
87.5	4.2	30.4	.9297	.0120
86.1	6.4	36.1	.8357	.0052
84.0	9.8	44.5	.7708	-----
83.4	12.3	46.9	.7042	.0030
82.1	14.9	52.0	.6848	-----
81.7	14.9	52.2	.6911	.0009
81.9	15.0	52.0	.6840	-----
80.6	18.5	53.6	.6212	.0253
79.1	35.0	59.6	.3526	.0828
79.7	35.9	57.9	.3738	.1004
78.8	58.6	60.4	.1886	.2785
79.1	58.6	60.9	.1920	.2695
78.8	60.9	60.9	.1764	.2969
78.8	70.2	60.4	.1106	.4208
79.1	91.9	68.5	.0469	.9112
84.3	98.7	75.9	-----	1.4646

1--Component 1

2--Component 2

*--Read from a plot of other values.





EXPERIMENTAL VAPOR LIQUID EQUILIBRIUM DATA
FOR
n-HEXANE¹-ETHANOL² AT 1545 mm. PRESSURE

FIGURE 37

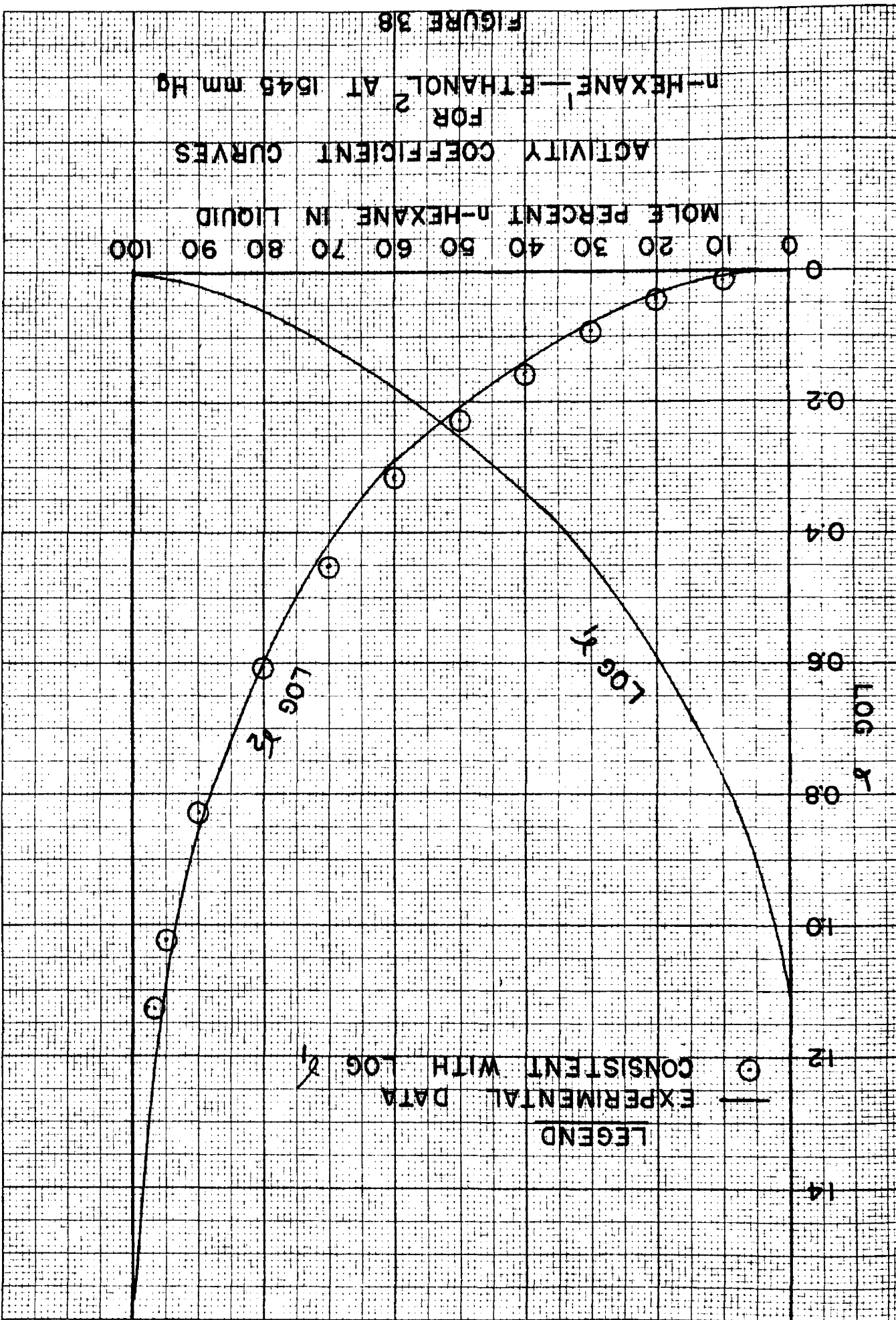
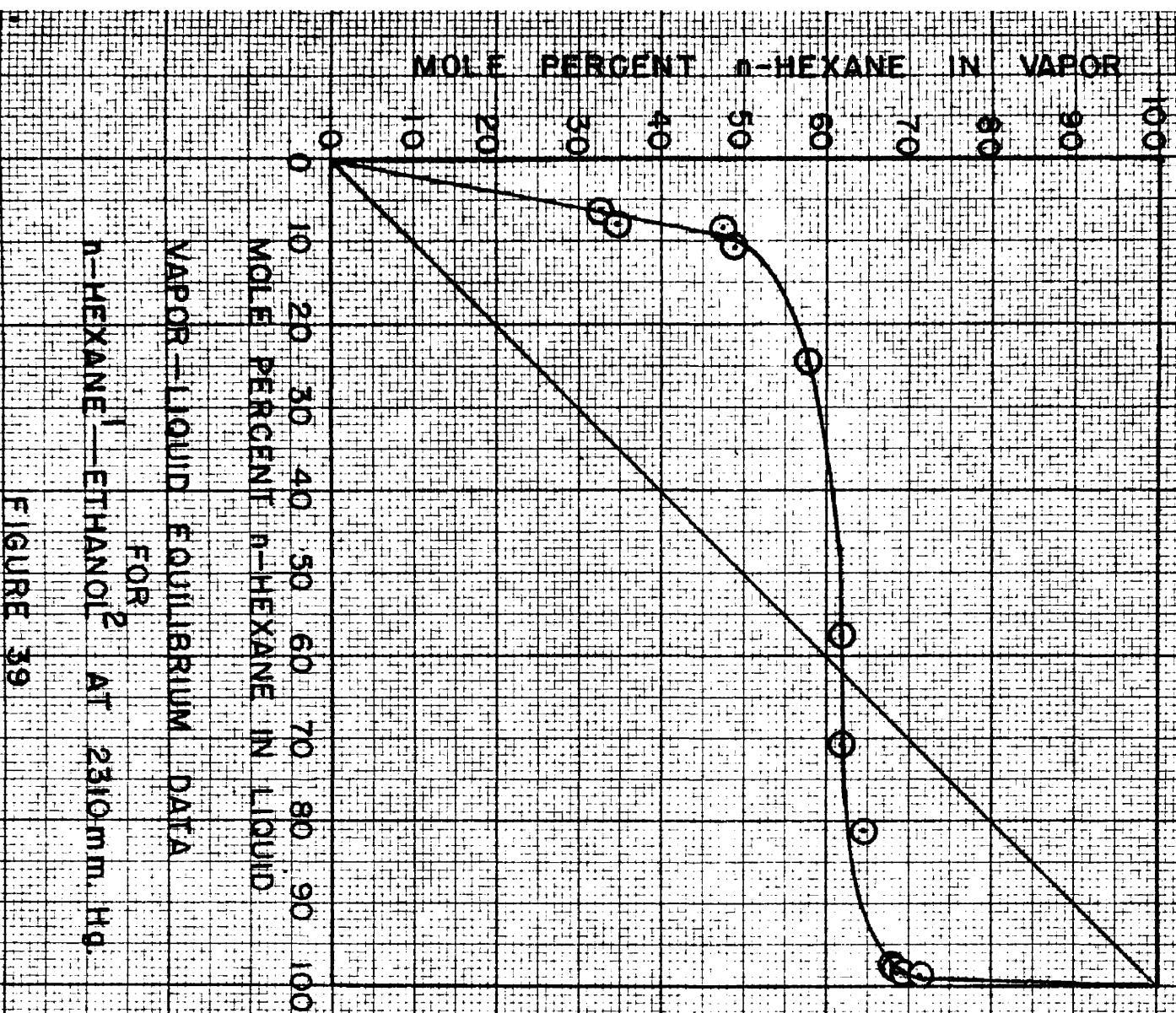


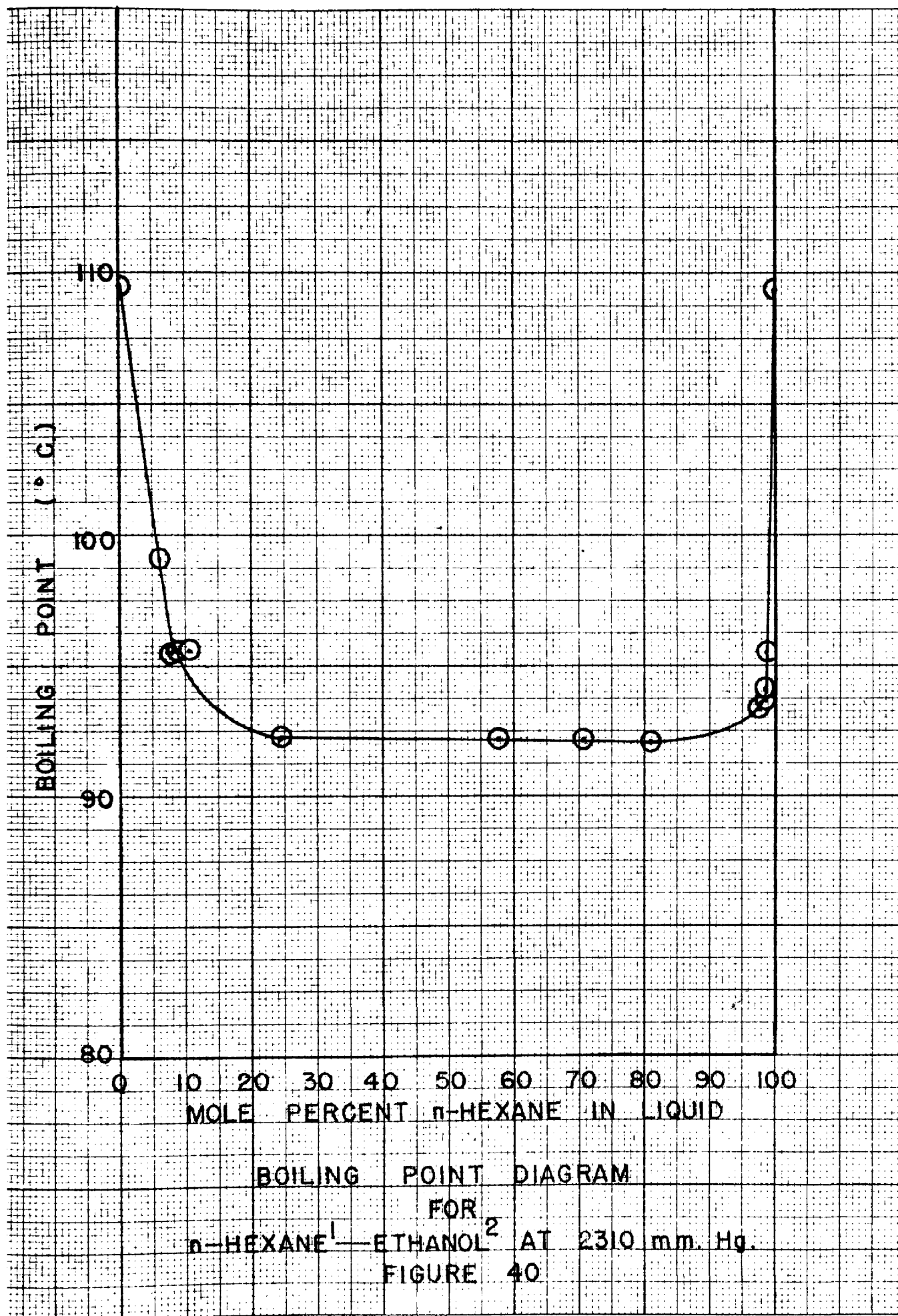
TABLE XII
 EXPERIMENTAL DATA ON n -HEXANE¹-ETHANOL² AT 2310 mm. Hg.
 TOTAL PRESSURE

TEMPERATURE °C.	MOLE PERCENT n -HEXANE ¹		LOG γ_1	LOG γ_2
	LIQUID	VAPOR		
99.1	6.1	32.5	.8311	.0018
95.5	8.0	34.6	.7698	.0517
95.5	8.2	47.4	.8953	-----
95.6	10.6	48.9	.7982	-----
92.2	24.5	57.7	.5394	-----
92.2	57.7	61.7	.1962	.1974
92.2	70.6	61.8	.1087	.3548
92.0	81.0	64.5	.0593	.5160
93.3	97.4	68.0	.0056	1.3149
93.4	97.9	68.0	.0104	1.4071
94.1	98.4	69.4	.0026	1.4951
93.6	98.5	68.6	.0026	1.5454
95.5	98.6	71.4	-----	1.5095

1--Component 1

2--Component 2





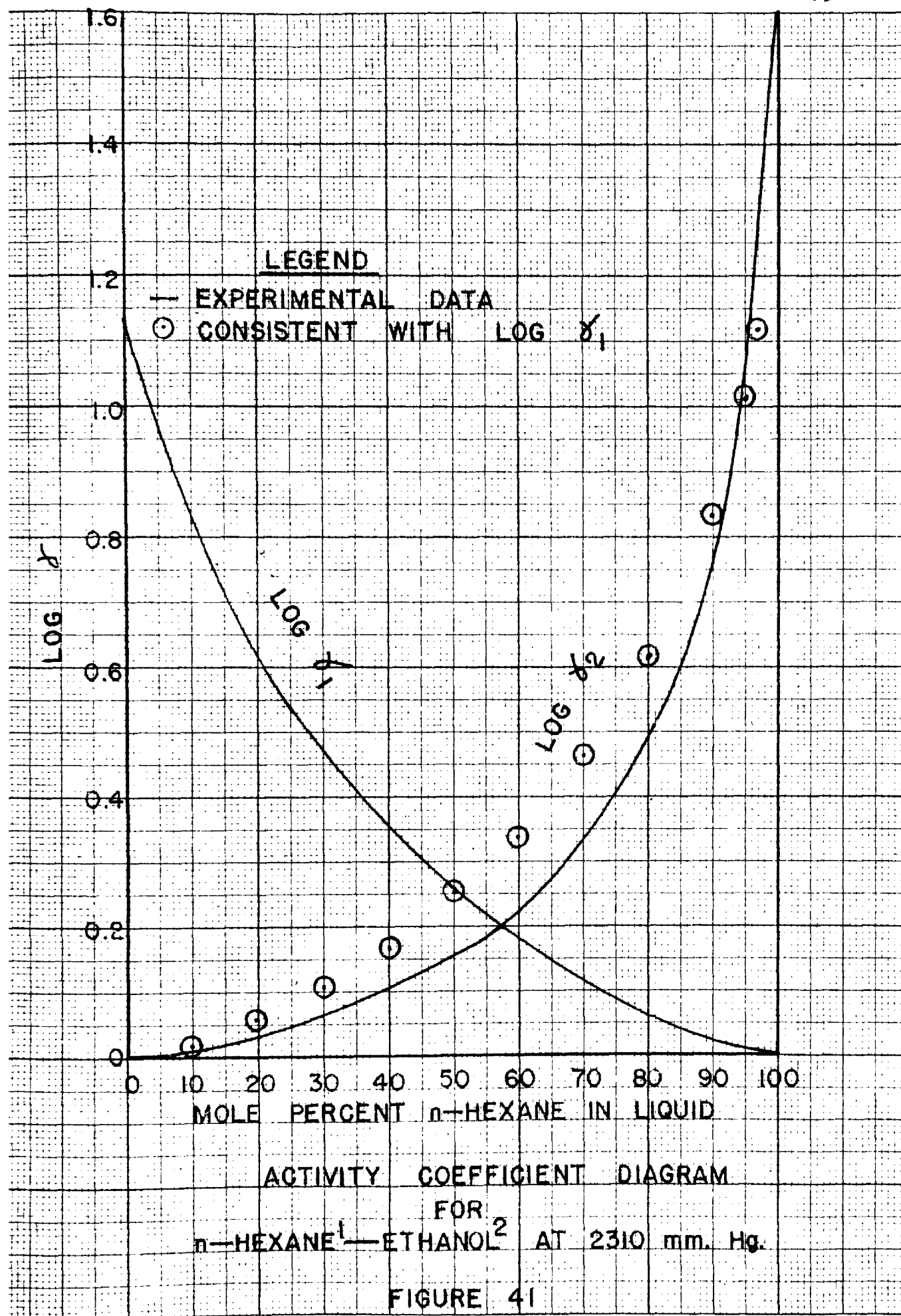
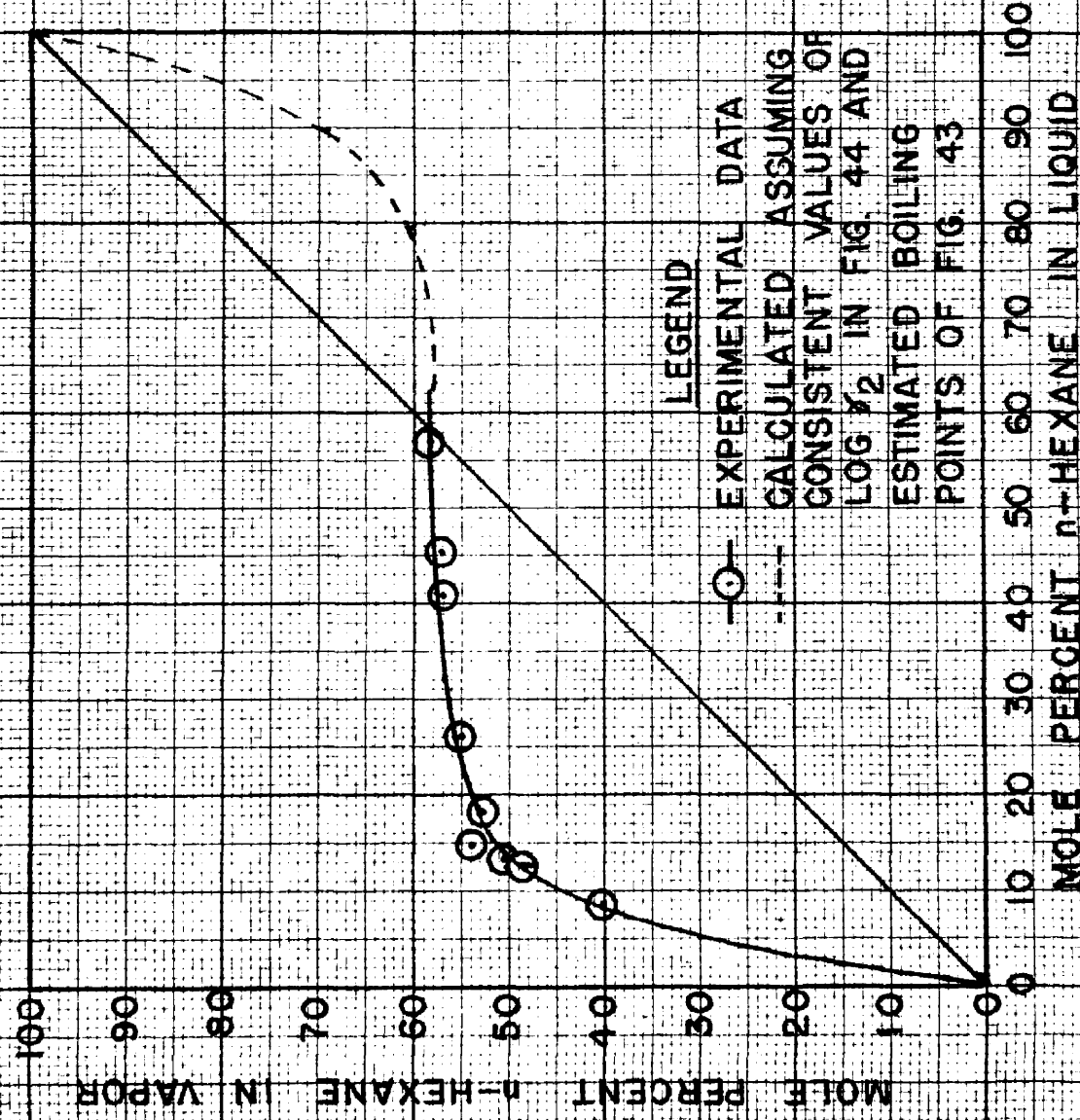


TABLE XIII
 EXPERIMENTAL DATA ON n-HEXANE¹ -ETHANOL² AT 2850 mm. Hg.
 TOTAL PRESSURE

TEMPERATURE °C.	MOLE PERCENT n-HEXANE ¹		LOG γ_1	LOG γ_2
	LIQUID	VAPOR		
107.0	8.7	40.0	.6713	----
101.1	12.6	47.5	.6448	----
101.1	13.1	50.3	.6516	----
99.0	14.9	54.0	.6493	----
99.7	18.4	52.5	.5449	----
98.9	26.0	55.0	.4154	.0135
98.5	40.7	57.0	.2354	.0899
98.8	45.2	57.0	.1902	.1241
98.7	57.0	58.4	.1002	.2148

1--Component 1

2--Component 2

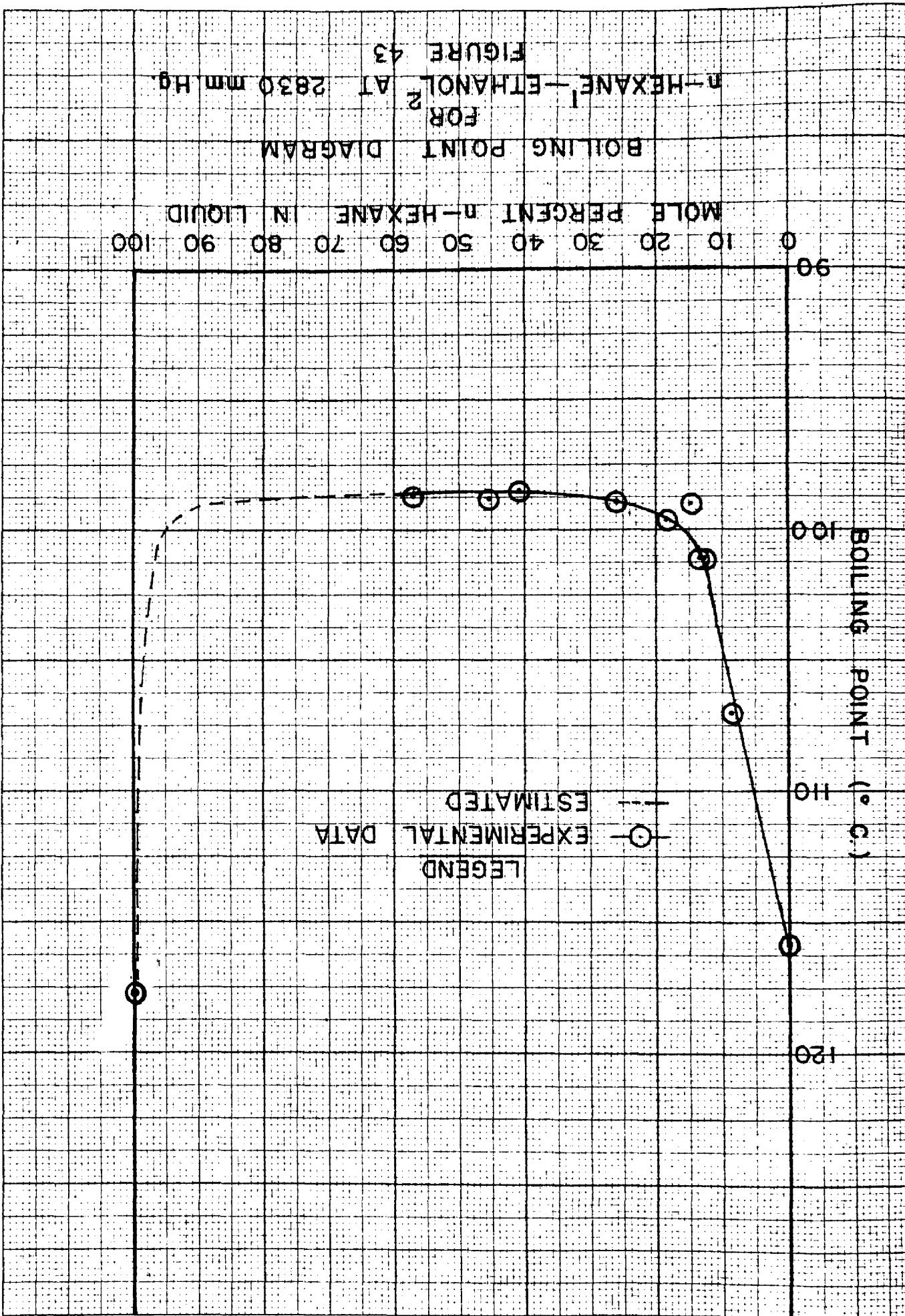


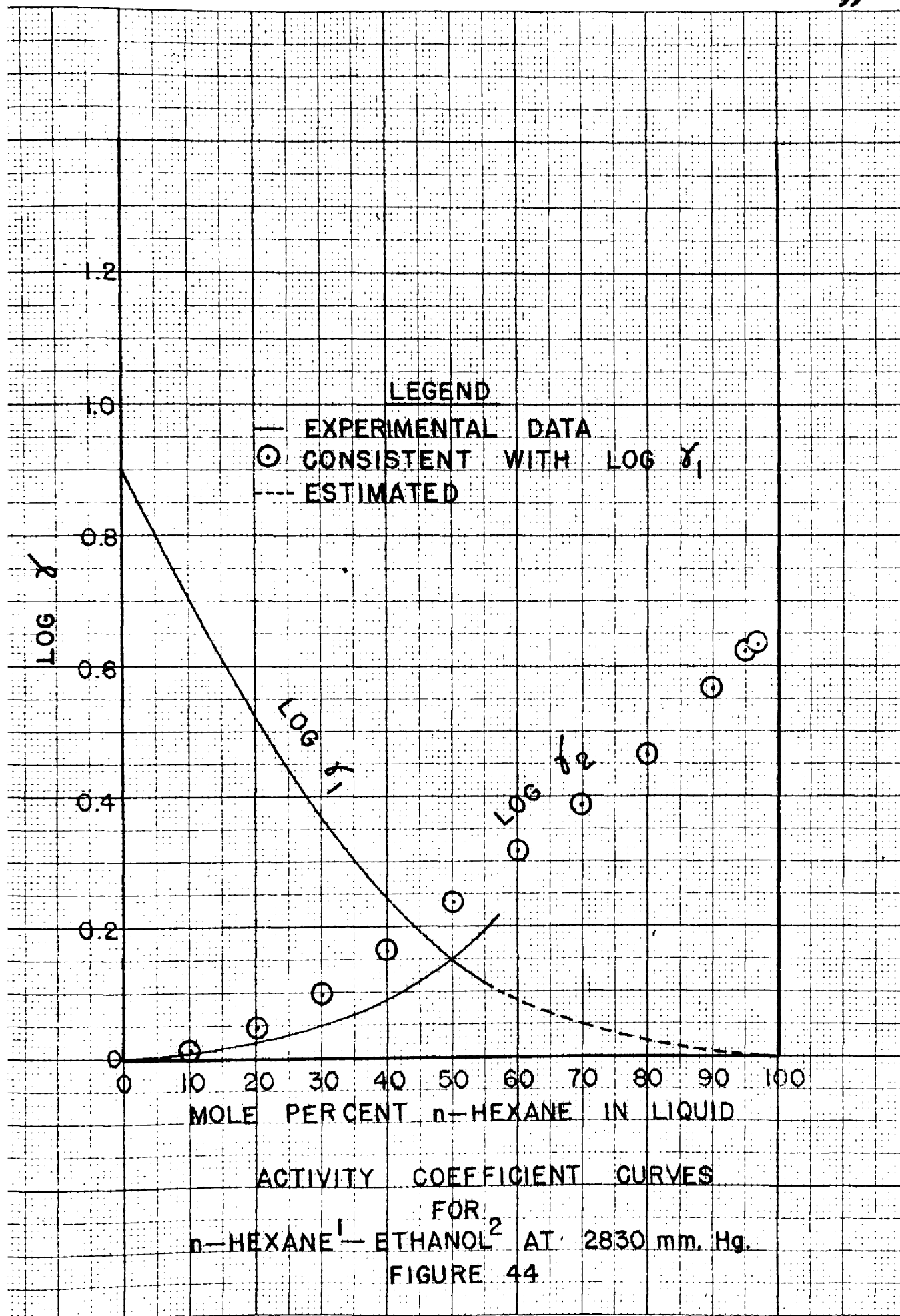
VAPOR—LIQUID EQUILIBRIUM DIAGRAM

FOR

n-HEXANE¹—ETHANOL² AT 2830 mm. Hg.

FIGURE 42





CHAPTER V

DISCUSSION OF RESULTS

The discussion of the results of this investigation is broken into parts to facilitate proper orientation of the material in the order of its occurrence.

A. DEVELOPMENT OF A MORE VERSATILE EQUILIBRIUM STILL

The new type equilibrium still proposed in Chapter III is the result of the combination of desirable features of stills already proposed with new features necessary to properly cope with some physical limitations which had not been satisfactorily overcome previously. The most notable of these difficulties was the adaptation of a recirculating type still so that partially miscible solutions could be handled.

The use of a centrifugal pump with a relatively large by-pass line as a condensed vapor receiver has several advantages: (1) Complete agitation is achieved so that any vapor that separates into two liquid phases on condensation behaves as a homogeneous liquid phase at least insofar as return to the total vaporizer is concerned. (2) The pump supplies the driving force necessary for recirculation of the condensed vapor and eliminates the necessity of sufficient liquid head to supply this driving force, thus reducing the overall size of the equipment. (3) Use of the pump eliminates slugging and the intermittent operation that is characteristic of the gravity return still of Jones, Schoenborn, and Colburn²² until the operating conditions are properly adjusted, thus the

still is more easily set in operation. (4) Centrifugal pumps come in a variety of sizes and materials of construction, so that choice of the pump can be suited to the type of system being handled and the volume of hold-up desired.

Use of a centrifugal pump as a condensed vapor receiver also possesses all the limitations characteristic of stuffing boxes when organic solvents are being handled. These difficulties can be overcome by proper choice of the packing material. Some of the plastic packing materials that have recently become available are especially resistant to organic solvents. Probably the most outstanding of these is Teflon, which is apparently impervious to chemicals and is also very stable over a wide temperature range. Teflon was used during this investigation as gaskets for the sight glass with complete success.

The total vaporizer is necessary if a still of the type described as category (b) in Chapter III is desired. The new still is of this type, so special care must be exercised in order to completely vaporize all of the feed coming from the condensed vapor receiver, but not to appreciably superheat the vapor. If superheated vapor enters the equilibrium chamber, evaporation of the liquid sample will occur as this sensible heat is lost on bubbling through the liquid. A "desuperheater" was installed as a feature of this vaporizer in the form of a nichrome spiral wound inside the inner tube through which the vapor must rise. This spiral will pick up superheat from the vapor and transfer it back to the cold incoming liquid.

No trouble was experienced with superheating since it was found there was sufficient heat to totally vaporize the feed at a temperature equal to

er lower than the boiling point of the liquid in the equilibrium chamber. This was true because the boiling point corresponding to the vapor composition is lower than that of the equilibrium liquid at all compositions other than the azeotropic composition where the two boiling temperatures are the same. The installation of a thermocouple at the entrance of the vapor to the equilibrium is a feature not previously used to insure that superheating of this vapor does not occur.

The liquid chamber was held at approximately the correct temperature by a vapor jacket. Any heat losses result in removal of superheat from the incoming vapor or condensation of a small portion of the vapor which is revaporized when it returns to the vaporizer.

Controlling the pressure by the rate of condensation of the vapor had been previously employed, but not on a still where a total vaporizer was used. For such a method to be successful, a balance of coolant rate, heat input, and rate of circulation must be attained. This balance is easily reached since at any set of conditions there is an equilibrium pressure. This equilibrium pressure can be adjusted to the desired value by changing any one or any combination of the controlled variables.

The data obtained on the systems Ethanol-Water and n-Butanol-Water, representative of miscible and partially miscible systems, were found to satisfactorily conform to the literature data within the limits of the experimental errors. Therefore it was concluded the still operated properly and data were obtained at several pressures on the system n-Hexane-Ethanol on which no data have been published.

In short the new still possesses the desirable characteristics of continuous operation with a definite small amount of miscible or partially miscible liquids at pressures ranging from below atmospheric to

considerably above atmospheric. The unit is of a simple, rugged design, easily constructed, and easily operated.

B. PROPOSED MODIFICATION OF EXISTING DESIGN

At the higher pressures some difficulty was encountered due to leaks. Such leaks are hard to detect and are disastrous to equilibrium measurements. The sight glass seemed to be the principal source of leaks, so a modified design with a smaller sight glass of different design is suggested. The volumetric capacity of the condensed vapor receiver is approximately sixty milliliters, and when this amount is charged it is not necessary to see the operating level. A sight glass of the type used in refrigerant lines would be sufficient to tell if there is circulation. The operation could be easily controlled by other criteria. This type of sight glass could be directly inserted into the line by screwed fittings eliminating the necessity for the special glange construction.

Placing the pressure gauge directly into the Y connecting the condenser and condensed vapor receiver would minimize the possibility of leaks. Charging and removal of the vapor sample could be easily effected through the sample valve at the bottom of the pump. The apparatus could be vented by the removable thermowell above the liquid chamber.

C. EXPERIMENTAL RESULTS

The experimental results on the system n-Hexane-Ethanol presented in Chapter IV are shown to be thermodynamically consistent for the pressures 250 mm., 393 mm., 760 mm., 1270 mm., and 1545 mm. The data at 2310 mm. and 2830 mm. are not quite as reliable as that at the lower pressures. Since the data up to 1545 mm. are consistent they are probably correct.

Analysis of this data shows that the vapor-liquid equilibrium line is displaced by increasing the pressure from 250 mm. to 760 mm. as has been postulated.³² However, at a pressure of 1270 mm. the line denoting the equilibrium compositions is not displaced throughout the composition range and the experimental azeotropic point is much lower than that predicted by the method of Othmer and Ten Eyck.³² The same is noted by comparison of the data at 1545 mm. with that at 1270 mm. and the lower pressures. At first it might seem this is due to erroneous data, but as already mentioned the data are consistent and in all probability are correct within the limits of the experimental error. However the vapor pressure curves for these two components are seen to cross at a pressure of 2500 mm. and a temperature of 112° C. (Figure 54--Appendix) A reversal of the volatility characteristics would be expected beyond this point. It seems this reversal begins when the conditions are such that the vapor pressures of the two components begin to converge thus resulting in the crossing of the equilibrium curves at two different pressures. The statements of Othmer and Ten Eyck³² are thus incorrect as they stand and should be qualified. Crossing of vapor pressure curves is not an unusual phenomena since several compounds that are not of the same homologous series exhibit this property.

No conclusions are drawn from the data at 2310 mm. and 2830 mm. since they have been shown to be inconsistent. An effort was made to determine the nature and amount of this inconsistency by adjustment of the activity coefficient curves for the 2310 mm. data until they were thermodynamically consistent. This was done by first assuming the curve representing $\log \gamma_1$ was correct and graphically integrating the Gibbs-Duhem equation to obtain

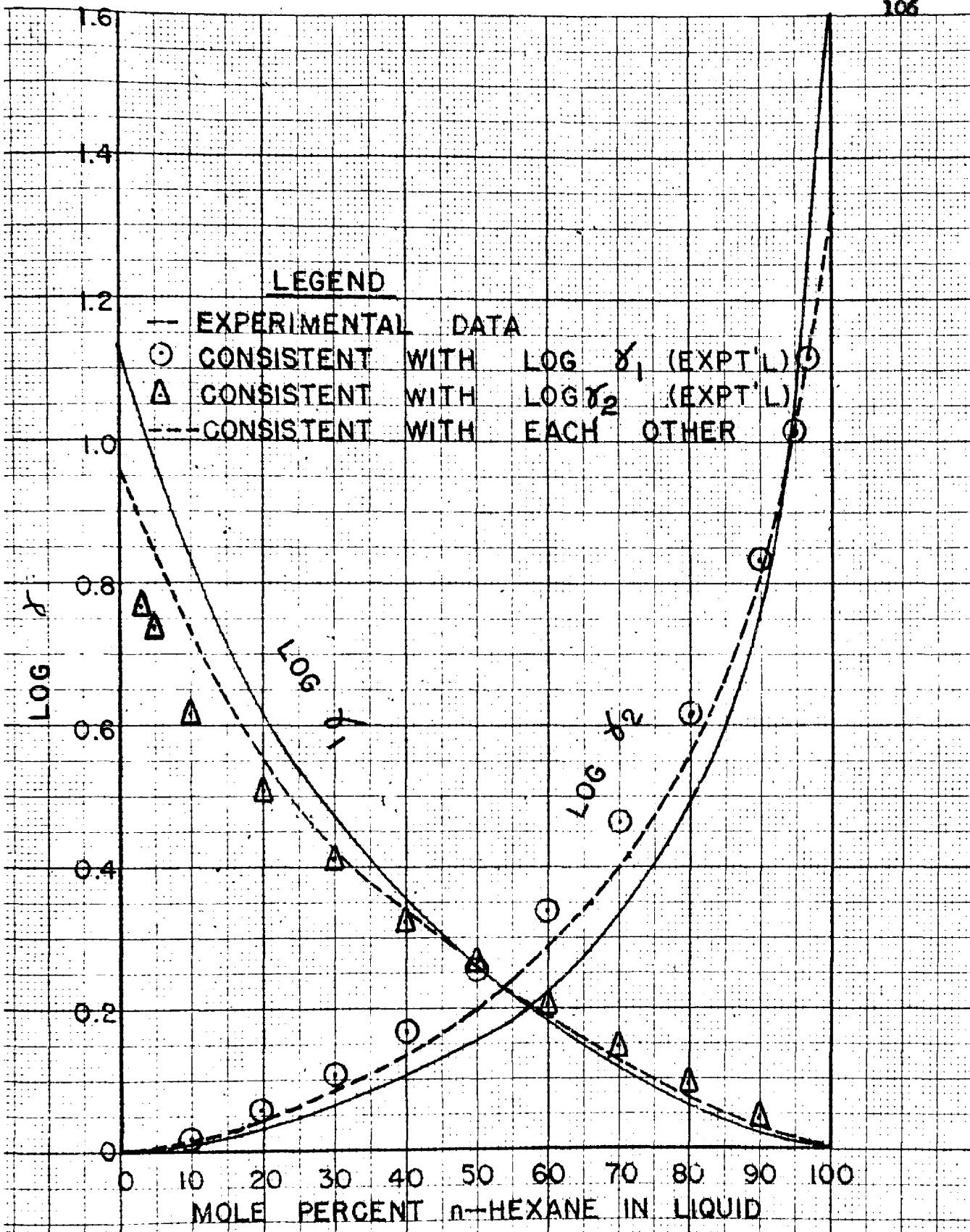
the curve representing $\text{Log } \gamma_2$ that would be thermodynamically consistent with $\text{Log } \gamma_1$ (Represented by circles on Figure 45). This makes the consistency appear to be poorer than it really is since all the inconsistencies of both curves are thrown into one. To account for this the curve representing $\text{Log } \gamma_2$ was assumed to be correct and the procedure repeated to find $\text{Log } \gamma_1$ that would be consistent with $\text{Log } \gamma_2$ (Represented by the triangles on Figure 45). Then somewhere in between the experimental curves and curves gotten by the procedure outlined there should be curves consistent with each other. The dashed lines on Figure 45 represent such curves, but being consistent does not make them correct. However assuming they were correct, new values for the equilibrium curve were calculated and are shown in Figure 46. The inconsistency seems to have occurred between 10 and 40 mole percent n-Hexane.

The experimental vapor pressures of the azeotrope of n-Hexane-Ethanol as a function of temperature were plotted on the Cox Vapor Pressure Plot (Figure 54--Appendix) where the behavior was the same as that for pure components even though the composition of the azeotrope changes with pressure. According to the method of Nutting and Horsley³⁰ the azeotrope of the n-Hexane-Ethanol system would disappear at a pressure greater than 10,000 mm. where the azeotrope vapor pressure curve and the Ethanol vapor pressure curve intersect.

D. CORRELATION OF DATA

The application of Equation (56) of Chapter II recommended previously for the correlation of activity coefficient data,

$$\text{Log } \frac{\gamma_1}{\gamma_2} = \text{Log } \frac{y_1 x_2}{x_1 y_2} + \text{Log } \frac{f_{P_2}}{f_{P_1}} + \text{Log } \frac{\sqrt{\pi_1}}{\sqrt{\pi_2}} + \frac{V_{M_2}(\pi - P_2)}{2.303 RT} - \frac{V_{M_1}(\pi - P_1)}{2.303 RT}$$



ACTIVITY COEFFICIENT DIAGRAM
FOR
n-HEXANE¹—ETHANOL² AT 2310 mm. Hg.

FIGURE 45

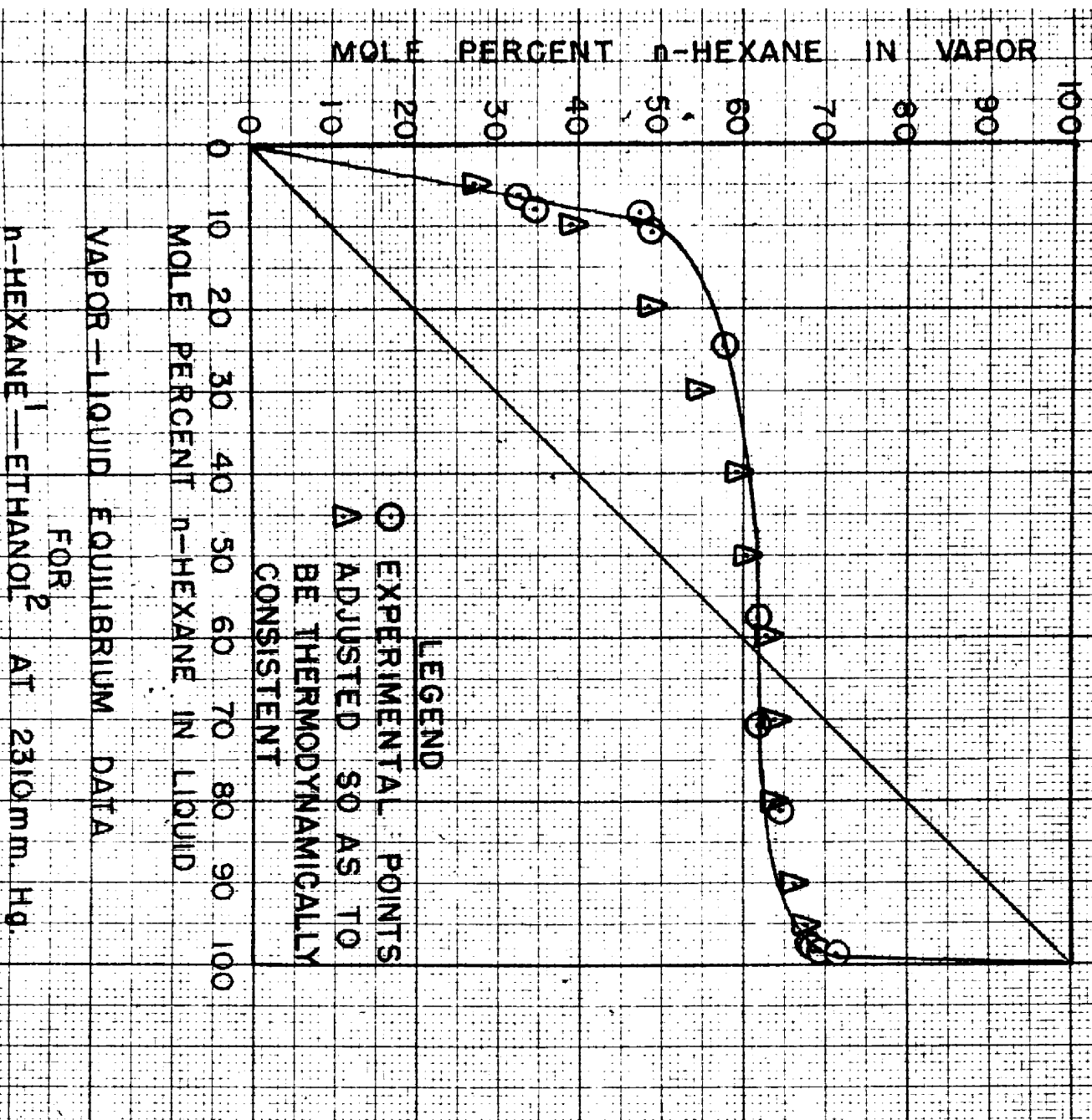


FIGURE 46

is illustrated in Figure 47 for the constant pressure data at 1545 mm. In this Figure all the component parts of the equation are plotted except the term $\frac{V_m(\pi-P)}{2.303 RT}$, each of which were of the order of magnitude of 0.0010 but of opposite sign so as to cancel. All the terms inside the brackets were calculated from a knowledge of the properties of the pure components, total pressure, and temperature. It should be noted that $\text{Log } \frac{\sqrt{\pi_1}}{\sqrt{\pi_2}}$ does not vary with composition for constant pressure data and $\text{Log } \frac{f_{P_2}}{f_{P_1}}$ does not vary for isothermal data. $\text{Log } \frac{y_1 x_2}{x_1 y_2}$ was determined experimentally and $\text{Log } \frac{\delta_1}{\delta_2}$ then calculated. Past investigators^{12, 27, 35} have developed empirical power series to express the data, but use of the above equation is simple and convenient when broken into its component parts and in addition adheres to the factors commonly used to express phase equilibrium.

According to Equation (50) of Chapter II

$$\int_0^1 \text{Log } \frac{\delta_1}{\delta_2} dx = 0$$

which means the positive and negative areas under the $\text{Log } \frac{\delta_1}{\delta_2}$ versus x_1 curve should be equal. This criteria is satisfactorily satisfied since the positive area as drawn is 0.254 units and the negative area is 0.249 units.

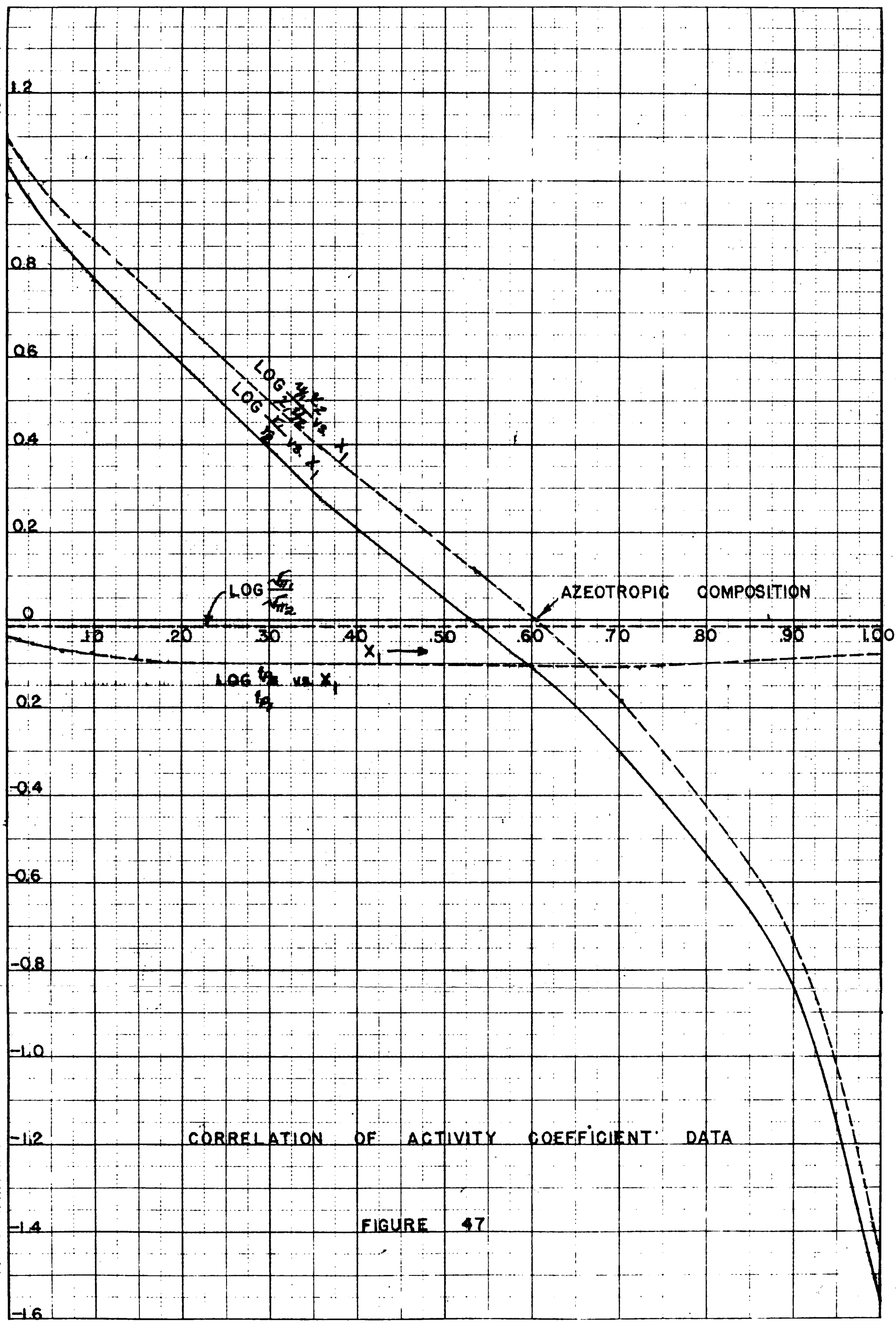
Since it has been shown in Chapter II that

$$\lim_{x_1 \rightarrow 0} \text{Log } \frac{y_1 x_2}{x_1 y_2} = \text{Log } k_1$$

and

$$\lim_{x_2 \rightarrow 0} \text{Log } \frac{y_2 x_1}{x_2 y_1} = \text{Log } k_2$$

FIGURE 47 (continued) NO. 1966



where k_1 is the Henry Law constant at $x_1 = 0$ and k_2 is the Henry Law constant at $x_2 = 0$, and which are the slopes of the x-y diagram at $x_1 = 0$ and $x_2 = 0$. This limiting slope can be used as an aid in drawing the equilibrium curve as shown in Example 1.

Example 1:

From Figure 47 at $x_1 = 0$, $\text{Log } \frac{y_1 x_2}{x_1 y_2} = \text{Log } k_1 = 1.10$.

Thus $k_1 = 12.6$ and a line having this slope is drawn through $x_1 = 0$ in Figure 48.

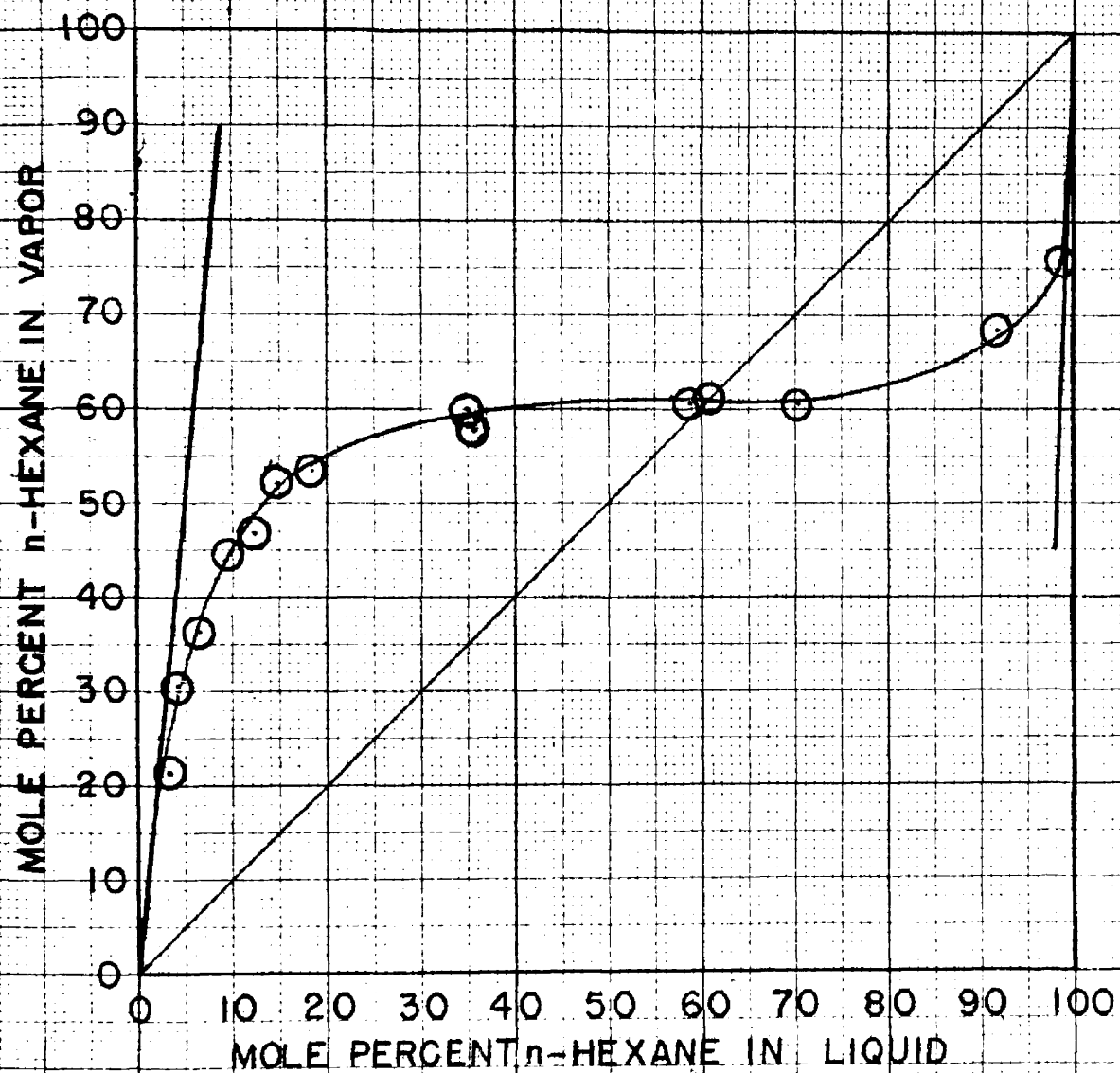
Similarly from Figure 47

$$\text{Log } \frac{y_2 x_1}{x_2 y_1} \bigg|_{x_2 = 0} = - \text{Log } \frac{y_1 x_2}{x_1 y_2} \bigg|_{x_2 = 0} = \text{Log } k_2 = 1.45$$

Then $k_2 = 28.2$ and a line having this slope is drawn through $x_2 = 0$ on Figure 48. The experimental data are seen to conform to these requirements.

Accurate prediction of activity coefficients and vapor-liquid equilibrium data from very limited data cannot be accomplished until a method is found to accurately predict the terminal values of the activity coefficients. At present the Van Laar equations are the most commonly used for this purpose. The limitations of these equations have already been pointed out and need no elaboration.

The following method is suggested for prediction of these end values based on a method presented by Hougen and Watson¹⁷ but made more accurate by substitution of fugacity for pressure. The following equations will hold for moderate pressures where the pressure correction terms, $\frac{V_M(\pi - P)}{RT}$, can be neglected.



EXPERIMENTAL VAPOR LIQUID EQUILIBRIUM DATA
FOR
n-HEXANE¹-ETHANOL² AT 1545 mm. PRESSURE

FIGURE 48

$$\delta_1 = \frac{y_1 \pi \sqrt{\pi_1}}{\chi_1 f_{P_1}}$$

$$\delta_2 = \frac{y_2 \pi \sqrt{\pi_2}}{\chi_2 f_{P_2}}$$

Then

$$y_1 \pi \sqrt{\pi_1} = \delta_1 \chi_1 f_{P_1}$$

$$y_2 \pi \sqrt{\pi_2} = \delta_2 \chi_2 f_{P_2}$$

Addition of these two equations gives

$$y_1 \pi \sqrt{\pi_1} + y_2 \pi \sqrt{\pi_2} = \delta_1 \chi_1 f_{P_1} + \delta_2 \chi_2 f_{P_2}$$

and since $y_1 + y_2 = 1$, and $\sqrt{\pi_1}$ and $\sqrt{\pi_2}$ are very near the same value the following can be written as an approximation.

$$\left(\frac{\sqrt{\pi_1} + \sqrt{\pi_2}}{2} \right) \pi = \delta_1 \chi_1 f_{P_1} + \delta_2 \chi_2 f_{P_2} \quad (1)$$

Rearrangement gives

$$\delta_1 = \frac{\left(\frac{\sqrt{\pi_1} + \sqrt{\pi_2}}{2} \right) \pi - \delta_2 \chi_2 f_{P_2}}{\chi_1 f_{P_1}} \quad (2)$$

As χ_1 approaches zero, δ_2 approaches zero and the following limits have been shown to hold¹⁷:

$$\lim_{\chi_1 \rightarrow 0} \delta_1 = \frac{\left(\frac{\sqrt{\pi_1} + \sqrt{\pi_2}}{2} \right) \pi - \chi_2 f_{P_2}}{\chi_1 f_{P_1}} \quad (3)$$

$$\lim_{\chi_2 \rightarrow 0} \delta_2 = \frac{\left(\frac{\sqrt{\pi_1} + \sqrt{\pi_2}}{2} \right) \pi - \chi_1 f_{P_1}}{\chi_2 f_{P_2}} \quad (4)$$

From accurate isobaric boiling point measurements over the entire composition range, apparent activity coefficients can be calculated and extrapolated to $x_1 = 0$ and $x_2 = 0$ at which point they are equal to the true activity coefficients. This should be more accurate than vapor-liquid equilibrium measurements because of the ease of making up a liquid of known composition thus eliminating an inaccurate analysis later in the process. Apparatus for accurately determining boiling points have been described⁴⁹. If there is considerable curvature, extrapolation to the zero concentrations is facilitated by use of the White⁵² method wherein $(T \log \gamma_1)^{-0.5}$ versus $\frac{x_1}{x_2}$ and $(T \log \gamma_2)^{-0.5}$ versus $\frac{x_2}{x_1}$ is plotted. The postulated straight line is not always observed, but it is sufficiently straight in the dilute ranges to permit accurate extrapolation.

Analysis of the Van Laar equations shows that the concentration at which $\log \frac{\gamma_1}{\gamma_2} = 0$ is given by

$$\pm \left(1 - \frac{1}{\chi_1}\right) = \sqrt{\frac{A}{B}}$$

And since $A = \log \gamma_1$ at $x_1 = 0$ and $B = \log \gamma_2$ at $x_2 = 0$, it follows that this concentration can be located by Equation (5).

$$\pm \left(1 - \frac{1}{\chi_1}\right) = \sqrt{\frac{(\log \gamma_1)_{\chi_1=0}}{(\log \gamma_2)_{\chi_2=0}}} \quad (5)$$

This is believed to be an adequate expression for this condition. At this point the actual values of γ_1 and γ_2 can be found by use of Equation (1). In many cases the boiling point curve will indicate the concentration at which the azeotrope occurs. At this point $\log \frac{y_1 x_2}{x_1 y_2} = 0$ and $\log \frac{\gamma_1}{\gamma_2}$

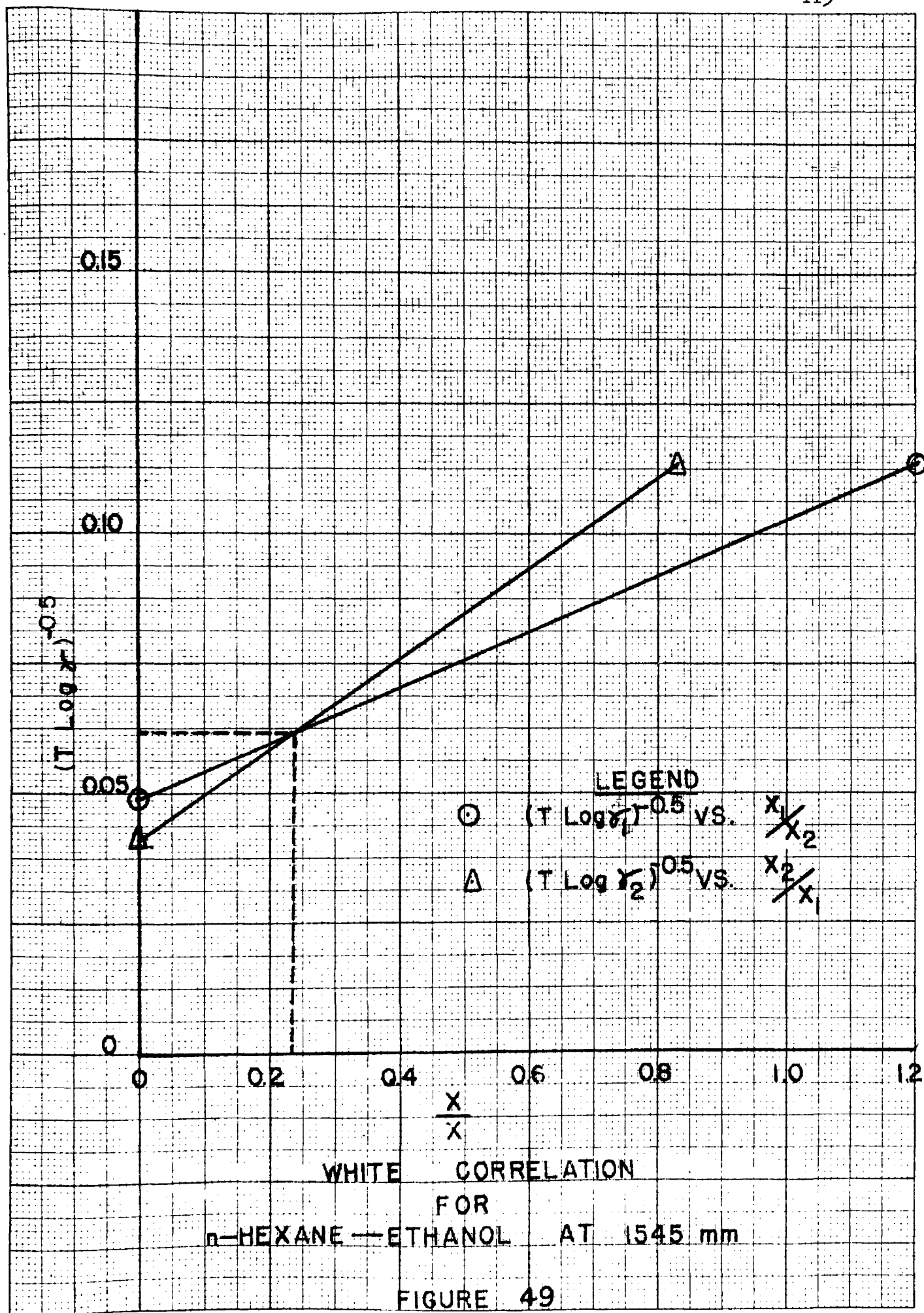
can be calculated from the equation proposed. This will give three or four points on the $\text{Log } \gamma_i$ versus x_1 curve which if used in conjunction with the specification

$$\int_0^1 \text{Log } \frac{\gamma_1}{\gamma_2} dx = 0$$

are sufficient to specify the activity coefficient curves. A check for consistency by integration of the Gibbs-Duhem equation should be performed and adjustments made.

This method was applied to the n-Hexane-Ethanol System at 1545 mm. assuming a knowledge of the boiling point diagram only (Figure 36--Chapter IV) as shown in Example 2. End values of $\text{Log } \gamma_1 = 1.11$ and $\text{Log } \gamma_2 = 1.60$ were predicted as compared with doubtfully extrapolated experimental values of $\text{Log } \gamma_1 = 1.11$ and $\text{Log } \gamma_2 = 1.60$ as seen in Figure 38 of Chapter IV. The predicted concentration at which $\text{Log } \frac{\gamma_1}{\gamma_2} = 0$ was $x_1 = 0.546$ as compared with the experimental value of $x_1 = 0.532$. The predicted value of $\text{Log } \gamma_1 = \text{Log } \gamma_2$ at this point is 0.221 as compared with an experimental value of 0.230.

To secure other points use is made of a characteristic brought out by White's method of plotting activity coefficients. This is illustrated in Figure 49 where it is seen that $\frac{x_1}{x_2} = \frac{x_2}{x_1} = 0.234$ and $T \text{Log } \gamma_1 = T \text{Log } \gamma_2$. This is indicated at $x_1 = x_2 = 0.189$. It has been found that these concentrations are correct for this characteristic but that the values of $\text{Log } \gamma$ obtained at this point do not conform to experimental data and will not be used. This is brought about by the assumption of a straight line for this plot which is not correct. The values obtained indicate that the high values of $\text{Log } \gamma$ are the ones in question, since there are two possible values.



Example 2:

From Figure 36 of Chapter IV the following data is obtained at 1545 mm. total pressure:

<u>x_1</u>	<u>x_2</u>	<u>B.P. °C.</u>
0.10	0.90	84.0
0.04	0.96	89.0
0.90	0.10	79.0
0.99	0.01	85.5

From these data and a knowledge of the vapor pressures and critical constants of the pure components the following can be calculated by methods presented in Chapter II:

<u>x_1</u>	<u> </u>	<u> </u>	<u> </u>	<u> </u>
0.04	0.951	0.966	939	1124
0.10	0.951	0.966	1063	1230
0.90	0.951	0.966	980	765
0.99	0.951	0.966	1130	940

Use of Equation (2) permits calculation of apparent values of γ_1 at the concentrations approaching $x_1 = 0$, and an analogous equation for γ_2 permits calculation of apparent values of γ_2 at concentrations approaching $x_2 = 0$.

<u>x_1</u>	<u>γ_1 apparent</u>	<u>Log γ_1 apparent</u>	<u>γ_2 apparent</u>	<u>Log γ_2 apparent</u>
0.04	9.25	.9661		
0.10	5.52	.7419		
0.90			7.63	.8819
0.99			36.80	1.565

When these values are plotted and extrapolated to $x_1 = 0$ or $x_2 = 0$ the end values of $\log \gamma_1$ and $\log \gamma_2$ are obtained.

$$(\log \gamma_1)_{x_1=0} = 1.11$$

$$(\log \gamma_2)_{x_2=0} = 1.60$$

To get the concentration at which $\gamma_1 = \gamma_2$

$$\frac{1}{\gamma_1} - 1 = \sqrt{\frac{1.11}{1.60}} = 0.829$$

$$\gamma_1 = \frac{1}{1.829} = 0.546$$

Now solving Equation (1) substituting γ_1 for γ_2 yields

$$\left(\frac{0.931 + 0.966}{2} \right) (1545) = 0.546 (990) \gamma_1 + 0.454 (765) \gamma_1$$

$$\gamma_1 = \gamma_2 = 1.661$$

$$\log \gamma_1 = \log \gamma_2 = 0.221$$

Using these values and the end point values the White correlation can be plotted as shown in Figure 49 and the concentrations found at which $\frac{x_1}{x_2} = \frac{\gamma_2}{\gamma_1}$ and simultaneously $(T \log \gamma_1)^{-0.5}$ equals $(T \log \gamma_2)^{-0.5}$.

$$\text{at } x_1 = 0, \frac{x_1}{x_2} = 0$$

$$(T \log \gamma_1)^{-0.5} = [370.6 (1.11)]^{-0.5} = 0.0492$$

$$\text{at } x_2 = 0, \frac{x_2}{x_1} = 0$$

$$(T \log \gamma_2)^{-0.5} = [366.1 (1.60)]^{-0.5} = 0.0413$$

$$\text{at } x_1 = 0.546, \frac{x_1}{x_2} = 1.203, \frac{x_2}{x_1} = 0.830$$

$$(T \log \gamma_1)^{-0.5} = (T \log \gamma_2)^{-0.5} = [352 (0.221)]^{-0.5} = 0.1135$$

From Figure 49 at the point of intersection of the two lines

$$\frac{x_1}{x_2} = \frac{x_2}{x_1} = 0.234, \text{ hence at } x_1 = 0.189 \text{ and } x_2 = 0.189 \text{ the logarithm}$$

of the activity coefficients are inversely proportional to their

absolute temperatures at the two indicated concentrations. That is,

$$\frac{(\log \gamma_2)_{x_2=0.189}}{(\log \gamma_1)_{x_1=0.189}} = \frac{(T)_{x_1=0.189}}{(T)_{x_2=0.189}}$$

Now the curve representing $\log \frac{\gamma_1}{\gamma_2}$ can be drawn satisfying the following conditions:

$$1. \quad \left(\log \frac{\gamma_1}{\gamma_2} \right)_{x_1=0} = (\log \gamma_1)_{x_1=0} = 1.11$$

$$2. \quad \left(\log \frac{\gamma_1}{\gamma_2} \right)_{x_1=1} = -(\log \gamma_2)_{x_2=0} = -1.60$$

$$3. \quad \log \frac{\gamma_1}{\gamma_2} = 0 \quad \text{at } x_1 = 0.546$$

$$4. \quad (T \log \gamma_1)_{x_1=0.189} = (T \log \gamma_2)_{x_2=0.189}$$

$$5. \quad \int_0^1 \log \frac{\gamma_1}{\gamma_2} dx = 0$$

For some systems where the azeotropic concentration can be accurately

predicted from the boiling point diagram the following condition can

also be specified:

$$6. \quad \log \frac{\gamma_1}{\gamma_2} = \log \frac{f_{P_2}}{f_{P_1}} + \log \frac{\sqrt{\pi_1}}{\sqrt{\pi_2}} + \frac{V_{M_2}(\pi - P_2)}{2.303 RT} - \frac{V_{M_1}(\pi - P_1)}{2.303 RT}$$

since $\log \frac{y_1 x_2}{x_1 y_2} = 0$ at that point.

It has been observed that for several systems a plot of $\log \frac{\gamma_1}{\gamma_2}$ versus

x_1 is almost a straight line from the zero concentration having the

lower value of $\log \gamma$ to the point where $\log \frac{\gamma_1}{\gamma_2} = 0$, so such a line would

probably be a very good first approximation. Also, the curve connecting the point where $\text{Log } \frac{\gamma_1}{\gamma_2} = 0$ to the higher end value of $\text{Log } \gamma$ shows quite pronounced curvature toward the concentration at which this high end value occurs. This can be seen by reference to Figure 47.

When the curve was drawn and properly adjusted according to the five points outlined, almost exact duplication of the experimental values was attained, hence the experimental curve of Figure 47 represents the predicted values and no second curve is drawn.

This method was also applied to the n-Butanol-Water system presented in Chapter III with the same good agreement being attained. Trials of this method on many systems should be carried out before definite conclusions as to its validity can be made, but it shows merit and is better than the methods previously used.

CHAPTER VI

SUMMARY

The literature pertaining to the determination and correlation of vapor-liquid equilibrium data for non-ideal liquid mixtures has been thoroughly surveyed. The proposed methods have been critically examined and their limitations pointed out. This examination showed a definite need for (1) better methods of determining vapor-liquid equilibrium, (2) better methods of correlating and extending experimental data to pressures and temperatures other than that determined, and (3) a dependable method for predicting vapor-liquid equilibrium from data easily and accurately determined.

A new continuous, recirculation type equilibrium still has been developed that will operate satisfactorily on miscible or partially miscible liquid systems at pressures ranging from below atmospheric to considerably above atmospheric pressure. This still and one similar in principle were then used to determine vapor-liquid equilibrium data on the binary systems, Ethanol-Water, n-Butanol-Water, Ethyl Acetate-Water, and n-Hexane-Ethanol. Data was also determined at total pressures of 250 mm., 393 mm., 1270 mm., 1545 mm., 2310 mm., and 2830 mm. on the system n-Hexane-Ethanol.

An equation for the correlation of activity coefficients derived from vapor-liquid equilibrium data is presented which is easily handled when broken into its component parts. At the same time this equation

shows the magnitude of the various factors influencing phase equilibrium. An aid to drawing the approach of the equilibrium curve to the end points is demonstrated.

In addition a method for predicting activity coefficients and vapor-liquid equilibrium data for any system at moderate pressures based on the method of correlation presented is successfully applied. The only data required is a knowledge of the vapor pressures of the components and accurate isobaric boiling points covering the entire composition range. Such data are much more easily and accurately obtained than reliable vapor-liquid equilibrium data.

It is sincerely hoped this work will stimulate more investigations along the same or related lines since much experimental data is necessary to adequately test and improve the methods presented.

SELECTED BIBLIOGRAPHY

1. Beatty, H. A., and Calingaert, G., Tests for the Accuracy of Vapor-Liquid Equilibrium Data, Ind. Eng. Chem., 26, 904 (1934).
2. Beebe, A. H. Jr., Coulter, K. E., Lindsay, R. A., and Baker, E. M., Equilibria in Ethanol-Water System at Pressures Less Than Atmospheric, Ind. Eng. Chem., 34, 1501 (1942).
3. Benedict, M., Johnson, C. A., Solomon, E., and Rubin, L. O., Azeotropic and Extractive Distillation--Theoretical Aspects, Trans. Am. Inst. Chem. Engrs., 41, 371 (1945).
4. Berg, C., and McKinnis, A. O., The Effect of Temperature on Liquid Phase Activity Coefficients, Ind. Eng. Chem., 40, 1309 (1948).
5. Carlson, H. O., Extractive Distillation, Trans. Am. Inst. Chem. Engrs., 41, 787 (1945).
6. Carlson, H. O., and Colburn, A. P., Vapor-Liquid Equilibria, Ind. Eng. Chem., 34, 581 (1942).
7. Colburn, A. P., Schoenborn, E. M., and Shilling, D., Equilibrium Still for Partially Miscible Liquids, Ind. Eng. Chem., 35, 1250 (1943).
8. Dodge, B. F., Chemical Engineering Thermodynamics, McGraw-Hill Book Company, Inc., New York, 1944.
9. Duhem, P., Compt. Rend., 102, 1449 (1886).
10. Gibbs, J. W., The Scientific Papers of J. Willard Gibbs: Thermodynamics, Longmans, Green, and Co., 1906.
11. Gillespie, D. T. C., Vapor-Liquid Equilibrium Still for Miscible Liquids, Ind. Eng. Chem., Anal. Ed., 18, 575 (1946).
12. Gilmont, R., Weinman, E. A., Kramer, F., Miller, E., Hashmall, F., and Othmer, D. F., Thermodynamic Correlation of Vapor-Liquid Equilibria, Ind. Eng. Chem., 42, 120 (1950).
13. Glasstone, S., Textbook of Physical Chemistry, Second Edition, D. Van Nostrand Company, Inc., New York, 1946.
14. Griswold, J., Haney, J. D., and Klein, V. A., Ethanol-Water System--Vapor-Liquid Properties at High Pressures, Ind. Eng. Chem., 35, 701 (1943).

15. Griswold, J., Andres, D., and Klein, V. A., Determination of High Pressure Vapor-Liquid Equilibria, Trans. Am. Inst. Chem. Engrs., 32, 223 (1943).
16. Hougen, O. A., and Watson, K. M., Chemical Process Principles, Part II, Thermodynamics, John Wiley and Sons, Inc., New York, 1947.
17. Hougen, O. A., and Watson, K. M., Chemical Process Principles Charts, John Wiley and Sons, Inc., New York, Figures 109 and 142, 1946.
18. Hougen, O. A., Phase Equilibria Review, Ind. Eng. Chem., 40, 1563 (1948).
19. Horsley, L. H., Table of Azeotropes and Non-Azeotropes, Ind. Eng. Chem., Anal. Ed., 19, 508 (1947).
20. Horsley, L. H., Graphical Method for Predicting Azeotropism and the Effect of Pressure on Azeotropic Constants, Ind. Eng. Chem., Anal. Ed., 19, 603 (1947).
21. International Critical Tables, McGraw-Hill Book Co., Inc., New York and London, 1935.
22. Jones, C. A., Schoenborn, E. M., and Colburn, A. P., Equilibrium Still for Miscible Liquids, Ind. Eng. Chem., 35, 666 (1943).
23. Lange, A. N., Handbook of Chemistry, Handbook Publishers, Inc., Sandusky, Ohio, 1946.
24. Lewis, G. N., Proc. Am. Acad., 37, 49 (1901).
25. Lewis, G. N., and Randall, M., Thermodynamics and the Free Energy of Chemical Substances, McGraw-Hill Book Co., Inc., New York and London, 1923.
26. Licht, Wm., Jr., and Denzler, O. G., Azeotropic Mixtures-- Variation of Boiling Point and Latent Heat with Pressure, Chemical Engineering Progress, 44, 627 (1948).
27. Margules, M., Anz. Akad. Wiss. Wien., Math. Naturw. Klasse, 104, II, 1243 (1895).
28. Mertes, T. S., and Colburn, A. P., Binary Mixtures of n-Butane, Isobutane, and 1-Butene with Furfural, Ind. Eng. Chem., 39, 787 (1947).
29. Norman, W. S., and Hands, C. H. G., The Dehydration of Allyl Alcohol By Azeotropic Distillation, Trans. Inst. of Chem. Engrs. (British), 23, 76 (1945).

30. Nutting, H. S., and Horsley, L. H., Graphical Method for Predicting Effect of Pressure on Azeotropic Systems, Ind. Eng. Chem., Anal. Ed., 19, 602 (1947).
31. Othmer, D. F., Correlating Latent Heat and Vapor Pressure Data, Ind. Eng. Chem., 32, 841 (1940).
32. Othmer, D. F., and Ten Eyck, E. H., Jr., Correlating Azeotropic Data, Ind. Eng. Chem., 41, 2897 (1949).
33. Othmer, D. F., and Gilmont, R., Correlating Vapor Compositions and Related Properties of Solutions, Ind. Eng. Chem., 36, 858 (1944).
34. Perry, J. H., Chemical Engineers' Handbook, McGraw-Hill Book Company, Inc., New York, Page 1361, 1941.
35. Redlich, O., and Kister, A. T., Thermodynamics of Nonelectrolyte Solutions, Ind. Eng. Chem., 40, 341 (1948).
36. Rieder, R. M., and Thompson, A. R., Vapor-Liquid Equilibria Measured by a Gillespie Still, Ind. Eng. Chem., 41, 2905 (1949).
37. Scatchard, G., Equilibria in Nonelectrolyte Solutions in Relation to the Vapor Pressures and Densities of the Components, Chem. Rev., 8, 321 (1931).
38. Scatchard, G., and Hamer, W. J., Application of Equations for the Chemical Potentials to Partially Miscible Solutions, J. Am. Chem. Soc., 57, 1805 (1935).
39. Scatchard, G., and Prentiss, S. S., Freezing Points of Aqueous Solutions, J. Am. Chem. Soc., 56, 1486 (1934).
40. Scatchard, G., and Raymond, C. L., Vapor-Liquid Equilibrium, J. Am. Chem. Soc., 60, 1278 (1938).
41. Scheibel, E. G., Activity Coefficient Correction Factor Nomograph, Ind. Eng. Chem., 41, 1076 (1949).
42. Scott, T. A., Jr., Refractive Index of Ethanol-Water Mixtures, Journal of Physical Chemistry, 50, 406 (1946).
43. Selected Values of Properties of Hydrocarbons, American Petroleum Institute Research Project 44, National Bureau of Standards, 1947.
44. Smith, T. E., and Bonner, R. F., Vapor-Liquid Equilibrium Still for Partially Miscible Liquids, Ind. Eng. Chem., 41, 2867 (1949).
45. Souders, M., Selheimer, C. W., Smith, R. L., and Brown, G. G., Pressure-Volume-Temperature Relations of Paraffin Hydrocarbons, Ind. Eng. Chem., 24, 513-22 (1932).

46. Steinhauser, H. H., and White, R. R., Vapor-Liquid Equilibria Data for Ternary Mixtures, Ind. Eng. Chem., 41, 2912 (1949).
47. Stockhardt, J. S., and Hull, C. M., Vapor-Liquid Equilibria and Boiling Point-Composition Relations for the Systems n-Butanol--Water and Isobutanol--Water, Ind. Eng. Chem., 23, 1438 (1931).
48. Stull, D. R., Vapor Pressure of Pure Substances, Ind. Eng. Chem., 39, 517 (1947).
49. Swietoslawski, W., Ebulliometric Measurements, Reinhold Publishing Corporation, New York, 1945.
50. Van Laar, J. J., Z. Physik. Chemie, 72, 723 (1910).
51. Van Laar, J. J., Z. Physik. Chemie, 185, 33 (1929).
52. White, R. R., Vapor-Liquid Equilibria of Non-Ideal Solutions, Trans. Am. Inst. Chem. Engrs., 41, 539 (1945).
53. Winsauer, W. O., Chu, P. L., and Griswold, J., Phase Equilibria in Ethyl Alcohol--Ethyl Acetate--Water System, Ind. Eng. Chem., 41, 2352 (1949).
54. Wehl, K., Thermodynamic Evaluation of Binary and Ternary Liquid Systems, Trans. Am. Inst. Chem. Engrs., 42, 215 (1946).
55. Wohl, K., Über den Gaszustand Niedrigsiedender Stoffe, Z. Physik. Chemie, B2, 77 (1929).

APPENDIX

NOMENCLATURE

- a -- activity
- a -- Van der Waal's constant
- a -- empirical constants in Equation (23)
- a_{12}, a_{21} -- empirical constants in Equations (38) and (39)
- A -- empirical constant, Van Laar or Margules
- b -- Van der Waal's constant
- b_1, b_2 -- empirical constants in Equations (38) and (39)
- B -- empirical constant, Van Laar or Margules
- B -- second virial coefficient
- C -- third virial coefficient
- d_4 -- specific gravity referred to water at 4°C.
- e -- Mathematical quantity, $e = 2.718$
- f -- fugacity
- f^0 -- fugacity in the standard state
- f_p -- fugacity of a pure substance under its own vapor pressure
- F -- free energy
- F -- partial molal free energy
- F^0 -- partial molal free energy in the standard state
- F^0 -- free energy in the standard state
- F_M -- free energy of mixing
- F^E -- excess free energy

H^* -- molal enthalpy at a pressure sufficiently low that the ideal gas laws hold

H° -- partial molal enthalpy at infinite dilution

H -- partial molal enthalpy

k -- Henry Law Constant

K -- empirical constant in Equation (43)

n -- number of moles of any component

N_D -- refractive index

p -- partial pressure

P -- total pressure

P -- vapor pressure

P_O -- critical pressure

P_R -- reduced pressure

P_{az} -- vapor pressure of the azeotrope at temperature, t

P_{az}^1 -- vapor pressure of the azeotrope at temperature, t^1

q -- effective molal volume

Q -- arbitrarily defined quantity of Equation (49)

R -- universal gas constant

t -- temperature

T -- absolute temperature

T_O -- critical temperature

T_R -- reduced temperature

v, V, V_m -- molal volume of pure component in the liquid

x -- mole fraction of any component in a liquid mixture

y -- mole fraction of any component in a vapor mixture

z -- effective volume fraction

z -- compressibility factor

Z -- correction factor defined by Equations (36) and (44)

π -- total pressure

π_R -- reduced pressure

γ -- activity coefficient

$\sqrt{\pi}$ -- fugacity coefficient corresponding to the total pressure, π

\sqrt{p} -- fugacity coefficient corresponding to the vapor pressure, P

α -- relative volatility

σ -- average standard deviation

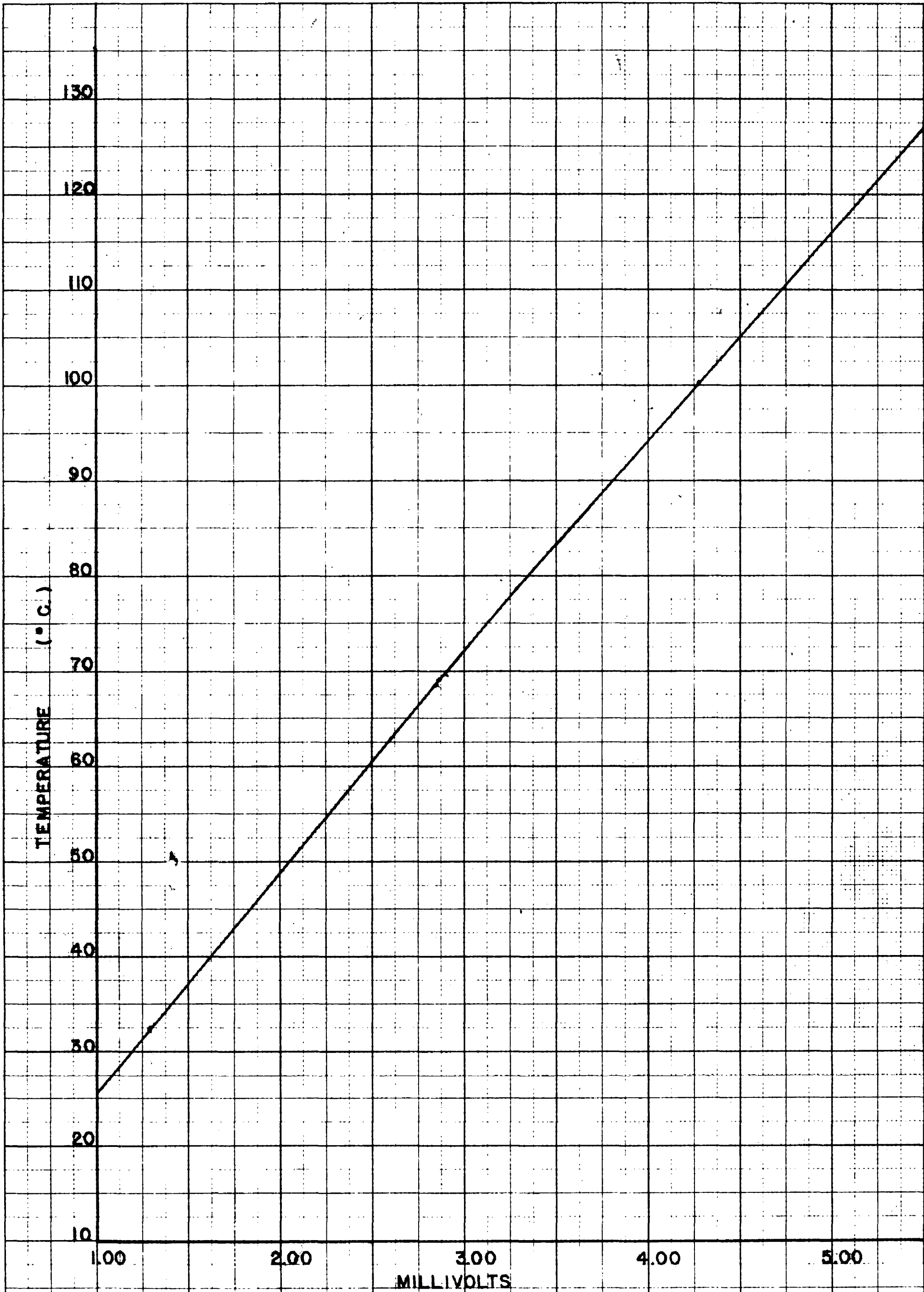
Subscripts

1, 2, 3 -- Component 1, 2, or 3

i, h, j, l - Component i, h, j, l

TABLE XIV
 CALIBRATION DATA FOR COPPER-CONSTANTAN THERMOCOUPLES
 (Reference Point--Ice Bath at 0°C.)

THERMO- COUPLE NUMBER	FIXED POINT	STANDARD USED	CORRECTED BAROMETER (INCHES OF MERCURY)	MILLI- VOLTS	TEMP. °C.
1	B.P.	Ethanol	30.28	3.283	76.67
	B.P.	n-Hexane	30.38	2.863	69.11
	B.P.	Water	30.13	4.274	100.20
	T.P.	Sodium Sulfate	-----	1.290	32.38
2	B.P.	Ethanol	30.28	3.283	78.67
	B.P.	n-Hexane	30.38	2.852	69.11
	B.P.	Water	30.13	4.274	100.20
3	B.P.	Ethanol	30.28	3.283	78.67
	B.P.	n-Hexane	30.38	2.862	69.11
	B.P.	Water	30.13	4.274	100.20



CALIBRATION CURVE FOR COPPER-CONSTANTAN THERMOCOUPLES

FIGURE 50

TABLE XV
SOLUBILITY⁴⁷ OF n-BUTANOL IN WATER

TEMP.	<u>Weight Percent n-Butanol in Water</u>	
<u>°C.</u>	<u>Water Rich Phase</u>	<u>Alcohol Rich Phase</u>
24	7.45	79.8
25	7.40	79.71
26	7.32	79.68
27	7.29	79.60
28	7.21	79.55
29	7.17	79.50
30	7.10	79.40

COMPOSITION VERSUS PHYSICAL PROPERTIES
FOR
n-BUTANOL¹ — WATER² AT 25° C

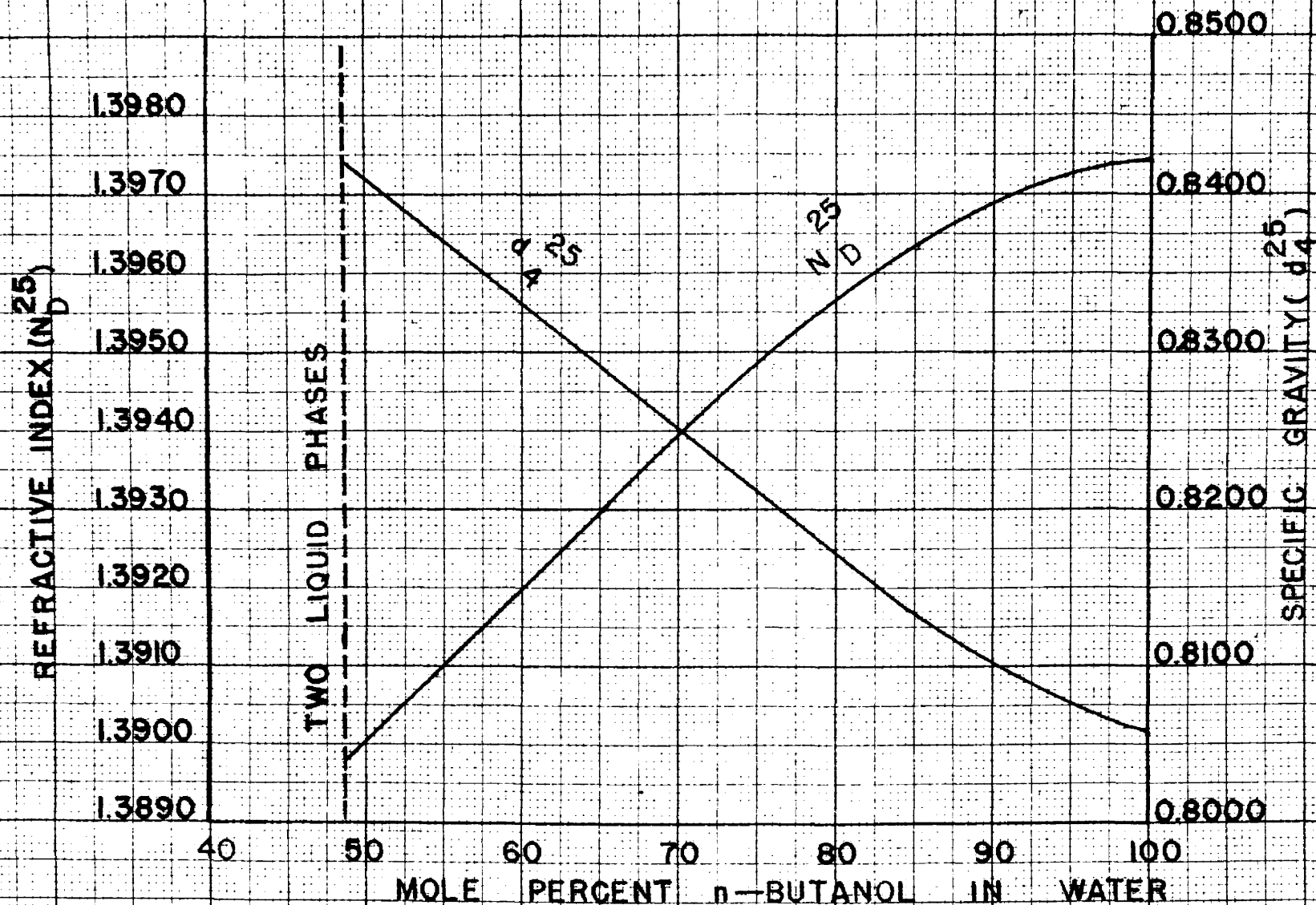


FIGURE 51

TABLE XVI
 SOLUBILITY²¹ OF ETHYL ACETATE IN WATER

TEMP. °C.	<u>Weight Percent Ethyl Acetate in Water</u>	
	<u>Water Rich Phase</u>	<u>Ethyl Acetate Rich Phase</u>
0	10.06	97.71
5	9.40	
10	8.93	97.39
15	8.29	
20	7.86	97.02
25	7.47	96.80
30	7.16	96.60
40	6.62	96.08
50		95.53
60		94.99

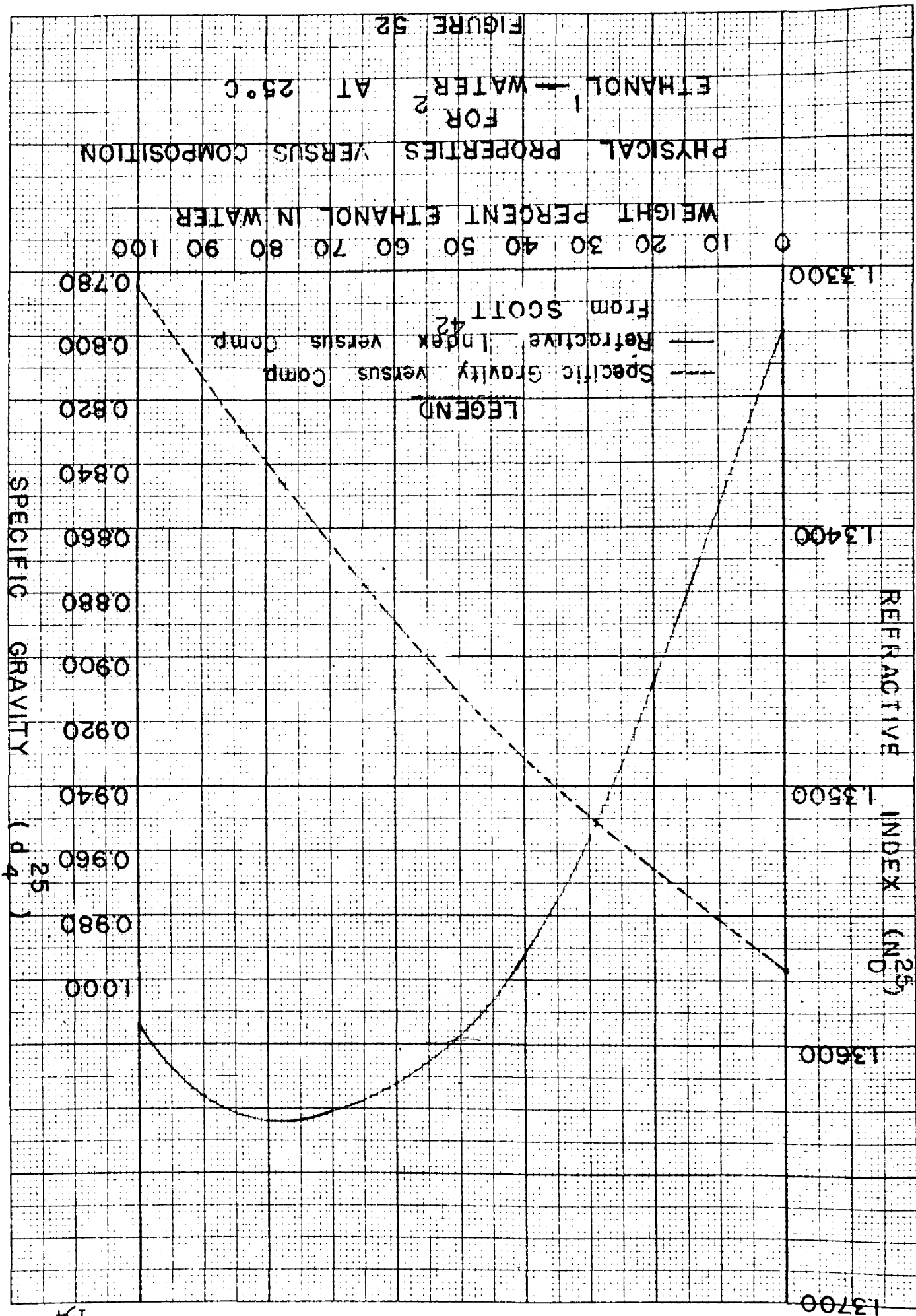
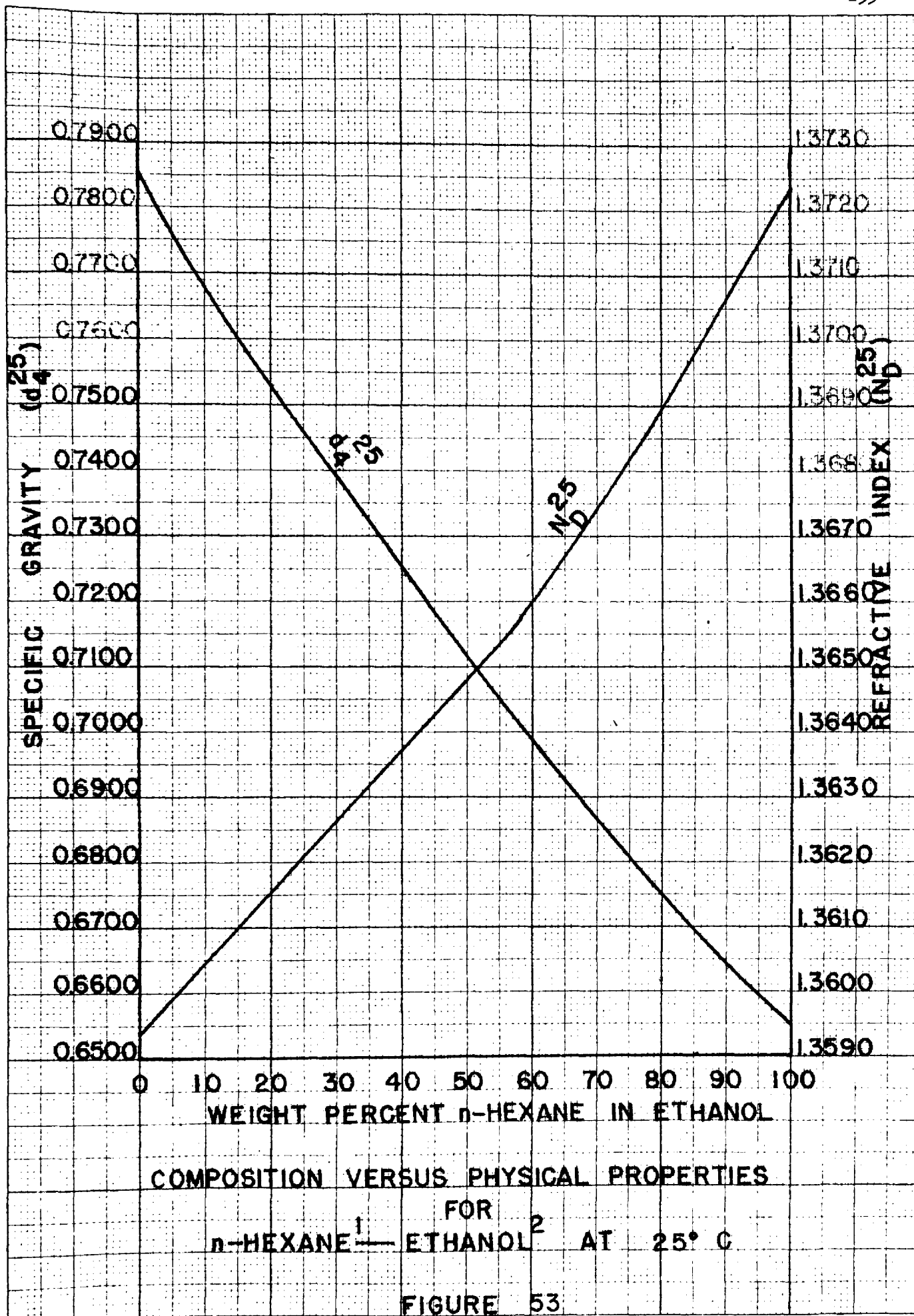


FIGURE 52

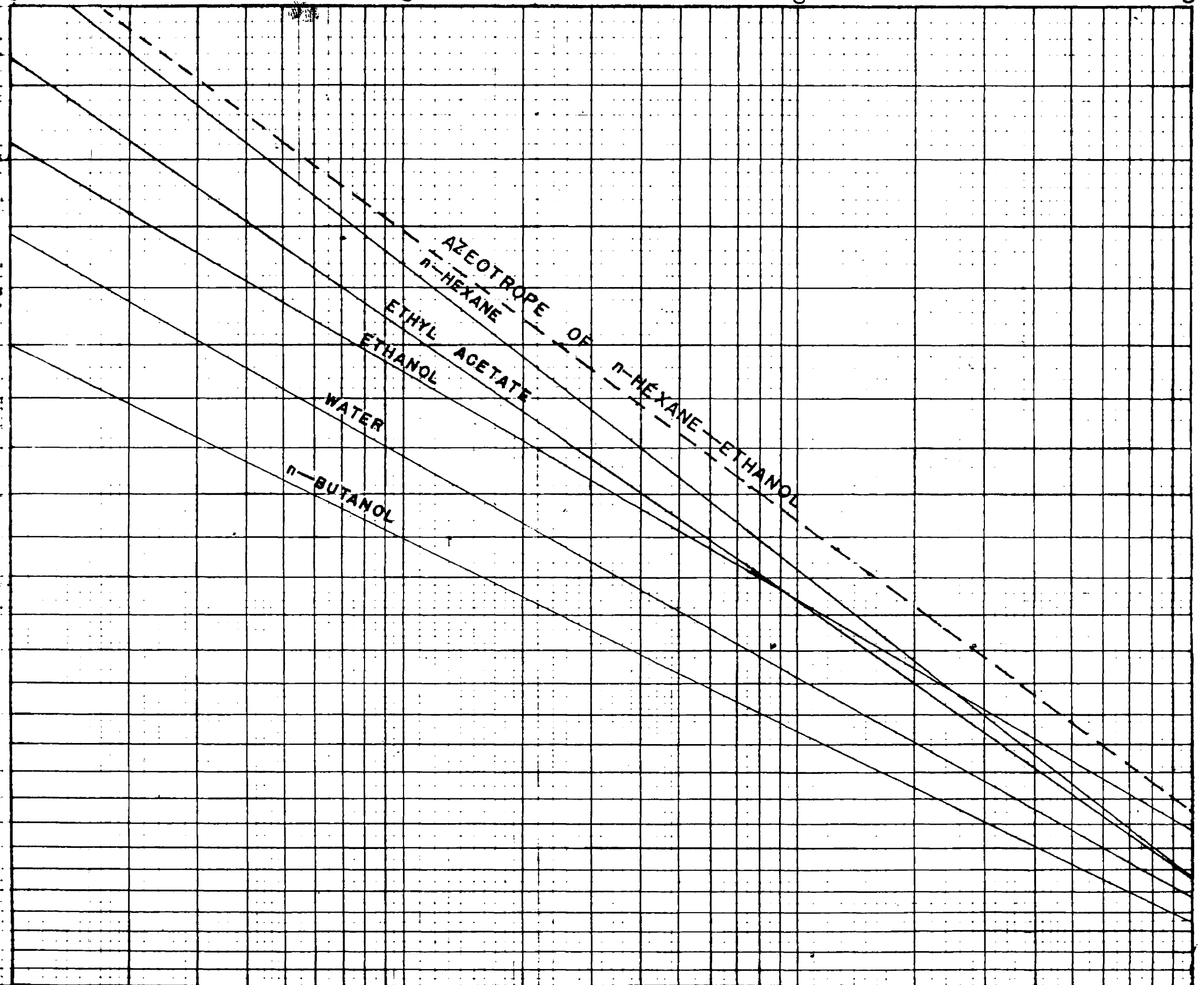


VAPOR PRESSURE (mm. Hg.)

COX VAPOR PRESSURE PLOT

FIGURE 5A

TEMPERATURE (°C.)



BIOGRAPHY

Virgil Orr was born in Glenmora, Louisiana on February 2, 1923. He attended Glenmora grammar and high schools and was graduated from Glenmora High School in 1940. In September of 1940 he enrolled at Louisiana Polytechnic Institute at Ruston, Louisiana and was graduated with the Degree of Bachelor of Science in Chemical Engineering in 1944.

He was employed by Cities Service Refining Corporation of Lake Charles, Louisiana as a shift analyst from July, 1944 until his induction into the Armed Services August 22, 1944.

After a brief training period he was assigned to the 29th Engineering Photomapping Battalion at Portland, Oregon, and later served in Manila, Philippine Islands.

He enrolled in the graduate school of Louisiana State University in September, 1946, and was appointed graduate assistant in the Department of Chemical Engineering in February, 1947. He was awarded the Degree of Master of Science in May of 1948, and at the present is a candidate for the Degree of Doctor of Philosophy.

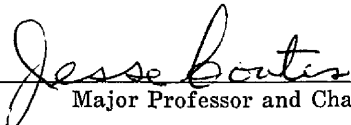
EXAMINATION AND THESIS REPORT

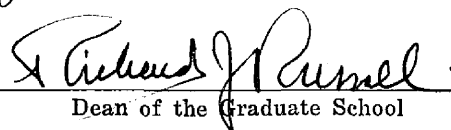
Candidate: Virgil Orr

Major Field: Chemical Engineering

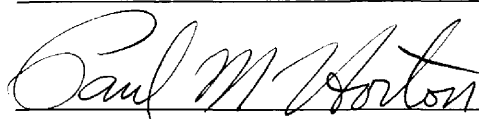
Title of Thesis: Vapor-Liquid Equilibrium of Non-Ideal Solutions.

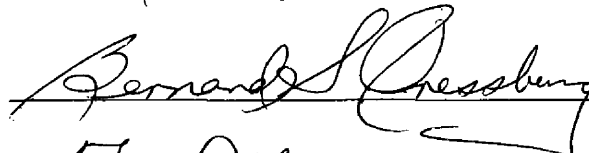
Approved:

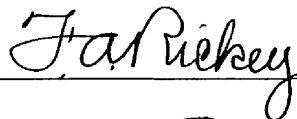

Major Professor and Chairman


Dean of the Graduate School

EXAMINING COMMITTEE:

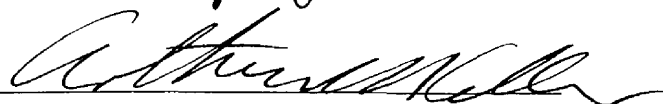












Date of Examination:

May 15, 1950